

DISSERTATION

*Development and quantification of new methods for the
determination and preparation of short-lived xenon isotopes for
the verification of the Comprehensive Nuclear Test Ban Treaty
(CTBT) in a laboratory*

ausgeführt zum Zwecke der Erlangung des akademischen Grades
eines Doktors der technischen Wissenschaften unter der Leitung von

Ao. Univ. Prof. Dr. phil. Manfred Tschurlovits

E141

Atominstitut der Österreichischen Universitäten

durchgeführt

im Forschungszentrum Seibersdorf
ARC Seibersdorf research GmbH, Health Physics, Risk & Safety

Betreuer.: *Mag. Dr. Erich Hrncsek*

eingereicht an der Technischen Universität Wien

Fakultät für Physik

von

Mag. Raith Maria
Matrikelnummer: 9401122
St. Wendelin-Gasse 6/7
1220 Wien

Wien, im März 2006



DANKSAGUNG

An erster Stelle möchte ich mich bei meinem Doktorvater Prof. Manfred Tschurlovits für seine großartige Unterstützung und Betreuung sowie die vielen anregenden Diskussionen bedanken.

Den Austrian research centers Seibersdorf GmbH danke ich herzlichst, dass sie die vorliegende Arbeit finanziert haben sowie mir die Gelegenheit gegeben haben, diese durchzuführen.

Persönlich gilt mein größter Dank Dr. Erich Hrncsek für seine wirklich tolle Betreuung und die großartige Zusammenarbeit, an welche ich mich bestimmt immer gerne zurück erinnern werde.

Allgemein möchte ich der Gruppe „Sicherheit und Risiko“ für die gute Zusammenarbeit in den drei Jahren danken.

Ein großer Dank auch für die Reaktorgruppe am Atominstitut der Österreichischen Universitäten, die mich immer unterstützt haben, wenn Proben bestrahlt wurden.

Größter Dank gebührt meinen Eltern, die mich immer tatkräftig unterstützt haben und mir immer, vor allem in schwierigen Zeiten, mit Rat und Tat zur Seite gestanden sind und stehen. Vor allem danke ich ihnen dafür, dass sie es mir ermöglicht haben, zu studieren und das Studium mit einer Doktorarbeit abzuschließen, sowie nun mit einer Zusatzausbildung, um in weiterer Folge als Medizinhysikerin tätig sein zu dürfen, zu beginnen.

Meinem Freund Norbert möchte ich für seinen Rückhalt, den er mir immer gibt und seine Unterstützung in jeder Hinsicht ganz besonders bedanken.

An dieser Stelle möchte ich auch meinen Bruder und seine Familie erwähnen und ihnen danken. Sie waren auch wesentlich daran beteiligt, dass diese Arbeit zu Stande gekommen ist. Danken möchte ich auch ihnen auch für die zahlreichen Gespräche, vor allem für jene, zu deren Zeitpunkt es für mich nicht so einfach war, alles zu bewerkstelligen.

Abstract

The conceptional background for this work is the Comprehensive Nuclear Test Ban Treaty (CTBT), which was adopted by the UN General Assembly on September 10th, 1996. This treaty will come into force after ratification by the member states mentioned in Annex II of the treaty.

Radionuclide systems were installed since the compliance with the comprehensive nuclear-test-ban treaty can only be verified by radionuclides. Every earthquake or explosions in mines can be detected by the other (seismic, infrasound and hydroacoustic) systems, but the radionuclide station can confirm whether a nuclear detonation has happened.

During a nuclear explosion radioactive elements are formed and can be detected both as solid particles and as noble gases. These nuclides are generated during fission from uranium- or plutoniumnuclides.

The aim of this work was the development of a measurement system for noble gas archive samples. In order to have a calibrated system, the production of relevant xenon isotopes was performed. Finally the exact isotopic composition could be prepared, as is vented during a nuclear explosion.

For this purpose a gaschromatographical method was developed by which the amount of stable xenon can be determined. Possible contaminations (radon and krypton) present in the sample can be eliminated in order to ensure that only xenon is measured in the following radiometric measurements.

A transfer line from an archive bottle to the gaschromatograph was constructed and had to be optimized. This optimization lead to a substantial reduce of losses from 30% in the beginning to 2% in the final stage.

A concept for radionuclide production was elaborated and 90% enriched uranium was irradiated at the TRIGA Mark II Reactor in Vienna at the Atomic Institute of the Austrian Universities. A theoretical calculation was performed first, the results of which afterwards were verified by using the program ORIGEN 2.2 developed especially for burn-up calculation.

The comparisons between calculation and experiments have shown that in this way the simulation of radionuclides released by nuclear explosions is possible.

Kurzfassung

Der Hintergrund für das vorliegende Thema ist das internationale Kernwaffenteststoppabkommen (CTBT), welches am 10. September 1996 von der UN-Generalversammlung angenommen wurde. Dieser Vertrag tritt in Kraft, sobald er von den im Anhang II genannten Staaten ratifiziert wurde.

Messsysteme, die speziell Radionuklide messen, wurden installiert, da die Einhaltung des Vertrages nur über diese verifiziert werden kann. Jedes Erdbeben und jede Minenexplosion kann mittels Seismik, Infraschall und Hydroakustik innerhalb des Messnetzes nachgewiesen werden, eine Radionuklid-Station jedoch kann eine Kernwaffenexplosion bestätigen.

Radioaktive Elemente entstehen bei einer Kernwaffenexplosion in der Form von sowohl festen Partikeln als auch Edelgasen und können auf diese Art nachgewiesen werden.

Das Ziel der vorliegenden Arbeit war die Entwicklung eines Messsystems für das nochmalige Messen von Archivproben, die Edelgas enthalten. Auch die Herstellung der relevanten Xenonisotope war ein Teil dieser Arbeit, um das bestehende radiometrische System zu testen und zu kalibrieren. Letzendlich konnte die relevante Zusammensetzung der Xenonisotope hergestellt werden, die den freigesetzten Isotopen einer Kernwaffenexplosion entspricht.

Dazu wurde mit einem Gaschromatographen ein Verfahren entwickelt, mit dessen Hilfe die Menge des stabilen Xenon in der Probe bestimmt werden kann. Kontaminationen wie Radon oder Krypton, die in

der Probe enthalten sein können, werden durch dieses Verfahren von Xenon sicher abgetrennt. Damit ist gewährleistet, dass in der nachfolgenden radiometrischen Messung nur Xenon gemessen wird.

Es wurde ein Transfersystem für den Proben transfer von der Archivflasche zum Gaschromatographen entwickelt und optimiert. Zu Beginn der Arbeit betrug der Transferverlust etwa 30% und konnte soweit verbessert werden, dass er am Ende dieser Arbeit im Bereich von 2% lag.

Die Isotopenherstellung wurde geplant und die Durchführung erfolgte durch Bestrahlung von 90% angereichertem U-235 im TRIGA Mark II Reaktor in Wien, am Atominstitut der Österreichischen Universitäten. Es wurden theoretische Berechnungen durchgeführt und deren Ergebnisse mit dem für Abbrandberechnungen von Brennelementen speziell entwickelten Programm ORIGEN 2.2 verifiziert.

Der Vergleich zwischen den Berechnungen und den durchgeführten Experimenten hat gezeigt, dass auf diese Art und Weise eine Simulation der Isotopenzusammensetzung eines durchgeführten Kernwaffentests möglich ist.

1 Index of contents

1 INDEX OF CONTENTS	8
LIST OF FIGURES	11
LIST OF TABLES	12
2 INTRODUCTION.....	15
2.1 NUCLEAR TESTS	15
2.2 DEVELOPMENT OF THE COMPREHENSIVE NUCLEAR TEST BAN TREATY - CTBT.....	18
2.3 VERIFICATION PROCEDURES.....	20
2.4 THE ROLE OF LABORATORIES	22
3 SCOPE OF WORK	24
4 SOURCE TERM.....	26
4.1 GENERAL	26
4.2 POSSIBLE SOURCES OF AIRBORNE XENON ISOTOPES.....	27
4.2.1 Reprocessing plants	27
4.2.2 Nuclear Power Plants.....	28
4.2.3 Nuclear Weapons.....	35
4.3 XENON ISOTOPES	41
4.3.1 Xe-131m.....	43
4.3.2 Xe-133.....	44
4.3.3 Xe-133m.....	46
4.3.4 Xe-135.....	47
4.4 WEAPONS TESTING AND REACTOR OPERATION	48

4.4.1	Release from reactor operation	49
4.4.2	Nuclear weapon testing	56
4.4.3	Conclusion	58
5	GAS TRANSFER AND MEASUREMENT	60
5.1	PURPOSE	60
5.1.1	Overview	62
5.1.2	Requirements and Design.....	63
5.1.3	Calibration	68
5.1.4	Validation.....	87
5.1.5	Comparison of the calibration data for the validation	90
5.1.6	Conclusion	92
5.2	GAS TRANSFER.....	93
5.2.1	Design	93
5.2.2	"TRANSFER 1"	97
5.2.3	Testing of the gas transfer system by using the sample loop of the gaschromatograph as cool trap with liquid nitrogen.....	103
5.2.4	Pumping the sample back and forth through the frozen sample loop.....	110
5.2.5	Transfer by adsorption on activated charcoal	114
6	PREPARATION OF RADIOACTIVE XENON ISOTOPES	115
6.1	INTRODUCTION.....	115
6.2	CALCULATIONS.....	116
6.2.2	Description of ORIGEN-2.2	130
6.3	EXPERIMENTAL.....	130
6.4	GAMMA SPECTROSCOPY OF SAMPLES	131

6.4.1 Calibration	131
6.5 RESULTS.....	133
6.5.1 Before separation	133
6.5.2 After separation.....	134
6.5.3 Conclusion	136
7 SUMMARY AND CONCLUSION	137
ANNEX A - DATA REGARDING CHAPTER 5.1.3.4	140
ANNEX B - ORIGEN 2.2 INPUT	144
ANNEX C-DETECTOR SPECIFICATION	145
ANNEX D-CALCULATION OF MDA	147
LITERATURE:.....	148
LEBENS LAUF	153

List of figures

Figure 4-1: Reprocessing plant Sellafield	27
Figure 4-2: Boiling water reactor	31
Figure 4-3: Basic design of a thermonuclear bomb	39
Figure 4-4: Number of reactors in operation, listed by countries	50
Figure 4-5: Relevant isotope ratios after a nuclear detonation.....	58
Figure 4-6: Xe135/Xe133 activity ratio for nuclear detonation and reactor operation	58
Figure 4-7: Xe133m/Xe133 isotope activity ratio nuclear detonation and reactor operation	59
Figure 5-1: Picture of the four possible archive sample geometries	61
Figure 5-2: Trace GC ultra.....	64
Figure 5-3: Design of the TCD	65
Figure 5-4: Design of the gaschromatograph.....	66
Figure 5-5: Inject and Load Position of ten port valve for sample injection...	66
Figure 5-6: Chromatogram belonging to the data of Table 5-4.	70
Figure 5-7: Gas mixture separated at 280°C down to 250°C.....	71
Figure 5-8: Gas mixture Xenon 50% with Silicagel	73
Figure 5-9: Gas mixture Xenon 50% without Silicagel	73
Figure 5-10: Calibration with a temperature ramp of 35°C/min.....	75
Figure 5-11: Overlay of the three chromatograms (26, 27, 28).....	77
Figure 5-12: Overlay of chromatograms of the gas mixtures 1-3.....	78
Figure 5-13: Calibration with a constant temperature program	79
Figure 5-14: Calibration with all mixtures, February 16th, 2005.....	80
Figure 5-15: Calibration with all gas mixtures,	81
Figure 5-16: Calibration with all gas mixtures on February 22 nd , 2005.....	82
Figure 5-17: Calibration on February 23 rd , 2005	83
Figure 5-18: Calibration with all gas mixtures on February 24 th , 2005.....	83
Figure 5-19: Calibration with all gas mixtures on February 25 th , 2005.....	84
Figure 5-20: Calibration with all gas mixtures on February 28 th , 2005.....	85
Figure 5-21: Stability of the calibration for one week	86
Figure 5-22: Increasing of carrier gas pressure from 4 to 5 bars	87
Figure 5-23: Calibration curve March 2005	89
Figure 5-24: Graphic illustration of the comparison of calibration of March. 90	
Figure 5-25: Graphic illustration of the comparison of February calibration 91	
Figure 5-26: Diagram of the connections for the first gas transfer.....	94
Figure 5-27: Diagram of the connection for the following gas transfers (graphic designed by DI Thales Schröttner)	97
Figure 5-28: Control panel for the calibration of the gaschromatograph	98
Figure 5-29: Graphic design of the calibration.....	100
Figure 5-30: Diagram of the connections for gas transfer experiments	108
Figure 6-1: Reactor core TRIGA-Mark II Research reactor	115
Figure 6-2: Decay scheme for the relevant isobaric chain 131	116
Figure 6-3: Decay scheme for the relevant isobaric chain 133	121

Figure 6-4: Decay scheme for the relevant isobaric chain 135	126
Figure 6-5: Detector ATL03_003	132
Figure 6-6: Spectrum of a sample irradiated for a short time.....	133
Figure 6-7: Spectrum after separation.....	135

List of tables

Table 4-1: Interesting Xenon isotopes and their half lives	26
Table 4-2: Known Xenon isotopes plus meta-stable states	42
Table 4-3: Energies emitted by Xe 131m.....	43
Table 4-4: Energies emitted by Xe-133	45
Table 4-5: Energies emitted by Xe-133m.....	46
Table 4-6: Energies emitted by Xe-135	48
Table 4-7: Reactor types in operation with generated capacity	49
Table 4-8: Release of Xenon from PWRs 1979	51
Table 4-9: Release of Xenon from PWRs 1988.....	53
Table 4-10: Release of Xenon from BWRs 1979.....	55
Table 4-11: Release of Xenon from BWRs 1988.....	56
Table 4-12: Calculated isotope ratios.....	57
Table 4-13: Comparison isotope activity ratios for reactor operation and nuclear detonation	59
Table 5-1: Archiving parameters of Xenon samples	61
Table 5-2: Summary of used gas mixtures	68
Table 5-3: Oven and TCD parameters for the first tests after installation	69
Table 5-4: Results of the analysis of the gas mixture after installation	69
Table 5-5: Oven and TCD parameters substantially changed	70
Table 5-6: Results of the measurement of gas mixture 4 at higher temperatures.....	71
Table 5-7: Comparison measurement with and without Silicagel SG, test of the new temperature program	72
Table 5-8: Oven and TCD parameters.....	72
Table 5-9: System parameters for the calibration with a temperature ramp of 35°C/min.....	74
Table 5-10: Results for the gas mixture 1	75
Table 5-11: Results for the gas mixture 2.....	75
Table 5-12: Results for the gas mixture 3.....	76
Table 5-13: Mean values and standard deviation for the calibration with a temperature ramp of 35°C/min (Figure 5-10)	76
Table 5-14: System parameters for the calibration with a constant temperature program of 180°C.....	76
Table 5-15: Results for the gas mixture 1	77
Table 5-16: Results for the gas mixture 2.....	77

Table 5-17: Results for the gas mixture 3.....	78
Table 5-18: Data used for the calibration diagram in Figure 5-13.....	79
Table 5-19: System parameters for the calibration with a constant temperature of 190°C.....	80
Table 5-20: Results of the calibration on February 16 th , 2005.....	80
Table 5-21: Calibration data for Figure 5-15.....	81
Table 5-22: Calibration data for Figure 5-16.....	82
Table 5-23: Data for the diagram in Figure 5-17.....	83
Table 5-24: Data for diagram in Figure 5-18.....	84
Table 5-25: Data used for diagram in Figure 5-19.....	84
Table 5-26: Mean values used for Figure 5-20.....	85
Table 5-27: Results of measurements of studying the influence of the carrier gas pressure.....	86
Table 5-28: Results of the calibration on March 1 st , 2005.....	87
Table 5-29: Results of the calibration on March 2 nd , 2005.....	88
Table 5-30: Results of calibration on 3 rd March 2005.....	88
Table 5-31: Results of the calibration on March 7 th , 2005.....	88
Table 5-32: Results of the calibration on March 14 th , 2005.....	88
Table 5-33: Results of the calibration on March 30 th , 2005.....	89
Table 5-34: Parameters for gas transfer.....	95
Table 5-35: Calibration of the gaschromatograph for 35% Xenon.....	95
Table 5-36: Amount of Xenon collected in the gas bag.....	95
Table 5-37: Results of the first transfer experiment.....	96
Table 5-38: Parameters of the gaschromatograph for the gas transfer Xenon proficiency test.....	99
Table 5-39: Measurements and results of the Xenon Exercise November 2004.....	100
Table 5-40: Results of sample injection with varying pressures with a gas mixture containing 10% of Xenon.....	102
Table 5-41: Decreasing of the pressure by carefully raising the flow of the sample and the time needed.....	104
Table 5-42: Results of the measurements for the analysis of the transfer experiment.....	104
Table 5-43: Pressures during pumping.....	111
Table 5-44: Results for the calibration of the gaschromatograph.....	111
Table 5-45: Pressures during pumping.....	112
Table 5-46: Pressures during pumping.....	113
Table 6-1: Independent and cumulative fission yield per 100 fissions of isobaric chain 131 for U-235, thermal fission.....	117
Table 6-2: Half life and decay constant for mass 131.....	117
Table 6-3: Independent and cumulative fission yield per 100 fissions of isobaric chain 133 for U-235, thermal fission.....	121
Table 6-4: Half life and decay constant for mass 133.....	121
Table 6-5: Independent and cumulative fission yield per 100 fissions of isobaric chain 135 for U-235, thermal fission.....	126
Table 6-6: Half life and decay constant for the mass 135.....	126

Table 6-7: KG-236-Nuclide list with activities for 01.01.2002	132
Table 6-8: Measured and calculated isotope ratios	134
Table 6-9: Measured and calculated isotope ratios for MR 14.....	135
Table- 7-1: Results of calibration on February 16 th 2005.....	140
Table - 7-2: Results of calibration on February 17 th 2005.....	140
Table -7-3: Results of calibration on February 22 nd 2005	140
Table -7-4: Results of calibration on February 23 rd 2005	140
Table-7-5: Results of calibration on February 24 th 2005.....	141
Table -7-6: Results of calibration on February 25 th 2005.....	141
Table -7-7: Results of calibration on February 28 th 2005.....	141
Table-7-8: Data used for testing the stability of the calibration for one week	142
Table 7-9: Results of calibration on March 1 st 2005	142
Table -7-10: Results of calibration on March 1 st 2005	142
Table 7-11: Results of calibration on March 3 rd 2005	142
Table 7-12: Results of calibration on March 7 th 2005.....	143
Table 7-13: Results of calibration on March 14 th 2005.....	143
Table 7-14: Results of calibration on March 30 th 2005.....	143
Table 7-15: Results of calibration on March 31 st 2005	143

2 Introduction

2.1 Nuclear tests

Different activities like production of energy by nuclear power plants, production of medical radionuclides or production and testing of nuclear weapons have lead and still lead to the release of radioactive materials into the environment. Due to extensive testing and escalating arms race, public concern was raised on these issues. Since the early 1950's arms control advocates have campaigned for adoption of a treaty banning all nuclear weapons testing. In the following, a short overview of the development of the international Comprehensive Test Ban Treaty (CTBT) is given.

The first nuclear tests were carried out by the United States of America in New Mexico on July 16th 1945 and this was the date when the age of nuclear weapons began. Between this date and December 31st 1953 more than 50 nuclear weapon tests were performed. [www.ctbto.org; http://www.ga.gov.au/oracle/nukexp_form.jsp]



Figure 2-1: "Romeo", March 26th 1954 [picture taken from www.nukeworker.com]

The first nuclear explosive test conducted by the United States of America on July 16th 1945 was named "Trinity" and detonated in Alamogordo/ New Mexico. The Soviet Union performed its first test in the atmosphere four years later on August 29th 1949. So did other countries like United Kingdom in 1952, China in 1964 and India in 1974. [UNSCEAR, 1977]

With the detonation of the first hydrogen bomb "Mike" on November 1st 1952 on the Eniwetok atoll carried out by the United States of America the age of the thermonuclear weapons began. This bomb was 500 times stronger than "Trinity" and the power of explosion was about 10.4 Mt TNT (1 t TNT is equivalent to $4.184 \cdot 10^9$ J, which is again equivalent to 11622,22 kWh).

Other states like the Soviet Union, United Kingdom, China and France as well tested a thermonuclear bomb. [UNSCEAR, 1977]

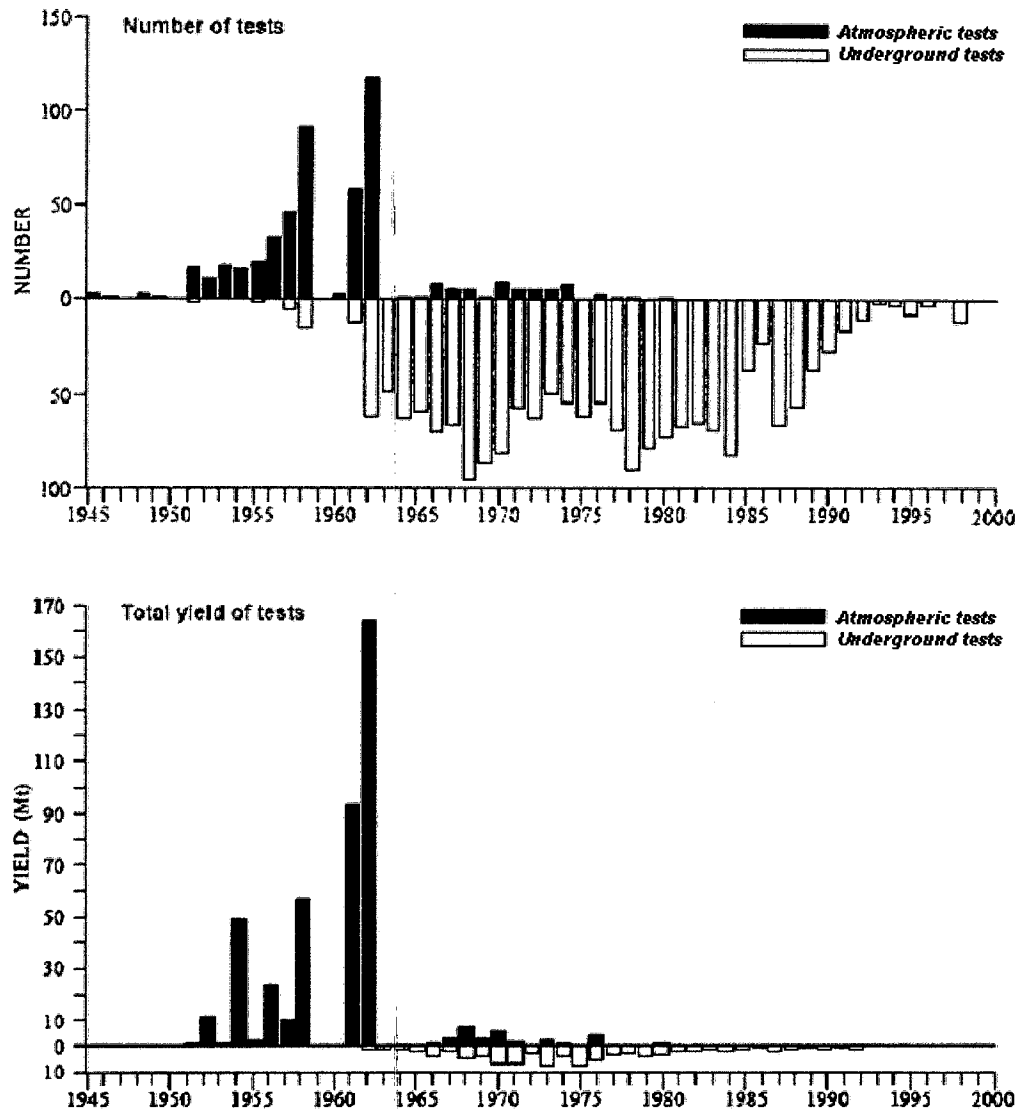


Figure 1. Tests of nuclear weapons in the atmosphere and underground.

Figure 2-2: Number and total yields of tests [UNSCEAR, 2000]

Nuclear testing was performed in the atmosphere, underground and underwater. Since 1945 a total of 2356 nuclear tests, 504 of them in the atmosphere and the other underground (including cratering tests by the USA and USSR), were performed. These numbers do not include the number of safety tests (39 tests), but include the combat use in World War II against Hiroshima and Nagasaki [UNSCEAR, 2000].

The Pugwash Conferences on Science and World Affairs is an international organization that brings together scholars and public figures to work towards reducing the danger of armed conflict and to seek solutions to global security threats. The background of the Pugwash conference is the Russell-Einstein-Manifesto, released in 1955, which called for a conference for scientists to assess the dangers of weapons of mass destruction. [www.pugwash.org; March 2006]

2.2 Development of the comprehensive nuclear test ban treaty - CTBT

In 1954 the general cessation of nuclear tests was proposed by Prime Minister Nehru of India [CTBTO, 2004]. At this time in the context of the cold war, there was great scepticism in the capability to verify compliance with a comprehensive nuclear-test-ban treaty.

However, in 1963, with the signing of the Partial Test Ban Treaty the first step was reached [PTBT, 1963]. This treaty banned nuclear tests in the atmosphere, underwater and in space. This agreement was neither signed by France nor by China, but it was signed by the Soviet Union, United Kingdom and the USA.

In 1968 the Nuclear Non-proliferation Treaty was signed with the objective of nuclear disarmament [NPT, 1968]. This treaty includes that non-nuclear weapon states were prohibited from, inter alia, possessing, manufacturing or acquiring nuclear weapons or other nuclear explosive devices.

The latest nuclear weapon tests were carried out in 1990 by the Soviet Union, 1991 by United Kingdom, 1992 by the USA and 1996 by France.

Negotiations for a comprehensive test ban treaty began in 1993. In 1996 France and China performed their last nuclear tests and intensive efforts were made over the next three years to draft the Treaty text and its two annexes, culminating in the adoption of the Comprehensive Nuclear-Test-Ban Treaty (CTBT) on 10th September 1996 by the United Nations General Assembly in New York [CTBT, 1996].

The CTBT, which prohibits all nuclear test explosions in all environments, was opened for signature in New York on 24 September 1996, when it was signed by 71 States, including the five nuclear-weapons States.

The most important facts of the treaty are given in article 1:

"BASIC OBLIGATIONS

1. Each State Party undertakes not to carry out any nuclear weapon test explosion or any other nuclear explosion, and to prohibit and prevent any such nuclear explosion at any place under its jurisdiction or control.

2. Each State Party undertakes, furthermore, to refrain from causing, encouraging, or in any way participating in the carrying out of any nuclear weapon test explosion or any other nuclear explosion." [CTBT, 1996]

This treaty is a very important part of the advancement of nuclear disarmament.

The Treaty will enter into force after ratification by the 44 States listed in its Annex 2. These 44 States formally participated in the 1996 session of the Conference on Disarmament, and possess nuclear power or research reactors.

2.3 Verification procedures

The verification of the compliance of the treaty is monitored by an International Monitoring System (IMS), which consists of 337 institutions (this number includes stations and laboratories). These institutions collect data worldwide and transmit them in real time to the International Data Centre (IDC) of the Comprehensive Test Ban Treaty Organisation (CTBTO). At present the CTBTO consists of a Preparatory Commission and a Provisional Technical Secretariat (PTS), which will be given up as soon as the treaty comes into force and then the CTBTO will consist of the Technical Secretariat, the Executive Council and The Conference of the States Parties. Presently the Preparatory Commission has the status of an international organisation and prepares the coming into force of the treaty. This commission monitors and coordinates the development of the International Monitoring System and the International Data Centre. The Provisional Technical Secretariat assists the Commission and carries out functions determined by the Commission, including the verification activities listed in the treaty. It receives, processes, analyses and reports on IMS data. The IMS consists of 170 seismic, 60 infrasound and 11 hydro acoustic monitoring stations, which register the seismic and acoustic waves generated in case of a nuclear detonation [Wotawa et al., 2003].

A total of 80 monitoring systems for radionuclides (40 of them will be noble gas stations), which are supported by 16 laboratories, analyze the air for artificial radioactive elements [Schulze et al.; 2000].

Preparatory Commission for the Comprehensive Nuclear-Test-Ban Treaty (CTBT)
Facilities of the CTBT International Monitoring System

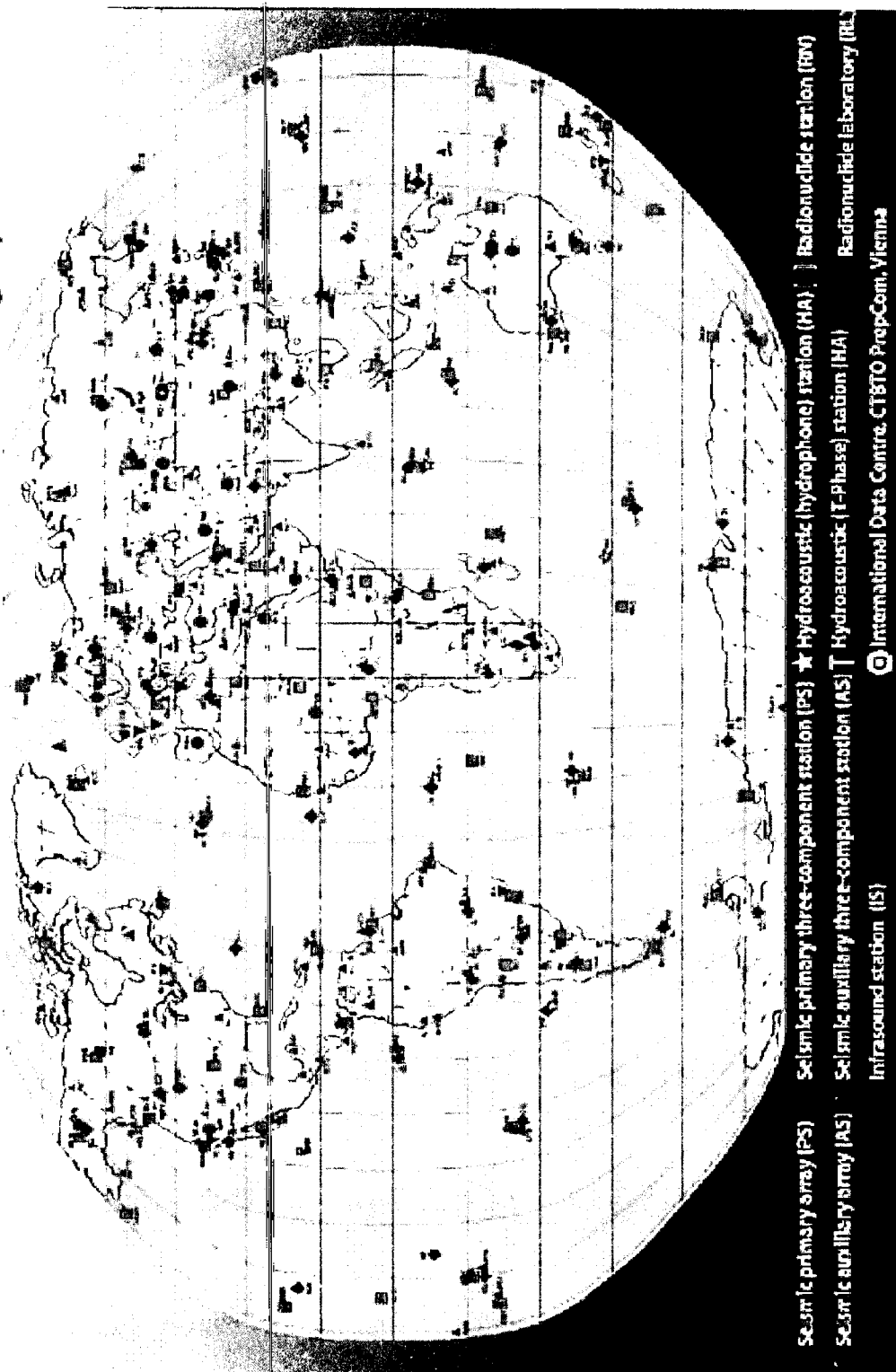


Figure 2-3: Map for the installation of measurement stations worldwide [picture taken from: www.ctbto.org]

Radionuclide systems have to be installed since the compliance with the comprehensive nuclear-test-ban treaty can only be verified by radionuclides. Every earthquake or explosion in mines may be detected by the other (seismic, infrasound and hydroacoustic) systems, but only the radionuclide station can affirm whether a nuclear detonation has happened.

During a nuclear explosion a long number of radioactive elements is formed including solids and noble gases. The detection regards specifically such nuclides, which can be found in the dust collected with specific aerosol filters. They are identified by gamma-spectroscopy of their decay radiation, regarding as well the noble gas xenon, especially xenon - 133, which is the last instable state in a decay chain which consists of very short living nuclides. These nuclides are generated during fission from uranium- or plutonium nuclides.

2.4 The role of laboratories

For checking the measurement results from radionuclide stations the air filter samples are sent to certified laboratories for "re-measurement".

The Radionuclide Laboratory ATL03 in the Austrian Research Centers Seibersdorf is the first certified laboratory worldwide for reference measurements in order to support the IMS (International Monitoring System) for verification of the Comprehensive Nuclear Test Ban Treaty (CTBT). Therefore air filter samples from different IMS-stations are re-measured gammaspectrometrically with an ultra low-level HPGe-system.

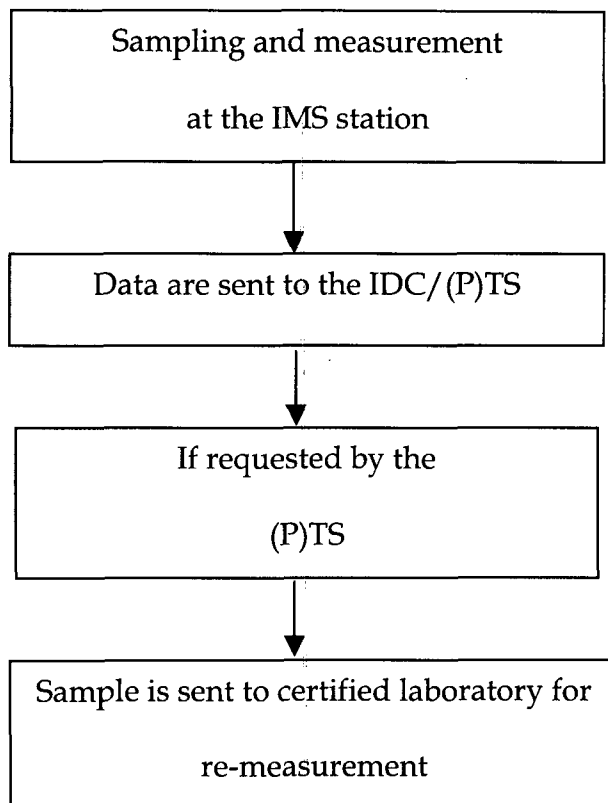


Figure 2-4: Path of the role of a laboratory for CTBT

3 Scope of work

The scope of this work was the development of a re-measurement system for noble gases and the production of relevant xenon isotopes for testing and calibration of the radiometric system and finally for simulation of nuclear weapons testing.

For this purpose a gaschromatographical method was developed by which the amount of stable xenon can be determined and contaminations, eventually present in the sample, can be eliminated in order to ensure that only xenon is measured in the following radiometric measurements.

This system was tested, calibrated with different parameters and optimized. The stability of this system was checked for a few months for validation.

A transfer line from an archive bottle to the gaschromatograph was built and had to be optimized. The design for such a transfer line was developed. First tests were performed by just freezing the sample out in the sample loop of the gaschromatograph, then it was tested to pump the sample back and forth in order to "collect" the xenon in the cool trap and finally activated charcoal was used because it gave the best transfer results. The system developed will be discussed in this work up to this point; however, further improvements will still have to be worked out in order to optimize the performance.

Since xenon isotopes were needed for the calibration of the radiometric system, a plan for isotope production was elaborated and 90% enriched uranium was irradiated in the TRIGA Mark II reactor at the Atomic Institute of the Austrian Universities in Vienna. A theoretical calculation was

done first, and afterwards ORIGEN 2.2, a program developed especially for the burn-up calculation was used for verification. These results were compared to the gamma spectrometric results for the estimation of nuclear weapons testing simulation or of reactor operation simulation. This is needed, since measuring equipment developed for On-Site-Inspections will be tested in the ATL03 laboratory and in Austria the possibility of measuring a xenon background is very low (no power plants).

4 Source Term

4.1 General

The main source of release of xenon in the atmosphere is reactor operation, but to a lesser extent medical and industrial use like reprocessing plants can be sources as well [Bowyer *et al.*, 1998; Bowyer *et al.*, 2002; Perkins and Casey, 1996].

During the detonation of a nuclear bomb four xenon isotopes with half-lives long enough for a determination are formed in an amount sufficient for detection even seven days after the event. These isotopes are listed in Table 4-1; they are generated by nuclear fission both directly and by decay of the respective radionuclides of iodine [Schulze *et al.*, 2000; Weiss *et al.*, 1997].

Isotope	T _{1/2}
Xe-135	9.1 h
Xe-133m	2.2 d
Xe-133	5.2 d
Xe-131m	11.8 d

Table 4-1: Interesting xenon isotopes and their half lives

These xenon isotopes are significant for verifying the Comprehensive Nuclear Test Ban Treaty, because noble gases will always leak from underground (clandestine tests) to the atmosphere in contrast to particles [Schulze *et al.*, 2000; Bowyer *et al.*, 2002].

4.2 Possible sources of airborne xenon isotopes

4.2.1 Reprocessing plants

Reprocessing plants are used for chemical reprocessing of spent fuel. This is a chemical process by separation of radioactive waste and reusable fissionable material like uranium and plutonium. Spent fuel consists of about 95% U-238, but about 1% non-fissioned U-235, too, and additionally about 1% plutonium together with other transuranium elements and 3% highly radioactive fission products. In reprocessing plants this material is separated in three categories: uranium, plutonium and waste, containing fission products. [<http://www.world-nuclear.org>; 2005]

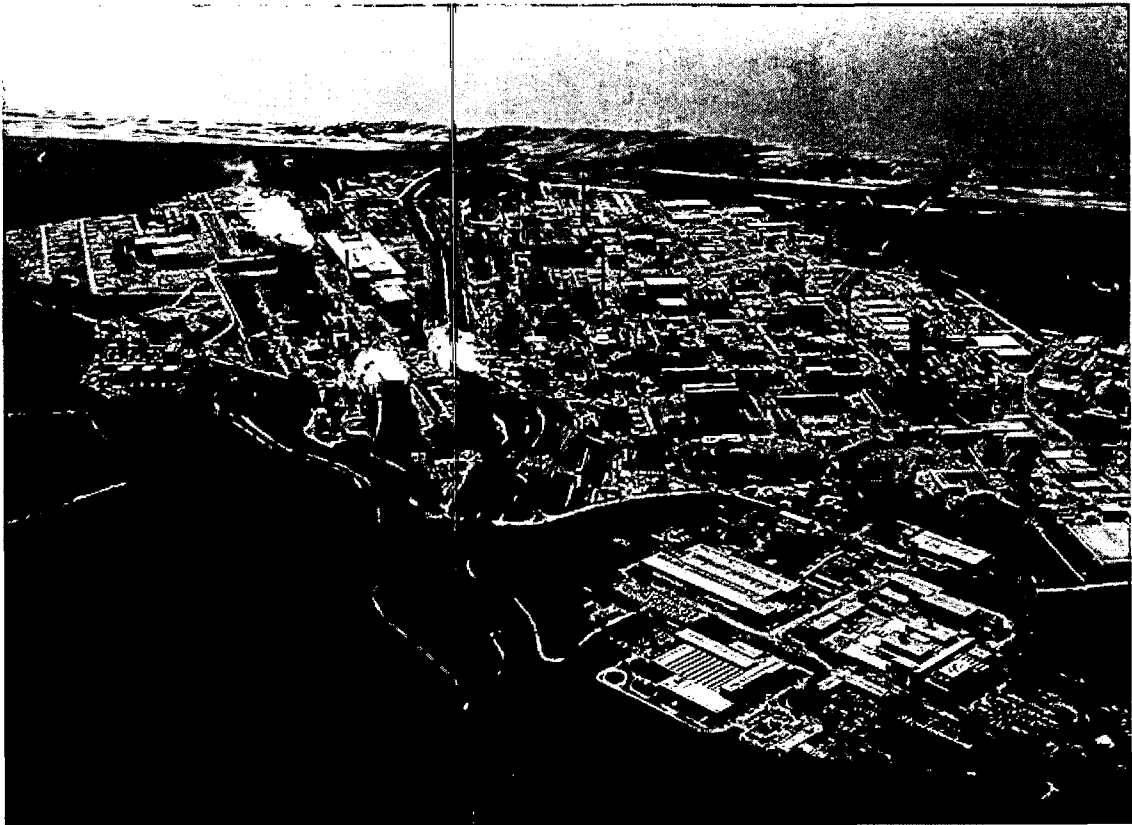


Figure 4-1: Reprocessing plant Sellafield [picture taken from <http://www.visitcumbria.com/wc/svc.htm>; 2005]

4.2.2 Nuclear Power Plants

In nuclear power plants the power is generated by controlled nuclear fission reactions. These reactions occur when sufficient quantities of e.g. uranium-235 mixed with a neutron moderator like e.g. graphite are concentrated in a small space. Introducing rods made of a material that absorbs the neutrons (like e.g. cadmium or boron) and therefore controls the rate of fission. By fission heat is produced; with a steam turbine this heat is converted into kinetic energy, and then electricity is produced with a generator.

Components common for most types of reactors:

FUEL – usually pellets of uranium oxide (UO_2) arranged in tubes to form fuel rods. The rods are arranged into the fuel assemblies in the reactor core.

MODERATOR – this is material, which slows down the neutrons released from the fission so that they cause more fissions. Usually it is water, but may be as well heavy water or graphite.

CONTROL RODS – these are made from neutron-absorbing material like cadmium, hafnium or boron and are inserted or withdrawn from the core to control the rate of reaction, or to halt it.

COOLANT – water circulating through the core to transfer the heat from it. In light water reactors the moderator acts as coolant as well.

PRESSURE VESSEL OR PRESSURE TUBES – usually a robust steel vessel containing the reactor core and moderator/coolant, but it may be a series of tubes holding the fuel and conveying the coolant through the moderator.

STEAM GENERATOR – part of the cooling system where the heat from the reactor is used to produce steam for running the turbine.

CONTAINMENT – the structure around the reactor core which is intended as protective shield against outside intrusion, and to protect those outside from the effects of radiation in case of any malfunction inside. Typically it is a metre-thick concrete and steel structure. [*Nuclear Power Reactors: <http://www.uic.com.au/nip64.htm>*]

There are a number of various reactor designs in use: Boiling Water Reactors (BWR), Pressurized Water Reactors (PWR), Gas Cooled Reactors (GCR), Pressurized Heavy Water Reactors (PHWR), Graphite and Water Reactors, Light Water Reactors, Cooled Heavy Water Reactors, Fast Breeders, Light Water Breeders, Boiling Heavy Water Reactors and others. All the various configurations and moderator/coolant combinations operate on the basic principle of heat produced by nuclear chain reaction being used to drive a turbine and thus generate power.

During the operation of a nuclear reactor radioactive fission- and activation products are produced. In great part these radioactive materials are retained within the fuel elements. Most radionuclides, which diffuse into or are formed within the coolant, are removed by the gaseous and liquid waste processing systems. Low-level releases, which occur during normal operation, are controlled and monitored closely. The type and the quantity of radioactive material released from reactors depend on the type of the reactor, and on the specific waste processing system used. Radionuclides come to the environment either through the gaseous or through the liquid effluent streams. In the airborne effluents fission noble gases (krypton and xenon isotopes), activation gases (^{41}Ar , ^{14}C , ^{16}N , and ^{35}S), tritium, radioactive halogens, and particulates are found. In the liquid effluents tritium, fission products, and activated corrosion products are found [UNSCEAR; 1971].

Most commonly used reactor types worldwide are the Pressurized Water Reactor (PWR), and the Boiling Water Reactor (BWR). The release of noble gases from these reactors will be discussed in chapter 4.4.1. All reactor types worldwide in use are listed in Table 4-7.

4.2.2.1 Boiling Water Reactor (BWR)

There are two types of the BWR: dual cycle and single cycle. In the dual cycle BWR there are two loops one of which delivers water to the reactor core to cool it, and the second, which delivers steam to the turbine. There are more BWR single cycle in use than dual cycle.

A steam separator on the top of the reactor vessel directs the steam to the turbines, and the water is recirculated through the core by the pumps. The water serves both as coolant and as moderator.

The dual cycle system also produces steam in the core, but rather than being channelled to the turbines it goes to a steam generator where its heat is used for the production of steam in the secondary loop which is then used to run the turbines.

The single cycle type is preferred since the thermal efficiency is better due to the direct formation of steam at the maximum cycle temperature. Besides it allows a lower capital investment for piping, heat exchangers, pumps and so on. Additionally it has - compared to the other type - lower operating costs.

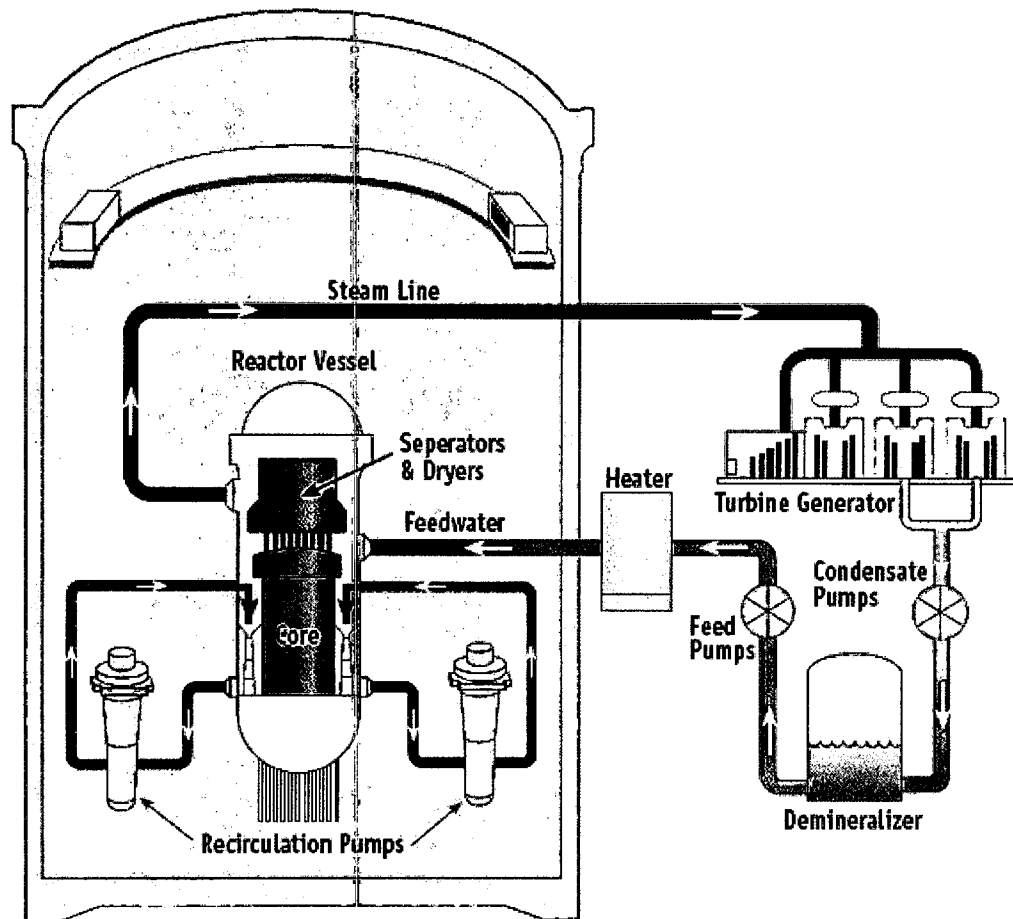


Figure 4-2: BWR (picture taken from <http://www.eia.doe.gov>; 2005)

The property of this type is that any fuel leak can contaminate the water, and radioactivity can reach the turbine and the rest of the loop.

The release of noble gases occurs due to the transport of in water solved gases and volatile substances via the turbine to the condensers. Therefrom they are released to atmosphere with the air of the reactor building by the chimney. For noble gas release of this type see chapter 4.4.1.2.

4.2.2.2 Pressurized Water Reactor (PWR)

This is the most common type, with over 230 in use for power generation and further several hundred in naval propulsion. The design originated as a submarine power plant. It uses ordinary water as both coolant and moderator. The design is distinguished by having a primary cooling circuit, which flows through the core of the reactor under very high pressure, and a secondary circuit in which steam is generated to drive the turbine.

A PWR has fuel assemblies consisting of 200-300 rods each, arranged vertically in the core, and a large reactor may have about 150-250 fuel assemblies with 80-100 tons of uranium.

The water in the reactor core reaches about 325°C, hence it must be kept under pressure to prevent it from boiling. Pressure is maintained by steam in a pressurizer (see Figure 4-3). In the primary cooling circuit the water is also the moderator, and if any of it is turned to steam the fission reaction slows down. This negative feedback effect is one of the safety features of the type. The secondary shutdown system involves adding boron to the primary circuit.

The secondary circuit is under lower pressure and the water here boils in the heat exchangers, which are thus steam generators. The steam drives the turbine to produce electricity, and is then condensed and returned to the heat exchangers in contact with the primary circuit. [<http://www.world-nuclear.org>; 2005]

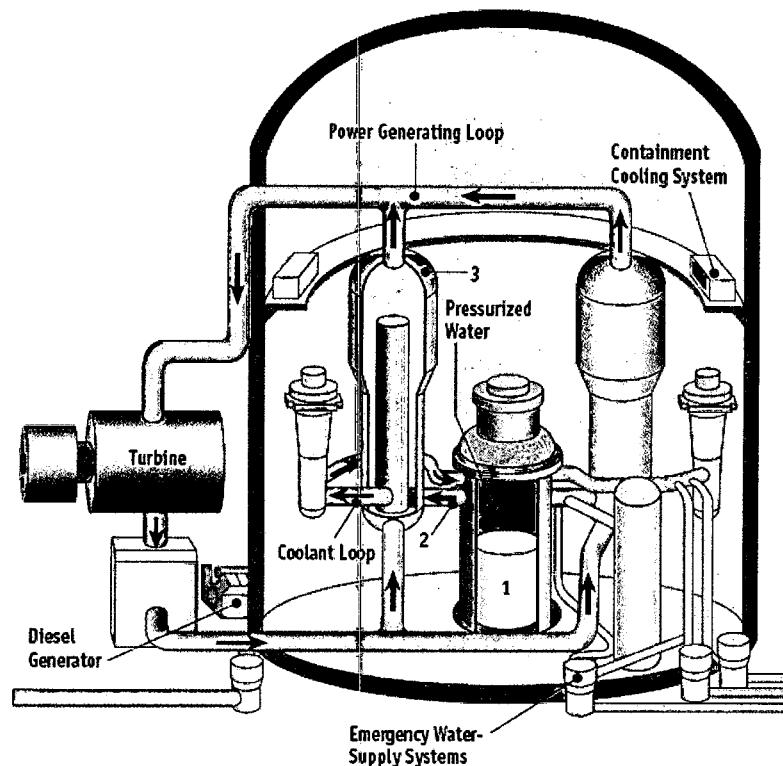


Figure 4-3: PWR (picture taken from <http://www.eia.doe.gov>; 2005)

Number labeling:

- 1.) The reactor core generates heat
- 2.) Pressurized-water in the primary coolant loop carries the heat to the steam generator
- 3.) Inside the steam generator heat from the primary coolant loop vaporizes the water in a secondary loop producing steam

The advantage of this reactor type is that it can operate at higher temperature and pressures, which provides a higher Carnot efficiency than for the BWR. Construction of these types is more expensive and more complicated.

For the release of noble gases of this reactor type see chapter 4.4.1.1

4.2.2.3 Reactor accidents

- Windscale (today Sellafield)

The fire started during the annealing procedure of the graphite structure. During normal operation, neutrons striking the graphite result in distortion of the crystal structure of the graphite, which again results in a build-up of stored energy in the graphite. This controlled heating annealing process was used to restore the graphite structure and release the stored energy. Unfortunately in this case, excessive energy was released resulting in fuel damage. The metallic uranium fuel and the graphite then reacted with air and started burning.

It was estimated that 100% of the xenon core inventory, 10% of the iodine, 10% of the tellurium and 0.1% of the antimony core inventory were released. [Finkelstein; 2001]

- Three Miles Island

This accident happened when Unit 2 of the pressurized water reactors was operating at full power. A series of events resulted in a substantial loss of primary coolant and more than 100 tons of fuel rods were subjected to varying degrees of oxidation, fragmentation and melting.

Noble gas release was estimated to be about 8-10% of the noble gas core inventory at the time of accident and during the first three days about 90%. [Finkelstein; 2001]

- Chernobyl

The reactor type was a graphite moderated boiling water reactor (RBMK, which means a high power reactor with channels) [Botsch, 2000]. It happened to come to a sudden and uncontrollable power surge. The fuel elements ruptured, and the resultant explosive force of steam lifted off the cover plate of the reactor, releasing fission products to the atmosphere. The release of noble gases was estimated to be > 90% [Finkelstein; 2001].

4.2.3 Nuclear Weapons

A nuclear weapon is a weapon where the destructive power of which is derived from nuclear fission and/or fusion. This destructive power of a nuclear weapon even with a small yield is by far higher than that of the largest conventional explosives.

Nowadays nuclear weapons are used primarily as a means of strategic threat (North Korea, Iran).

The first atomic bombs tested on July 16th 1945 (test name: Trinity), and used against Japan on August 6th 1945 (Little Boy, over Hiroshima) and on August 9th 1945 (Fat Man, over Nagasaki) were pure fission weapons containing U-235 and Pu-239 respectively. Little Boy had a force equal to 13.000 t TNT equivalent and was the first nuclear weapon used in warfare. Fat man was the second weapon used in warfare and had a force equal to 20.000 t TNT equivalent. It was a powerful plutonium implosion weapon. [www.atomicmuseum.org]

4.2.3.1 *Types of nuclear weapons*

Basically there are two principles for the function of atomic bombs: Bombs built according to the nuclear fission - principle („classic“ atomic bombs), or according to the principle of nuclear fusion (Hydrogen- or H-bombs). The simplest nuclear weapons derive their energy from nuclear fission.

In case of the “classic” atomic bomb a mass of fissile material is rapidly assembled into a critical mass, in which a chain reaction starts and grows exponentially, releasing tremendous amounts of energy.

A mass of fissile material is called critical when it is capable to sustain a chain reaction. This capability depends upon the size, geometry and purity of the material as well as upon the reflector. The neutron multiplication factor k is a numerical measure for the criticality of a mass:

$$k = f - l$$

where f is the average number of neutrons released per fission event and l is the average number of neutrons lost by either leaving the system or being captured in a non-fission event.

When

$k = 1$: critical mass,

$k < 1$: subcritical mass, and

$k > 1$: supercritical mass.

A fission bomb works by rapidly changing a subcritical mass of fissile material into a supercritical assembly, causing a chain reaction which rapidly releases large amounts of energy.

This reaction is accomplished by rapidly creating supercriticality, either by shooting one piece of subcritical material into another, or compressing a subcritical mass. A major challenge in all nuclear weapon designs is ensuring that a significant fraction of the fuel is consumed before the weapon destroys itself.

In case of a fission bomb a super-critical quantity (how much this is depends on the geometry and on the construction of the bomb – the smallest critical mass is achieved with one globe) of U-235 or Pu-239 is compressed by explosive material to a small volume. From a certain relation of mass and surface of the nuclear material on, neutrons formed in occasion of the spontaneous decomposition of single nuclei can split other nuclei in the material which again supply some neutrons. A nuclear chain reaction occurs in the course of which more and more nuclei are split.

With the more advanced nuclear weapons, the fusion bombs, first a fission bomb is ignited, the energy of which is used to trigger nuclear fusion, releasing even more energy. In such a weapon, the x-ray thermal radiation from a nuclear fission explosion is used to heat and compress a capsule of tritium, deuterium, or lithium, in which fusion takes place. These weapons, colloquially known as hydrogen bombs or more formally as thermonuclear bombs, can be many hundreds of times more powerful than fission weapons. The so-called “Teller-Ulam-design” is intended for application in the construction of thermonuclear weapons in the megaton - range.

4.2.3.2 Fission bomb

A classical nuclear fission bomb (atomic bomb) is constructed in such a way that at the intended moment parts of the nuclear material are united so that together they exceed the critical mass, but every single part alone is below the critical mass. As soon as the critical mass is achieved the neutron source starts to emit neutrons, which then initiate a chain reaction in the

nuclear material. The number of neutrons newly formed by nuclear fission is larger in every fission generation than the number of neutrons escaped from the material and the number absorbed in the material without fission. An often used neutron source is the combination polonium/beryllium, which has to mix at the right moment. In case of polonium/beryllium – sources alpha-particles which are emitted by the plutonium, react with beryllium.

4.2.3.3 Fusion bomb

In case of the fusion bomb a fission bomb is used for initiating the chain reaction. The tamper is moved inwards by the detonation of the explosives and together with the beryllium reflector (intended for stopping neutrons from escaping and for multiplying neutrons by $(n, 2n)$ -reactions) inside hits the plutonium pit. Within a time of much less than one second radiation is emitted from the plutonium pit which has become a critical mass by the contact with the tamper. With initiating neutrons produced by a neutron source the plutonium pit is as well the place where the chain reactions start. The next step is a nuclear implosion by which the tritium/deuterium mixture, injected into the centre is compressed to such an extent that fusion reactions take place and high energy neutrons are formed which initiate new fission chains in the plutonium. After this the plutonium falls apart. The fission energy is at least doubled by this process. The boosting process supplies energy, which is not very large in comparison to the boosted fission energy. In total, the plutonium fission induced by high-energy neutrons is not an important part of the total fission process.

An intense stream of x-rays leaves the primary once it is heated to a temperature of many millions of degrees. This stream travels down the chamber where geometry and materials are designed to guide photons onto the heavy pusher around the fusion fuel. High levels of energy are absorbed in the outer layers of the pusher, resulting in material being build off and a strong inward momentum being generated. An extremely large force builds

up, squeezing the fusion fuel to super density. The central string of fissile material, the spark plug, if present, is highly compressed and becomes supercritical and fission begins. This process increases the density and temperature further, thus improving the conditions for thermonuclear burning. The fission neutrons contribute to tritium production through reactions with lithium in the thermonuclear fuel. It is essential that the fusion fuel is highly compressed, to avoid it being transparent to the bremsstrahlung produced by the electrons in the plasma, as this would reduce the temperature below what is required for fusion reactions to continue. [Technical report, 1998]

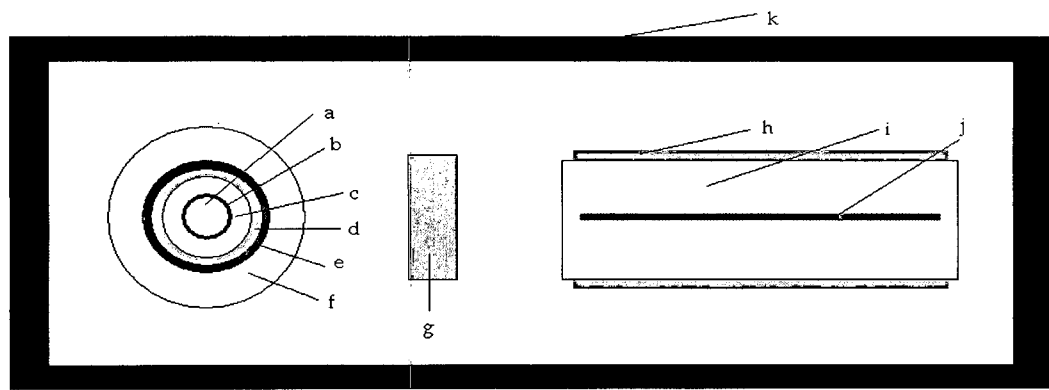


Figure 4-3: Schematic structure of the thermonuclear bomb

a...mixture of Tritium and Deuterium gas, b...plutonium pit, c... gap, d...beryllium reflector, e...Tamper, f...high explosives, g...radiation shield, h...pusher (e.g. depleted U, ^{235}U , Pb or W), i...Lithium Deuterium, j...spark plug (e.g. ^{235}U), k...walls of heavy material

Nuclear weapons which utilize nuclear fusion can have much more increased yields compared to weapons which use only fission, as fusion releases even more energy per reaction than fission, and can also be used as a source for additional neutrons. So is the efficiency for a fission weapon about 20% whereas it is for fusion weapons about 40%. The light weight of the elements used as fusion fuel, combined with the larger energy release means that fusion is a very efficient fuel by weight, making it possible to build extremely high yield weapons which are still portable enough to deliver

easily. Fusion is the combination of two light atoms, usually isotopes of Hydrogen, to form a more stable heavy atom and release excess energy. The fusion reaction requires the atoms involved to have a high thermal energy, which is why the reaction is called thermonuclear. The extreme temperatures and densities necessary for a fusion reaction are easily generated by a fission explosion. A pure fusion weapon is a hypothetical design that does not first need a fission, but no weapons of this sort have ever been developed up to our knowledge.

4.2.3.4 Fission-fusion-fission weapons

The largest modern fission-fusion-fission weapons include a fissionable outer shell of U-238, the more inert waste isotope of uranium, or x-ray mirrors constructed of polished U-238. This otherwise inert U-238 would be detonated by the intense fast neutrons from the fusion stage, increasing the yield of the bomb by many times. For example, in the Castle Bravo test (performed 1954 by the United States on an artificial island in the Bikini atoll), the largest US test ever, of the total of 15 megaton yield, 10 megatons were derived from fission of the natural uranium tamper. For even higher yield, however, moderately enriched uranium can be used as a jacket material.

4.2.3.5 The neutron bomb

Another variant of the thermonuclear weapons is the enhanced radiation weapon, or neutron bomb, which is a small thermonuclear weapon in which the burst of neutrons generated by the fusion reaction is intentionally not absorbed inside the weapon, but allowed to escape, what means that the bomb produces minimal blast and heat, but releases large amounts of lethal radiation. This intense burst of high-energy neutrons is the principal destructive mechanism. High energy neutrons are more penetrating than other types of radiation, and therefore many shielding

materials that work well against gamma rays practically do not work. The term "enhanced radiation" refers only to the burst of ionizing radiation released at the moment of detonation, not to any enhancement of residual radiation in fallout.

4.3 Xenon isotopes

In this chapter the origin and the nuclear data of the interesting relevant xenon isotopes are discussed. For the isobaric chain yield and decay scheme see chapter 6.2.

xenon has 38 isotopes, not including 6 metastable states (see Table 4-2). In total there are 44 entities, 9 are stable and 27 have half-lives below 6 hours, which is the lower limit for CTBT relevance. So eight isotopes fulfilling the half life requirement are left. But four of them are not produced in fission or by activation in a nuclear weapons testing, therefore these isotopes (namely Xe-122, Xe-125, Xe-127 and Xe-129m) are not CTBT relevant, too. [De Geer; 2002]

A	T _{1/2}	Decay mode
110	~ 0,2 s	EC, α
111	(0,74 \pm 0,20) s	EC, α
112	(2,7 \pm 0,8) s	EC, α
113	(2,74 \pm 0,08) s	EC, α , p
114	(10,0 \pm 0,4) s	EC
115	(18 \pm 4) s	EC, p
116	(59 \pm 2) s	EC
117	(61 \pm 2) s	EC, p
118	(3,8 \pm 0,9) min	EC
119	(5,8 \pm 0,3) min	EC
120	(40 \pm 1) min	EC
121	(40,1 \pm 2,0) min	EC
122	(20,1 \pm 0,1) h	EC
123	(2,08 \pm 0,02) h	EC
124	< 1,1 · 10 ¹⁷ years	2 EC

125	$(16,9 \pm 0,2)$ h	EC
125m	$(56,9 \pm 0,9)$ s	IT
126	STABLE	
127	$(36,4 \pm 0,1)$ days	EC
127m	$(69,2 \pm 0,9)$ s	IT
128	STABLE	
129	STABLE	
A	$T_{1/2}$	Decay mode
129m	$(8,88 \pm 0,02)$ days	IT
130	STABLE	
131	STABLE	
131m	$(11,934 \pm 0,021)$ days	IT
132	STABLE	
133	$(5,243 \pm 0,001)$ days	β^-
133m	$(2,19 \pm 0,01)$ days	IT
134	STABLE	
134m	(290 ± 17) s	IT
135	$(9,14 \pm 0,02)$ hours	β^-
135m	$(15,29 \pm 0,05)$ min	IT, β^-
136	$> 3,6 \cdot 10^{20}$ years	2 β^-
137	$(3,818 \pm 0,013)$ min	β^-
138	$(14,08 \pm 0,08)$ min	β^-
139	$(39,68 \pm 0,14)$ s	β^-
140	$(13,60 \pm 0,10)$ s	β^-
141	$(1,73 \pm 0,01)$ s	β^- , n
142	$(1,22 \pm 0,02)$ s	β^- , n
143	$(0,30 \pm 0,03)$ s	β^-
144	$(1,15 \pm 0,20)$ s	β^-
145	$(0,9 \pm 0,3)$ s	β^- , n
146		β^-
147	< 150 ns	β^- , n

Table 4-2: Known xenon isotopes plus meta-stable states [<http://ie.lbl.gov>; 11.03.2006]

4.3.1 Xe-131m

4.3.1.1 Origin of Xe-131m

This radioisotope is present in irradiated nuclear fuel and enters the atmosphere when it is released from fuel during reprocessing.

In general the time delay between irradiation and reprocessing is long (> 200 days), and the amounts released are not relevant because of the short half-life of 11.87 days. If the nuclear fuels are stored for more than one year, this isotope is not a significant source of atmospheric xenon. It is also a by-product in the production of Xe-133 (see chapter 4.3.2) for medical applications [Perkins and Casey, 1996].

4.3.1.2 Nuclear data of Xe-131m

Half-life: 11.87d

Production mode: Thermal neutron activation

Decay mode: Isomeric transition, branching (%): 100

Gammas from ^{131m}Xe (11.87 d)		
E_γ (keV)	I_γ (%)	Decay mode
163.930	1.91	IT
X-rays emitted by ^{131m}Xe (11.87 d)		
E (keV)	I (%)	Assignment
29.112	0.00159	Xe $K_{\alpha 3}$
29.461	15.6	Xe $K_{\alpha 2}$
29.782	28.8	Xe $K_{\alpha 1}$
33.562	2.65	Xe $K_{\beta 3}$
33.624	5.11	Xe $K_{\beta 1}$
33.881	0.052	Xe $K_{\beta 5}$
34.419	1.55	Xe $K_{\beta 2}$
34.496	0.299	Xe $K_{\beta 4}$

Table 4-3: Energies emitted by Xe 131m

4.3.2 Xe-133

4.3.2.1 Origin of Xe-133

The radionuclide Xe-133 is produced for medical diagnostics - for lung function tests - by neutron irradiation of Xe-gas ($\text{Xe132}(n, \gamma) \rightarrow \text{Xe-133}$), but the main source is reactor operation [Schulze et al., 2000].

Measurements of the activity concentrations of Xe-133 in the Northeast United States (50 operating nuclear power plants) have shown a value between $< 1\text{mBq/m}^3$ and $< 9\text{mBq/m}^3$ [Perkins and Casey, 1996], whereas typical mean values for the activity concentration are between 3 and 10 mBq/m^3 [Schulze et al., 2000].

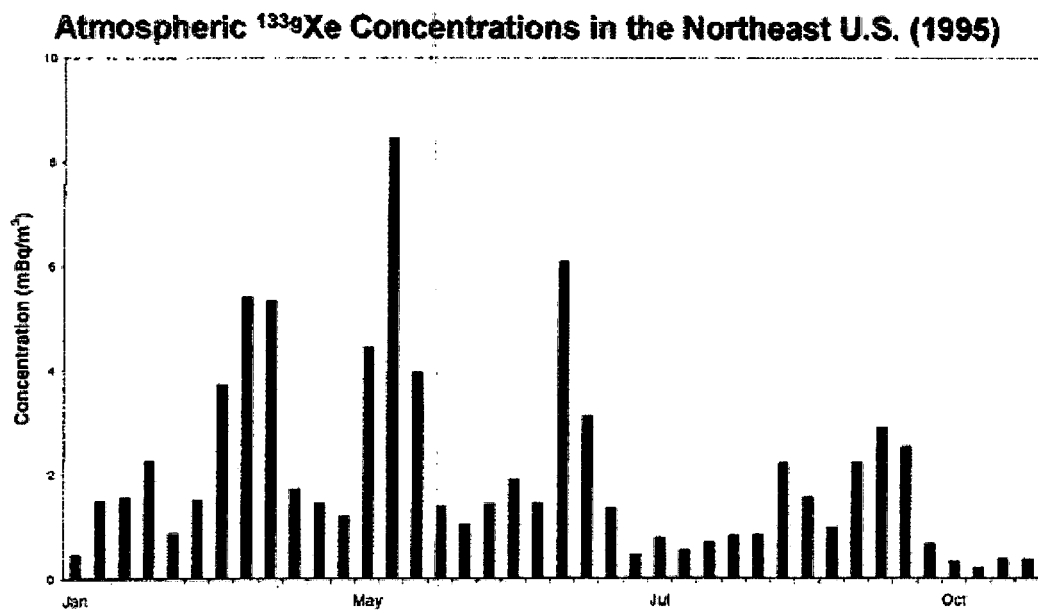


Figure 4-4: Atmospheric Xe-133 concentrations in the Northeast U.S. (1995) [Perkins and Casey, 1996]

This range is in accordance with the activity, which can be measured at a monitoring place after an underground test [Perkins and Casey, 1996].

4.3.2.2 Nuclear data

Half-life: 5,243d

Production mode: Fission product, fast neutron activation, and thermal neutron activation

Decay mode: β^- , branching (%): 100

Gammas from ^{133}Xe (5,243 d)		
E_γ (keV)	I_γ (%)	Decay mode
79.6139	0.27	β^-
80.9971	38.0	β^-
160.613	0.066	β^-
223.234	0.00012	β^-
302.853	0.0048	β^-
383.851	0.0024	β^-
X-rays from ^{133}Xe (5,243 d)		
E (keV)	I (%)	Assignment
30.270	0.00165	Cs $K_{\alpha 3}$
30.625	14.4	Cs $K_{\alpha 2}$
30.973	26.5	Cs $K_{\alpha 1}$
34.920	2.46	Cs $K_{\beta 3}$
34.987	4.76	Cs $K_{\beta 1}$
35.252	0.0505	Cs $K_{\beta 5}$
35.818	1.48	Cs $K_{\beta 2}$
35.907	0.306	Cs $K_{\beta 4}$
Betas from ^{133}Xe (5,243 d)		
E_β endpoint (keV)	I_β (%)	Decay mode
43.55	0.0076	β^-
266.79	0.81	β^-
346.4	99	β^-

Table 4-4: Energies emitted by Xe-133

4.3.3 Xe-133m

4.3.3.1 Origin of Xe-133m

Main source is nuclear weapons testing [Perkins and Casey, 1996].

4.3.3.2 Nuclear data

Half life: 2.19 d

Production mode: Fission product, fast neutron activation, thermal neutron activation

Decay mode: Isomeric transition, branching (%): 100

Gammas from ^{133m}Xe (2,19 d)		
E_γ (keV)	I_γ (%)	Decay mode
233.221	10	IT
X-rays from ^{133m}Xe (2,19 d)		
E (keV)	I (%)	Assignment
29.112	0.00165	Xe $K_{\alpha 3}$
29.461	16.2	Xe $K_{\alpha 2}$
29.782	29.9	Xe $K_{\alpha 1}$
33.562	2.75	Xe $K_{\beta 3}$
33.624	5.30	Xe $K_{\beta 1}$
33.881	0.0539	Xe $K_{\beta 5}$
34.419	1.60	Xe $K_{\beta 2}$
34.496	0.311	Xe $K_{\beta 4}$

Table 4-5: Energies emitted by Xe-133m

4.3.4 Xe-135

4.3.4.1 Origin of Xe-135

Main source is nuclear weapons testing (see chapter 4.4.2) and this is the most important nuclide, since it is more abundant than the other relevant radioxenons during the first days after a detonation has happened. Its ambient background from reactor operation is negligible due to its short half time [Perkins and Casey, 1996].

4.3.4.2 Nuclear data

Half life: 9,14h

Production mode: Fission product, fast neutron activation, thermal neutron activation

Decay mode: β^- , branching (%):100

Gammas from ^{135}Xe (9.14 h)		
E_γ (keV)	I_γ (%)	Decay mode
158.260	0.290	β^-
200.19	0.012	β^-
249.770	90	β^-
358.384	0.221	β^-
373.13	0.015	β^-
408.009	0.359	β^-
454.2	0.0036	β^-
573.36	0.0048	β^-
608.151	2.90	β^-
654.296	0.0451	β^-
731.634	0.055	β^-
812.635	0.0704	β^-
1062.41	0.0041	β^-
X-rays from ^{135}Xe (9.14 h)		
E (keV)	I (%)	Assignment
30.270	1.71E-04	Cs $K_{\alpha 3}$
30.625	1.49	Cs $K_{\alpha 2}$
30.973	2.75	Cs $K_{\alpha 1}$
34.920	0.255	Cs $K_{\beta 3}$
34.987	0.492	Cs $K_{\beta 1}$

35.252	0.00522	Cs K _{β5}
35.818	0.153	Cs K _{β2}
35.907	0.0316	Cs K _{β4}
Betas from ¹³⁵ Xe (9.14 h)		
E _β endpoint (keV)	I _β (%)	Decay mode
88.62	0.123	β ⁻
169.6	0.075	β ⁻
542.85	3.11	β ⁻
742.97	0.59	β ⁻
901.23	96	β ⁻

Table 4-6: Energies emitted by Xe-135

All nuclear data are taken from the web “WWW Table of Radioactive Isotopes” with following URL: <http://ie.lbl.gov/toi/> (01.10.2005)

4.4 Weapons Testing and Reactor Operation

These different ways of origin enables differentiation of the source like reactor operation and nuclear weapons testing. [Weiss et al., 1997]

The main indicator for nuclear explosion is the short lived Xe-135, since its release from reactor operation is negligible. During nuclear explosions also the other radionuclides are released to the atmosphere, but since there is a xenon background, nuclear weapons testing cannot be proved by measuring of only one relevant xenon isotope, but by measuring the isotope activity ratios.

The activity ratios are dependent from the source, and therefore it might be possible to distinguish the origin of release - nuclear explosion or reactor operation [Bowyer et al.; 1996].

4.4.1 Release from reactor operation

In the following the releases from PWR and BWR reactor operation will be discussed, since these types are the main reactor types operating worldwide.

Following table gives an overview about the reactor types in operation and under construction worldwide plus the electrical capacity generated by them per year:

Type	Operational		Under construction	
	No. of Units	Total MW(e)	No. of Units	Total MW(e)
PWR Pressurized Water Reactor	214	205365	2	2466
BWR Boiling Water Reactor	89	78047	1	1067
WWER Water Water Energy Reactor	53	35870	10	9499
PHWR Pressurized Hot Water Reactor	41	20963	7	2645
LWGR Light Water Gas Cooled Reactor	16	11404	1	925
AGR Advanced Gas Cooled Reactor	14	8380	0	0
GCR Gas Cooled Reactor	8	2284	0	0
ABWR Advanced Boiling Water Reactor	4	5259	2	2600
FBR Fast Breeder Reactor	3	1039	1	470
Total	442	368611	24	19672

Table 4-7: Reactor types in operation with generated capacity [data taken from Power Reactor Information System PRIS;2005]

Number of Reactors in Operation Worldwide (as of 31 of October 2005)

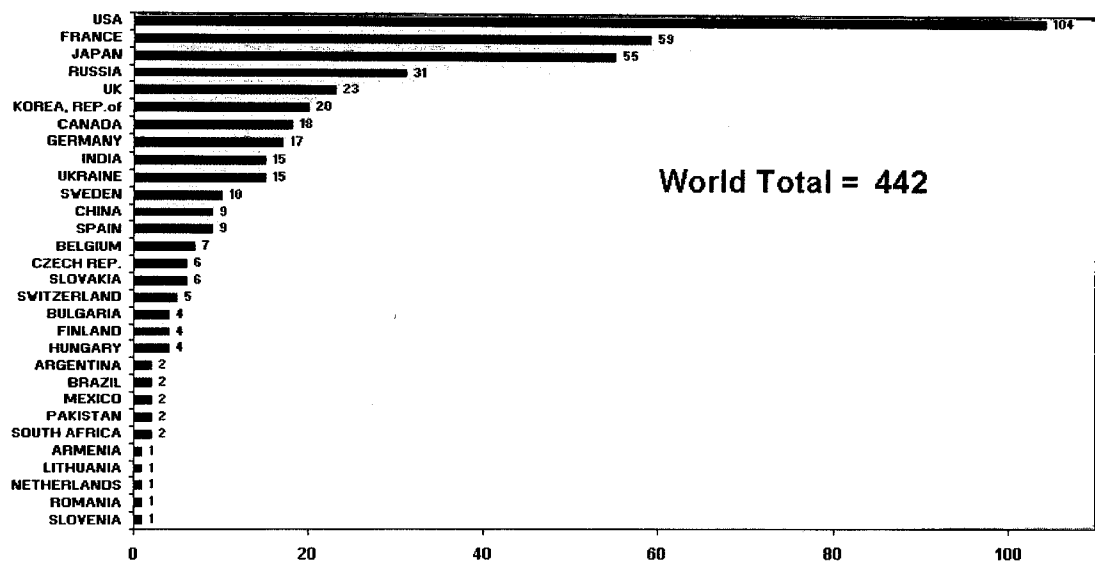


Figure 4-5: Number of reactors in operation, listed by countries [picture taken from Power Reaction Information System PRIS, 2005]

4.4.1.1 Normalized releases of PWR

Releases [TBq/(GW[e]a)] of the relevant xenon isotopes from PWRs reactor types located in the United States in 1979 [UNSCEAR, 1982] and 1988 [UNSCEAR, 1993] are listed in following tables:

1979	Reactor	Startup year	GW(e) a	Release [TBq]				Isotope ratio	
				Xe-131m	Xe-133m	Xe-133	Xe-135	Xe133m/Xe133	Xe135/Xe133
	Arkansas 1	1974	0,397	0,11	2,80	289	24	0,0097	0,0830
	Arkansas 2	1979	0,916	0,001		143	19	0,0000	0,1329
	Beaver Valley	1976	0,221	18	1,6	45	0,027	0,0356	0,0006
	Calvert Cliffs 1, 2	1975/1977	1,161	0,048	0,14	363	13	0,0004	0,0358
	Cook 1, 2	1975/1978	1,373		0,88	70	7,8	0,0126	0,1114
	Crystal River	1977	0,453	36	49	2290	212	0,0214	0,0926
	Davis Besse	1977	0,381	0,019	0,023	3,3	0,24	0,0070	0,0727
	Joseph M. Farley	1978	0,211	3,5	1,4	95	5,1	0,0147	0,0537
	Fort Calhoun	1973	0,44		0,19	25	0,24	0,0076	0,0096

<i>R.E. Ginna</i>	1969	0,355	0,036	0,018	25	1,9	0,0007	0,0760
<i>Haddam Neck</i>	1967	0,493	1,5	0,29	155	1,1	0,0019	0,0071
<i>Indian Point</i>	1973	1,142	3,8	3,6	297	11	0,0121	0,0370
<i>Kewaunee</i>	1974	0,412		0,007	1,1	0,41	0,0064	0,3727
<i>Maine Yankee</i>	1972	0,537	2,4		67	1,4	0,0000	0,0209
<i>Millstone Point</i> 2	1975	0,52			648	0,64	0,0000	0,0010
<i>North Anna</i>	1978	0,507	0,12	0,58	224	7,3	0,0026	0,0326
<i>Oconee 1, 2, 3</i>	1973/1974	1,708	14	27	1646	29	0,0164	0,0176
<i>Palisades</i>	1971	0,415	0,021	0,002	2,4	0,007	0,0008	0,0029
<i>Point Beach 1, 2</i>	1970/1972	0,808		0,11	11,3	12	0,0097	1,0619
<i>Prairie Island 1,</i> 2	1973/1974	0,865		0,068	25	0,71	0,0027	0,0284
<i>Rancho Seco</i>	1974	0,687	0,085	0,92	300	24	0,0031	0,0800
<i>H.B. Robinson</i>	1970	0,482			56	0,87	0,0000	0,0155
<i>Salem</i>	1976	0,25		0,12	8,4	0,56	0,0143	0,0667
<i>St. Lucie</i>	1976	0,592	31	4,9	492	9,4	0,0100	0,0191
<i>San Onofre</i>	1967	0,401	0,1	0,073	19	0,53	0,0038	0,0279
<i>Surry 1, 2</i>	1972/1973	0,343		0,36	63	2,5	0,0057	0,0397
<i>Three Miles</i> <i>Island 1</i>	1974	0,266	0,093	0,26	81	0,95	0,0032	0,0117
<i>Trojan</i>	1975	0,631	0,092	0,28	32	1,4	0,0088	0,0438
<i>Turkey Point</i>	1972/1973	0,811	0,075	0,25	389	1,1	0,0006	0,0028
<i>Yankee Rowe</i>	1960	0,149	0,012	0,069	4,3	0,94	0,0160	0,2186
<i>Zion</i>	1973	1,238	8,8	0,63	1132	118	0,0006	0,1042
<i>Normalized release</i>			6,3	5	469	26	0,0107	0,0554

Table 4-8: Release of xenon from PWRs 1979 [UNSCEAR, 1982]

1988	Release [TBq]				Isotope ratio	
Reactor	Xe-131m	Xe-133m	Xe-133	Xe-135	Xe133m/Xe133	Xe135/Xe133
Arkansas One 1	0,0618	0,0374	42,9	2,96	0,0009	0,0690
Arkansas One 2	1,42	0,0833	66,2	12,2	0,0013	0,1843
Beaver Valley 1-2	0,139	0,00107	0,858	0,125	0,0012	0,1457
Braidwood 1	0,0197	0,00999	1,49	0,0141	0,0067	0,0095
Braidwood 2	0,0327	0,00403	1,35	0,00138	0,0030	0,0010
Byron 1-2	0,249	0,463	64	0,633	0,0072	0,0099
Callaway 1	0,0888	0,0947	20,7	1,38	0,0046	0,0667
Calvert Cliffs 1-2	0,944	1,44	181	13,8	0,0080	0,0762
Catawba 1	0,451	0,574	55,9	0,666	0,0103	0,0119
Catawba 2	0,451	0,574	55,9	0,666	0,0103	0,0119
Crystal River 3	1,59	0,15	121	2,67	0,0012	0,0221
Davis-Besse 1	0,00071	0,00588	3,77	0,0414	0,0016	0,0110
Diablo Canyon 1-2	0,577	0,0339	10,7	0,433	0,0032	0,0405
Donald C. Cook 1-2	0,0299	0,0463	9,07	0,3	0,0051	0,0331
Fort Calhoun	0,633	0,126	27,9	0,0599	0,0045	0,0021
H.B. Robinson 2	0,166	0,244	31	2,23	0,0079	0,0719
Haddam Neck	0,15	0,285	84	2,01	0,0034	0,0239
Harris 1		1,2	71,8	4,18	0,0167	0,0582
Indian Point 1-2		0,0161	7,59	0,418	0,0021	0,0551
Indian Point 3	0,308	0,0747	10,6	0,305	0,0070	0,0288
Joseph M. Farley 1	0,0426	0,0807	6,77	2,23	0,0119	0,3294
Joseph M. Farley 2		0,00703	2,74	0,881	0,0026	0,3215
Kewaunee	0,00005	0,00053	0,238	0,00184	0,0022	0,0077
McGuire 1	0,396	0,903	66,2	2,62	0,0136	0,0396
McGuire 2	0,396	0,903	66,2	2,62	0,0136	0,0396
Millstone 2	0,0907	0,0633	27,1	4,77	0,0023	0,1760
Millstone 3	0,00751	0,0186	2,87	0,221	0,0065	0,0770
North Anna 1-2	0,0722	0,0216	17,5	0,0962	0,0012	0,0055
Oconee 1-3	13,8	6,92	866	6,92	0,0080	0,0080
Palisades	0,0257	0,0264	88,8	0,179	0,0003	0,0020

<i>Palo Verde 1</i>	0,259	0,23	58,1	2,54	0,0040	0,0437
<i>Palo Verde 2</i>	2,04	0,411	104	1,54	0,0040	0,0148
<i>Palo Verde 3</i>	0,00899	0,00411	4,55	0,154	0,0009	0,0338
<i>Point-Beach 1-2</i>		0,0124	2,23	0,131	0,0056	0,0587
<i>Prairie Island 1-2</i>		0	0,0007	0,00002	0,0000	0,0286
<i>R.E. Ginna</i>	0,00729	0,00104	1,28	0,466	0,0008	0,3641
<i>Rancho Seco 1</i>	0,566	0,357	54	0,936	0,0066	0,0173
<i>Salem 1</i>	0,29	0,0366	18,5	0,703	0,0020	0,0380
<i>Salem 2</i>	0,0981	0,225	41,4	1,27	0,0054	0,0307
<i>San Onofre 1</i>	0,145	0,988	105	3,27	0,0094	0,0311
<i>San Onofre 2-3</i>	0,57	0,235	174	11,8	0,0014	0,0678
<i>Sequoyah 1-2</i>	0,0403	0,0788	7,99	0,136	0,0099	0,0170
<i>South Texas 1</i>		0,00218	3,54	0,0474	0,0006	0,0134
<i>St. Lucie 1</i>	0,00043	0,202	44,4	7,51	0,0045	0,1691
<i>St. Lucie 2</i>	0,128	3,22	296	35,2	0,0109	0,1189
<i>Summer 1</i>	0,0562	0,0392	11	0,84	0,0036	0,0764
<i>Surry 1-2</i>	0,0729	0,0223	13,1	0,169	0,0017	0,0129
<i>Three Miles Islands 1</i>	0,437	0,533	66,2	1,33	0,0081	0,0201
<i>Three Miles Islands 2</i>						
<i>Trojan</i>	0,0929	0,0503	14,2	0,239	0,0035	0,0168
<i>Turkey Point 3</i>	0,577	0,257	44,4	0,692	0,0058	0,0156
<i>Turkey Point 4</i>	0,511	0,278	45,5	0,718	0,0061	0,0158
<i>Vogtle 1</i>		0,00201	2,87	0,232	0,0007	0,0808
<i>Waterford 3</i>	0,648	0,189	188	6,96	0,0010	0,0370
<i>Wolf Creek 1</i>	0,151	0,283	28	0,696	0,0101	0,0249
<i>Yankee Rowe 1</i>	0,0407	0,0766	3,77	1,44	0,0203	0,3820
<i>Zion 1-2</i>	0,0238	0,0132	51,4	2,05	0,0003	0,0399
Normalized activity [TBq/(GWa)]		0,53	82	3,5	0,0065	0,0427

Table 4-9: Release of xenon from PWRs 1988 [UNSCEAR, 1993]

4.4.1.2 Normalized releases of BWR

Normalized releases [TBq/(GW[e]a)] of the relevant xenon isotopes from BWRs reactor types located in the United States in 1979 [UNSCEAR, 1982] and 1988 [UNSCEAR, 1993]:

1979			Release [TBq]				Isotope ratio	
Reactor	Startup year	GW(e) a	Xe-131m	Xe-133m	Xe-133	Xe-135	Xe133m/Xe133	Xe135/x133
Big Rock Point 1	1962	0,013	0,11	0,32	5,8	20	0,0552	3,4483
Browns Ferry 1, 2, 3	1973/1977	2,393			319	38	0,0000	0,1191
Brunswick 1,2	1975/1977	0,81		29	84	1217	0,3452	14,4881
Cooper	1974	0,591	1,7	11	310	358	0,0355	1,1548
Dresden 1	1959				6,8		0,0000	0,0000
Dresden 2, 3	1970/1971	1,013			219	466	0,0000	2,1279
Duane Arnold	1974	0,352			212	42	0,0000	0,1981
J.A. Fitzpatrick	1974	0,349	4,6	1,2	70	29	0,0171	0,4143
Edwin Hatch	1974	0,401	14	1,2	110	2,1	0,0109	0,0191
Lacrosse	1967	0,024	0,35	3	27	120	0,1111	4,4444
Millstone Point 1	1970	0,505	81		12	74	0,0000	6,1667
Monticello	1970	0,522	0,07	0,02	10	2,1	0,0020	0,2100
Nine Mile Point	1969	0,354				5,1		
Oyster Creek	1969	0,541			1298	8362	0,0000	6,4422
Peach Bottom 2, 3	1973/1974	1,74	5	72	3922	566	0,0184	0,1443
Pilgrim	1972	0,574			71	19	0,0000	0,2676
Quad Cities 1, 2	1971/1972	1,075			481	97	0,0000	0,2017

<i>Vermont Yankee</i>	1972	0,414			164	8,1	0,0000	0,0494
<i>Normalized release</i>			9,1	10	630	980	0,0159	1,5556

Table 4-10: Release of xenon from BWRs 1979 [UNSCEAR, 1982]

1988	Release [TBq]				Isotope ratio	
Reactor	Xe-131m	Xe-133m	Xe-133	Xe-135	Xe133m/Xe133	Xe135/xs133
<i>Big Rock Point</i>			1,58	19,7	0,0000	12,4684
<i>Browns Ferry 1-3</i>						
<i>Brunswick 1-2</i>		0,0418	16,1	22,6	0,0026	1,4037
<i>Clinton 1</i>				0,161		
<i>Cooper</i>		0,0426	4,85	4,85	0,0088	1,0000
<i>Dresden 1-3</i>			0,833	4,14	0,0000	4,9700
<i>Duane Arnold</i>		0,027	8,47	13,4	0,0032	1,5821
<i>Edwin I, Hatch 1-2</i>	2,52	0,0925	87,3	9,99	0,0011	0,1144
<i>Fermi 2</i>				0,0253		
<i>Grand Gulf 1</i>			0,00105	0,04	0,0000	38,0952
<i>Hope Creek 1</i>			0,13	0,329	0,0000	2,5308
<i>Humboldt Bay 3</i>						
<i>James A. Fitzpatrick</i>	0,466	2,19	52,2	38,9	0,0420	0,7452
<i>Lacrosse</i>						
<i>Lasalle 1-2</i>			89,5	6,73	0,0000	0,0752
<i>Limerick 1</i>		0,00365	3,96	1,57	0,0009	0,3965
<i>Millstone 1</i>			15	1,97	0,0000	0,1313
<i>Monticello</i>	0,0304	0,295	59,9	2,29	0,0049	0,0382
<i>Nine Mile Point 1</i>			0,544	0,122	0,0000	0,2243
<i>Nine Mile Point 2</i>			0	0,0314		
<i>Oyster Creek</i>			33,3	66,2	0,0000	1,9880
<i>Peach Bottom 2-3</i>						
<i>Perry 1</i>	0,0984	0,54	29,2	9,21	0,0185	0,3154
<i>Pilgrim 1</i>						
<i>Quad Cities 1-2</i>			0,0636	0,0132	0,0000	0,2075
<i>River Bend 1</i>				0,0759		

<i>Susquehanna 1-2</i>			2,68			
<i>Vermont Yankee</i>						
<i>WNP-2</i>	0,231	1,48	20,9	4,26	0,0708	0,2038
<i>Normalized activity [TBq/(GWa)]</i>	0,22	0,28	26	12	0,0108	0,4615

Table 4-11: Release of xenon from BWRs 1988 [UNSCEAR, 1993]

It must be taken into account that these data (for the PWR and for the BWR) do not consider whether the reactor was shut down for changing the fuel elements and coming into operation again. A reason for some high Xe-135 concentrations may be due to the starting up of the respective reactor (e.g. Oyster Creek).

The calculated isotope ratios cannot be seen as an indicator for nuclear weapons testing since these are mean values for a whole year, the calculation shall demonstrate the different releases from different reactor types and year of construction.

Furthermore it must be taken into account that nowadays the equipment for retention of noble gases is much better and in this way provides decay of most Xe-135 before release [Bowyer *et al.*, 1996]. This can be well seen by comparing the data between 1979 and 1983.

4.4.2 Nuclear weapon testing

Since no experimental data for the release of noble gases during nuclear detonations are available, values were calculated by simulation of nuclear weapons testing with Origen 2.2 (distributed by NEA – Nuclear Energy Agency). The estimation was based on an explosion with an 1kt U-235 and 1kt Pu-239 bomb [Bowyer *et al.*, 1996].

Following figure shows the isotope ratios versus time after detonation. The respective data are listed in Table 4-12.

Ratio	time after detonation t [min]	U-235	Pu-239
Xe135/Xe133	0	640.1	388.3
	2	688.5	419.5
	5	639.8	435.8
	10	467.5	408.8
	30	183	239.3
	120	62.5	81.3
	300	36.6	43.3
	600	22.7	25.6
	1200	10.5	11.5
Xe133m/Xe133	0	7.92	7.85
	2	6.8	7.28
	5	4.86	6.3
	10	2.64	4.74
	30	0.61	1.79
	120	0.15	0.38
	300	0.096	0.179
	600	0.081	0.121
	1200	0.072	0.092

Table 4-12: Calculated isotope ratios [Bowyer et al., 1996]

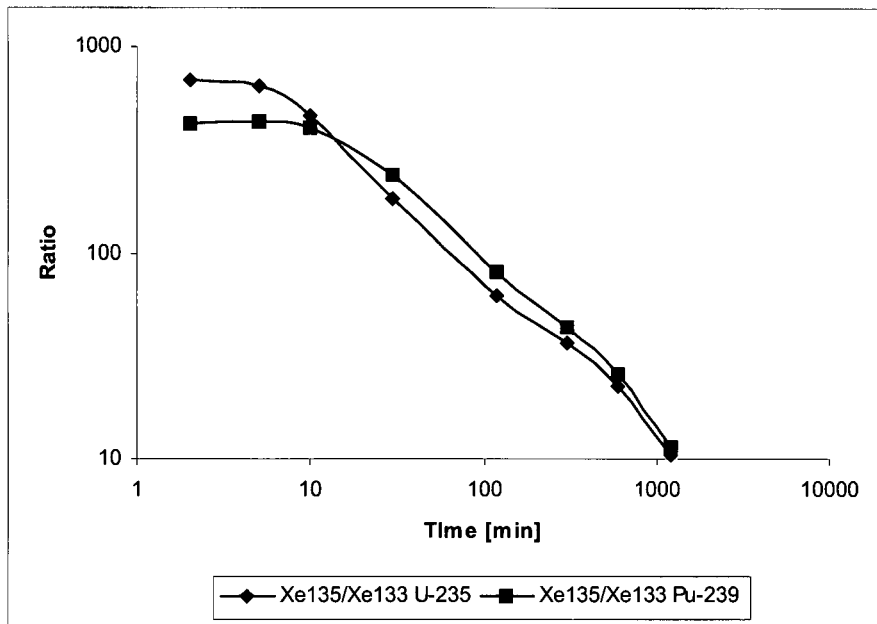


Figure 4-6: Relevant isotope ratios after a nuclear detonation (U-235 and Pu-239)

4.4.3 Conclusion

Differentiation between nuclear weapon testing and reactor operation is possible by means of isotope activity ratios dependent from the source.

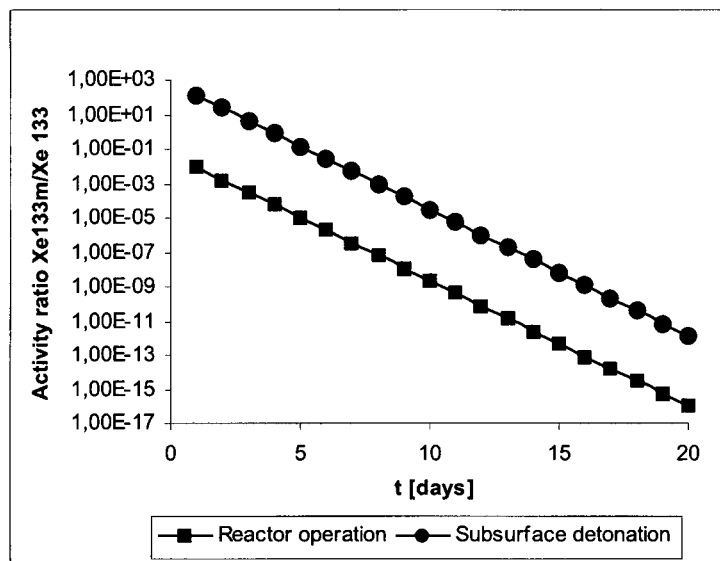


Figure 4-7: $\text{Xe135}/\text{Xe133}$ activity ratio for nuclear detonation (uranium) and reactor operation

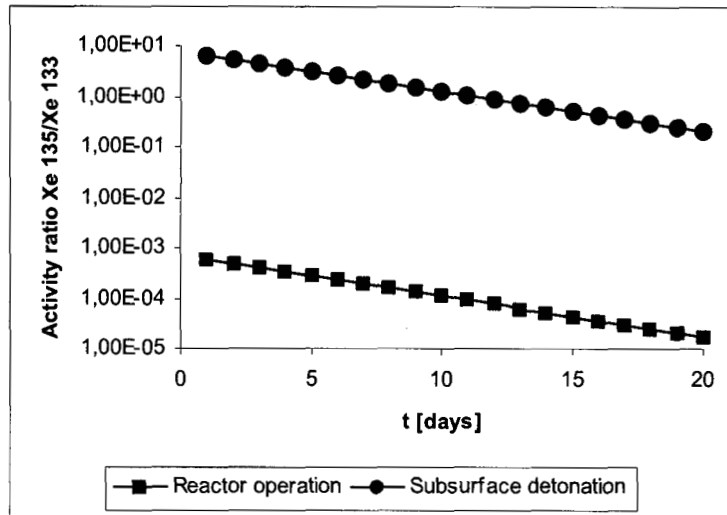


Figure 4-8: Xe133m/Xe133 isotope activity ratio nuclear detonation (uranium) and reactor operation

Summarizing following guide value can be given:

	reactor equilibrium	Nuclear detonation
Xe133m/Xe133g	< 0.01-0.1	About 100 times higher
Xe135/Xe133	~ 0.01	About 10.000 times higher

Table 4-13: Comparison isotope activity ratios for reactor operation and nuclear detonation [Perkins and Casey, 1996; Bowyer et al., 1998]

Measuring only one isotope means that there is no possibility for differentiating the source since a high Xe-133 concentration can be caused by leakage in power reactors but as well by nuclear weapons testing. If a high ratio of Xe135/Xe133 is measured, then also a higher ratio of Xe133m/Xe-133 can be detected (see Figure 4-8).

Another important point is the changing of isotope ratios during long lasting transport times. If an archive bottle needs more time than can be taken into account, so it is possible that just one isotope can be measured any more. Then the sample analysis has to be made very careful by determination of other CTBT-relevant nuclides.

5 Gas Transfer and Measurement

5.1 Purpose

A gas transfer system had to be designed for two possible applications:

- Measurement of archive samples of IMS stations:

Since the samples coming from International Monitoring System - IMS stations are stored under varying conditions and in different containers, a transfer system, designed especially for this purpose had to be developed to guarantee standardized conditions. Furthermore the determination of the quantity of the stable xenon is required by the (Provisional) Technical Secretary - (P)TS. Measurement of stable xenon is performed by gaschromatography.

- Testing of the equipment developed especially for on-site inspections

Requirements for on site inspection equipments:

Separation capability of water and carbon dioxide, Purification capability of xenon isotopes regarding radon and sensitivity to Xe-133g at a concentration of 1 mBqm³ for 10m³ of gas [PTS, 2003]

The requirements for a laboratory are at least the same as for the equipment for on site inspection.

A possible design had to be developed, which removes traces of impurities like CO₂, Rn, Ar and Kr from the sample for the check of the requirements of the PTS.

The requirement for this transfer system is a transfer with minimal sample loss during the transport to the gaschromatograph and then the transfer to the measurement geometry for radiometric analysis.

Altogether there are four different sample geometries, which can be seen in following picture and the storage container parameters are given in Table 5-1:

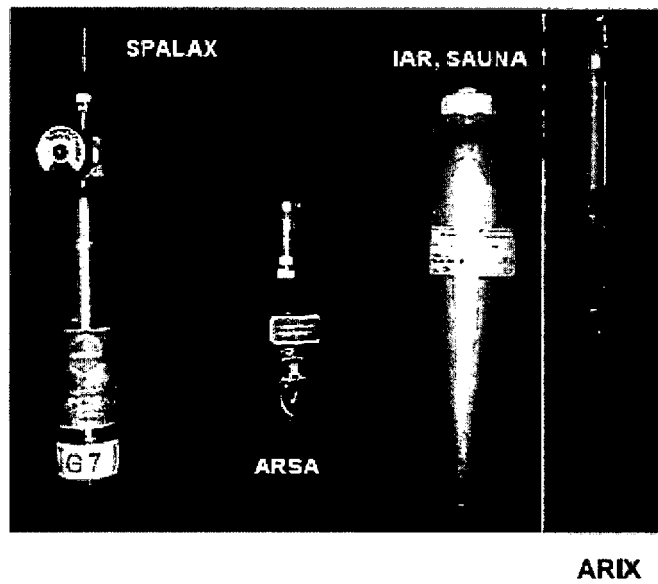


Figure 5-1: Picture of possible archive sample geometries [Auer M., 2002]

Name	SPALAX	ARIX	ARSA	SAUNA	SAUNA II
Container volume [ml]	300	210	150	1000	500
Total gas volume [ml@STP]	25	6	3	6	351
Container pressure (kPa) at 20°C	9.062	3.107	2.175	0.652	76.341
Composition of gas mixture	30 % Xe > a few thousand ppm CO ₂ 70% N ₂	0,7 ml Xe 0,3 ml N ₂ +O ₂ 3 ml He 2 ml CO ₂	35 % Xe 61 % N ₂ 4 % CO ₂	0.5 ml Xe 5.5 ml He	1 ml Xe 350 ml He

Table 5-1: Archiving parameters of xenon samples [data from CTBTO/IMS/RM; 2004]

Figure 5-1 shows the different sample geometries. The Swedish group (SAUNA) has developed an additional bottle, therefore in Table 5-1 listing all the archiving parameters are five bottles mentioned.

The first step was the development and the planning of the best possible gaschromatographical system and afterwards the design of the transfer system.

In the following the design of the gaschromatograph and its validation, and the development of a transfer system are described in detail.

5.1.1 Overview

Chromatography is a physico-chemical method for the separation of substances. The mobile phase flows over a steady state phase, where the interactions with sample components are different. The result is a distribution of the components between mobile and steady state phase. Depending on the distribution coefficients the components are analyzed earlier or later. In general the mobile phase is either gaseous or liquid and the steady state phase is either solid or liquid.

Therefore the separation of the different elements in a solution is the result of their different flow rates in the steady state phase. However, this is just an apparent effect, since the actual solution of the substance in the mobile phase is constant. The difference is given by numerous de- and adsorption sequences. [Böcker J., 1997]

In this case gaschromatography was used for separation of xenon from other elements and substances like krypton, argon, nitrogen, oxygen, methane and radon and for the determination of the quantity of stable xenon.

5.1.2 *Requirements and Design*

Due to expected large sample volumes (from 0.5 ml to about 10 ml) packed columns are used. In general typical volumes for gaschromatography are in the μl - range, therefore capillary columns with an inner diameter of 0.53 mm are used, but for larger sample volumes and for the separation of noble gases packed columns like molecular sieves are better.

The system has to fulfil the following requirements:

Processing of large sample volumes (range 15-20 ml), these samples may consist of approximately 0.1 - 10 ml xenon, which must be separated. The xenon fraction has to be cut from the gas stream after the detection of xenon, and transferred to a measurement cell for analysis of radioactivity (gamma-spectrometry). Other elements or substances which can be present in the sample are methane, helium and nitrogen used at the IMS-station as carrier gases, furthermore carbon dioxide and traces of oxygen may be present. In our case for subsequent activity analysis it must be guaranteed, that neither krypton nor radon are present in the sample after separation.

Due to varying archiving parameters, the plan was to transfer all archive samples into a plastic bag for sample analysis and for separation by gaschromatography.

The instrument used is TRACE GC ultra (Thermo Electron Austria) with the following specifications:

The temperature range of the column oven reaches from some degrees above ambient temperature up to 450°C, the program ramps 0.1 to 120°C/min through seven ramps and the cooling time is 250 s from 450°C to 50°C and the heating time is 420 s from 50°C to 450°C.

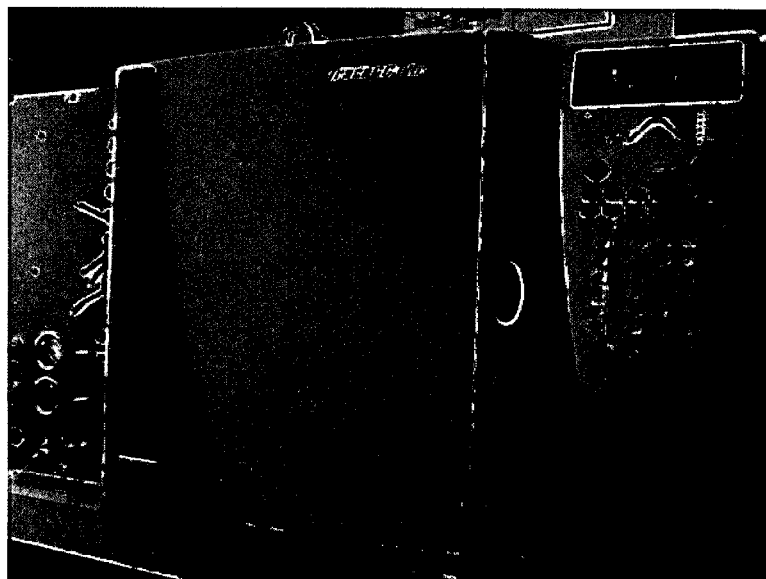
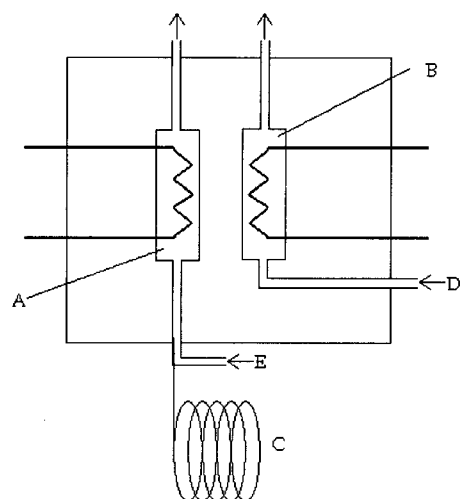


Figure 5-2: View of Trace GC ultra

The detector used is a thermal conductivity detector (TCD) which consists of filaments which are built up like a Wheatstone bridge. The detector measures the change in thermal conductivity of the gas flowing around it. Changes in thermal conductivity cause a temperature rise in the element which is sensed as a change in resistance. The TCD is not as sensitive as other detectors but it is non-specific and non-destructive.

The internal cell volume of the thermal conductivity detector is 200 μl and two different operating modes are possible: constant temperature and constant voltage. The minimum detectable amount is specified by typically 600 pg Ethane/ml He carrier. The TCD is linear up to the factor 10^6 and compatible with packed and capillary columns.



- A ... Measurement cell
- B ... Reference cell
- C ... Column (Mol Sieve 5A)
- D ... Reference gas
- E ... Make up gas (not used)

Figure 5-3: Design of the Thermal Conductivity Detector - TCD

The molecular sieve used is Molecular Sieve 5A (Chrompack, Catalog No. 318768685, Column No. 3612, The Netherlands) with a mesh size of 80-100, the material of the column consists of stainless steel with a length of 2.0 m and an inside diameter of 4 mm. The outside diameter is ¼ inch and the fittings are made of brass. The maximum temperature this column can be worked with is 400°C and it was conditioned in the factory at 300°C for 16 hours.

The Silicagel used as adsorbent for CO₂ is type Silicagel GC Grade (Chrompack, Catalog No. 318768685, Column No. 3614, The Netherlands) with a mesh size of 80-100. The other components (length, diameter) are the same as for the molecular sieve. This column was conditioned by the producer at 180°C for 16 hours and can be operated up to a maximum temperature of 200°C.

Sample inlet is in front of the gaschromatograph, where a plastic gas bag can be connected. The sample loop is connected at both sides with a

Sample injection for the calibration gas:

The calibration gas is connected to Sample IN (Figure 5-4), the magnetic valves MV3 and MV4 are open and the position of the ten port valve is "LOAD" (Figure 5-5). The gas flows the way 9-10 over the sample loop and along 8-7 towards the vacuum pump to Sample OUT (see red line in Figure 5-4). During this time, the molecular sieve is flushed with helium (1-2). In the same way Silicagel is flushed with helium, which in this case is called auxiliary carrier gas (via 4-3 into the column and via 6-5 out).

If a sample is measured, then the sample (in a gas bag) is connected to Sample IN, the valve of the gas bag is closed, MV3 and MV4 are opened, and the connection is evacuated. Then MV4 is closed and the valve from the gas bag is opened, so that the sample flushes into the sample loop. Then MV3 is closed again and the procedure is performed as follows.

After flushing the calibration gas for 3 minutes, MV3 is closed and afterwards MV4 is closed as well in order to obtain atmospheric pressure in the sample loop. The LOAD position is changed to INJECT position (blue lines are connected, see Figure 5-4), helium flushes over 1-10 to the sample loop containing the sample, then the gas streams via 7-6 over the Silicagel, along 3-2 over the Molecular sieve and then to the TCD. After the measurement in the sieve the gas is let out to air or, if a sample is measured, can be cut by switching the four port valve after the TCD to the red line and can be collected in the gas bag.

After a defined injection time the ten port valve is switched again to the "load" position in which the Silicagel is flushed by the auxiliary carrier gas and traces of carbon dioxide are removed.

5.1.3 Calibration

For the calibration three different gas mixtures of helium with xenon with certified concentrations were used¹. These gas standards have a certificate of analysis which declares them as test gas of category 1. This category guarantees that the rate of addition has a manufacturer's tolerance of $\pm 1\%$ rel. and a measurement uncertainty of $\pm 1\%$ rel.

The mixtures were chosen to contain 50% vol., 35 % vol., 20 % vol. and 10 % vol. xenon, respectively injection of these mixtures corresponds to 1 ml, 0.7 ml, 0.4 ml and 0.2 ml xenon in the 2 ml sample loop. Therefore it can be said, that this design is able to detect the minimum quantity which will be stored in an archive sample, since the minimum quantity is about 0.5 ml of xenon. The 20% vol. mixture contains additionally oxygen, nitrogen, krypton, argon, methane and carbon dioxide in order to test whether CO₂ is held back in the Silicagel column and the other elements can be separated well. With these certified gas mixtures calibration curves were established. For testing the calibration and evaluation of the separation performance, the certified gas mixture with O₂, N₂, CH₄, Kr, Ar, He, Xe and CO₂ was used.

	Xe[%]	He[%]	Ar[%]	Kr[%]	CO ₂ [%]	O ₂ [%]	CH ₄ [%]	N ₂ [%]
Mixture 1	50.05	49.95	-	-	-	-	-	-
Mixture 2	35	65	-	-	-	-	-	-
Mixture 3	10.5	89.5	-	-	-	-	-	-
Mixture 4	19.9	-	3.02	3.08	11	2.98	30.3	29.72

Table 5-2: Summary of used gas mixtures

¹ Supplier: Linde Gase, Austria

5.1.3.1 First tests

After setting in operation of the gaschromatograph first tests were performed in order to check the accordance with the requirements. Therefore the instrument was built up with both columns, Silicagel and Molecular Sieve 5A. These first tests after installation were performed with the parameters given in Table 5-3.

Oven parameters		TCD parameters	
Initial temperature [°C]	180	Block temperature [°C]	150
Initial time [min]	10	Transfer temperature [°C]	150
Number of ramps	1	Filament temperature [°C]	250
Rate #1 [deg/min]	20	Filament voltage [V]	10
Final temperature [°C]	150	Reference flow [ml/min]	30
Hold time [min]	7.5		

Table 5-3: Oven and TCD parameters for the first tests after installation

Test 5a					
Peak	Ar, O ₂	N ₂	Kr	CH ₄	Xe
Retention time [min]	5.395	6.8167	9.6467	10.3483	19.92
Peak Area [mVs]	9.86·10 ⁶	4.68·10 ⁷	5.41·10 ⁶	3.00·10 ⁷	3.10·10 ⁷

Table 5-4: Results of the analysis of the gas mixture after installation

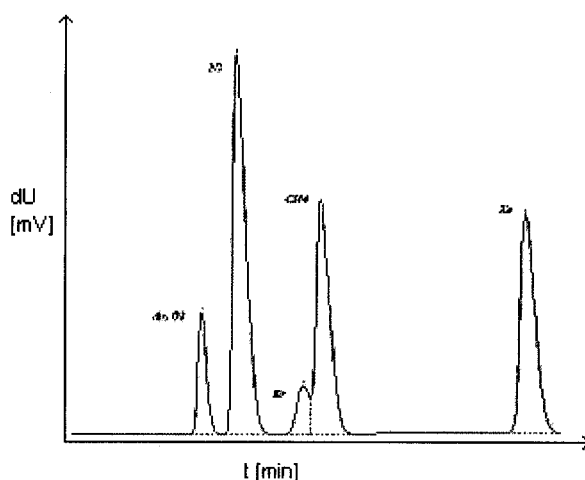


Figure 5-6: Chromatogram belonging to the data of Table 5-4. For relevant retention time values see Table 5-4.

Krypton and methane were not separated completely, so both components are still mixed together. For the separation of these components a new, higher temperature program had to be written.

Therefore measurement with gas mixture 4 was performed with higher oven temperature for separation of the compounds krypton and methane (Table 5-5):

<i>Oven parameters</i>		<i>TCD parameters</i>	
Initial temperature [°C]	280	Block temperature [°C]	260
Initial time [min]	8	Transfer temperature [°C]	260
Number of ramps	1	Filament temperature [°C]	350
Rate #1[deg/min]	20	Filament voltage [V]	10
Final temperature [°C]	250	Reference flow [ml/min]	30
Hold time (min)	10		

Table 5-5: Oven and TCD parameters substantially changed

Peak	Ar, O ₂	N ₂	Kr	CH ₄	Xe
Retention Time [min]	1.8333	2.5983	3.5333	4.04	11.46
Peak Area [mVs]	$2.99 \cdot 10^6$	$1.43 \cdot 10^7$	$2.00 \cdot 10^6$	$1.18 \cdot 10^7$	$1.83 \cdot 10^7$

Table 5-6: Results of the measurement of gas mixture 4 at higher temperatures

Higher temperatures lead to a shorter retention time which can be seen clearly by comparison with the earlier experiment (Table 5-4).

Chromatogram from this experiment shows that the peak from krypton and methane is separated well (Figure 5-7):

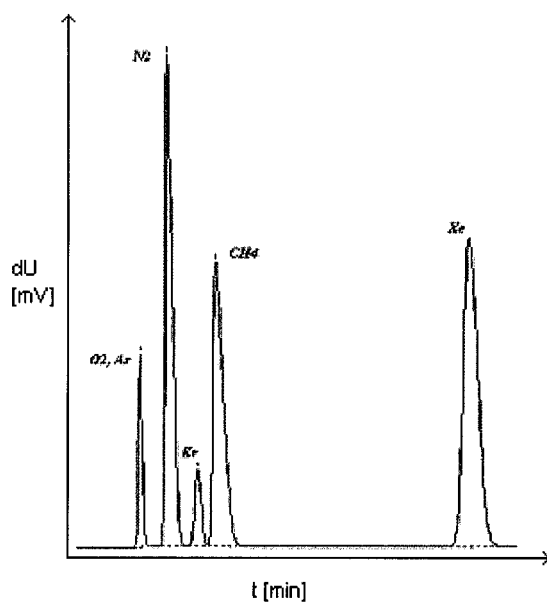


Figure 5-7: Gas mixture separated at 280°C down to 250°C belonging to the data of Table 5-5, for relevant retention time data see Table 5-6.

Since the Silicagel is just necessary for the separation of carbon dioxide it was removed from the system and measurements were performed with the gas mixture containing 50% of xenon.

Test 6	With SG	Without SG
Retention time [min]	19.11	16.3567
Peak area [mVs]	$1.88 \cdot 10^7$	$7.92 \cdot 10^7$

Table 5-7: Comparison measurement with and without Silicagel SG, test of the new temperature program

<i>Oven parameters</i>	<i>With SG</i>	<i>Without SG</i>
Initial temperature [°C]	60	60
Initial t [min]	10	10
Number of Ramps	1	1
Rate #1[deg/min]	20	20
Final temperature [°C]	150	150
Hold time [min]	10	10
<i>TCD parameters</i>	<i>With SG</i>	<i>Without SG</i>
Block temperature [°C]	150	150
Transfer temperature [°C]	150	150
Filament temperature [°C]	250	250
Filament voltage [V]	10	10
Reference flow [ml/min]	30	30

Table 5-8: Oven and TCD parameters

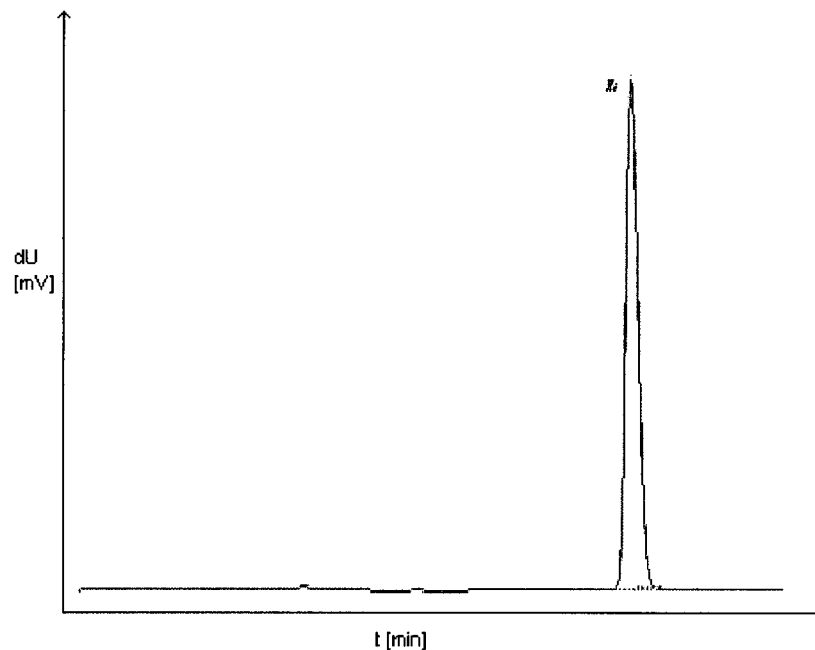


Figure 5-8: Gas mixture xenon 50% with Silicagel and temperature program as given in Table 5-8, for relevant retention time data see Table 5-7.

The small peaks which can be seen in the chromatogram result from traces of air and from the switching of pneumatic valves since the TCD is very sensitive for impacts from outside.

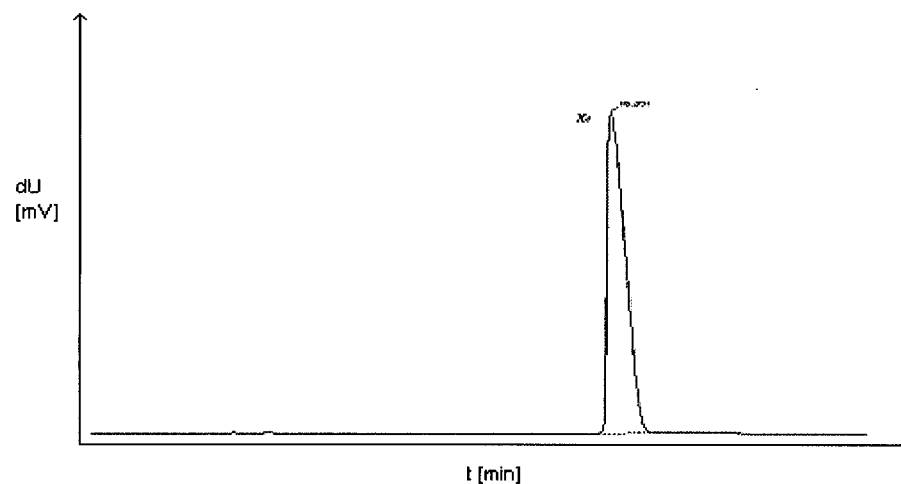


Figure 5-9: Gas mixture xenon 50% without Silicagel and temperature program as given in Table 5-8, for relevant retention time data see Table 5-7.

These first tests showed that the system is in accordance with the requirements, since all elements and substances could be separated and carbon dioxide is held back in the Silicagel column.

5.1.3.2 Calibration: temperature ramp of 35°C/min from 60°C-150°C

The temperature program was changed by raising the temperature ramp from 20°C/min for the first tests to 35°C/min which had the effect that the retention time became shorter.

All equations of the calibration curve and the detection limit were calculated by Origen 6.1. with the method "fit linear".

In Table 5-9 the parameters used for the gaschromatograph are given:

<i>Oven parameters</i>		<i>TCD parameters</i>	
Initial temperature [°C]	60	Block temperature [°C]	150
Initial time [min]	8.5	Transfer temperature [°C]	150
Number of ramps	1	Filament temperature [°C]	250
Rate #1[deg/min]	35	Filament voltage [V]	10
Final temperature [°C]	150	Reference flow [ml/min]	30
Hold time (min)	6		

Table 5-9: System parameters for the calibration with a temperature ramp of 35°C/min

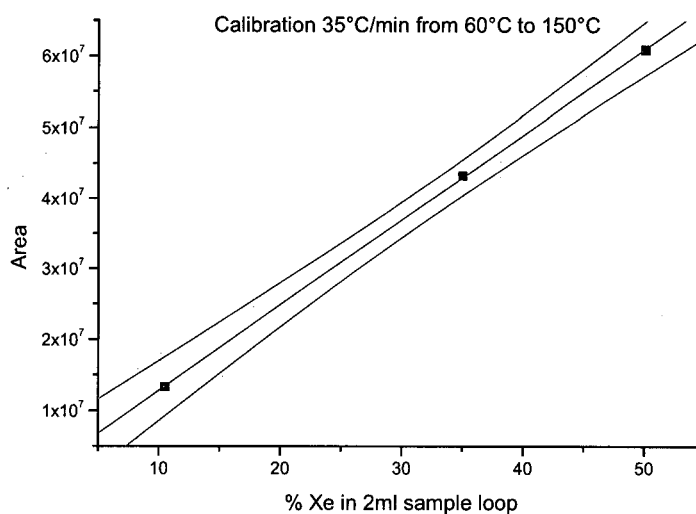


Figure 5-10: Calibration with a temperature ramp of 35°C/min

$$y = 0.78064 \cdot 10^6 + 1.20521 \cdot 10^6 x \quad \text{Equation 1}$$

Detection limit: 0.006 µl

Measurements:

- 50.05% xenon

	Area [mVs]	Retention time [min]
11-11.12.2003	$6.095 \cdot 10^7$	14.96
12-11.12.2003	$6.092 \cdot 10^7$	14.97
13-11.12.2003	$6.094 \cdot 10^7$	14.97
14-11.12.2003	$6.094 \cdot 10^7$	14.95

Table 5-10: Results for the gas mixture 1

- 35% Xenon

	Area [mVs]	Retention time [min]
09-11.12.2003	$4.325 \cdot 10^7$	15.07
10-11.12.2003	$4.324 \cdot 10^7$	15.06

Table 5-11: Results for the gas mixture 2

- 10.5% Xenon

	Area [mVs]	Retention time [min]
03-11.12.2003	$1.334 \cdot 10^7$	15.29
05-11.12.2003	$1.330 \cdot 10^7$	15.28
06-11.12.2003	$1.330 \cdot 10^7$	15.95
07-11.12.2003	$1.334 \cdot 10^7$	15.26
08-11.12.2003	$1.335 \cdot 10^7$	15.27

Table 5-12: Results for the gas mixture 3

Mean values for the calibration with a temperature ramp of 35°C/min from 60°C to 150°C are given in Table 5-13:

% Xenon	Area [mVs]
10.5	$1.333 \cdot 10^7 \pm 0.003 \cdot 10^7$
35	$4.324 \cdot 10^7 \pm 0.001 \cdot 10^7$
50.05	$6.093 \cdot 10^7 \pm 0.001 \cdot 10^7$

Table 5-13: Mean values and standard deviation for the calibration with a temperature ramp of 35°C/min (Figure 5-10)

It is necessary to calibrate the gaschromatograph regularly, because influences from outside like varying pressure or temperatures can have an impact on the measurements.

5.1.3.3 Calibration with a constant temperature of 180°C

<i>Oven parameters</i>		<i>TCD parameters</i>	
Initial temperature [°C]	180	Block temperature [°C]	150
Initial time [min]	10	Transfer temperature [°C]	150
Number of ramps	1	Filament temperature [°C]	250
Rate #1[deg/min]	35	Filament voltage [V]	10
Final temperature [°C]	180	Reference flow [ml/min]	30
Hold time (min)	15		

Table 5-14: System parameters for calibration with constant temperature program of 180°C

The measurements were performed without Silicagel and the oven temperature was held constant, since there were no other elements in the sample, which had to be separated from xenon.

50.05% Xenon

	Area [mVs]	Retention time [min]
26-15.12.03	$4.138 \cdot 10^7$	4.94
27-15.12.03	$4.140 \cdot 10^7$	4.94
28-15.12.03	$4.147 \cdot 10^7$	4.94

Table 5-15: Results for the gas mixture 1

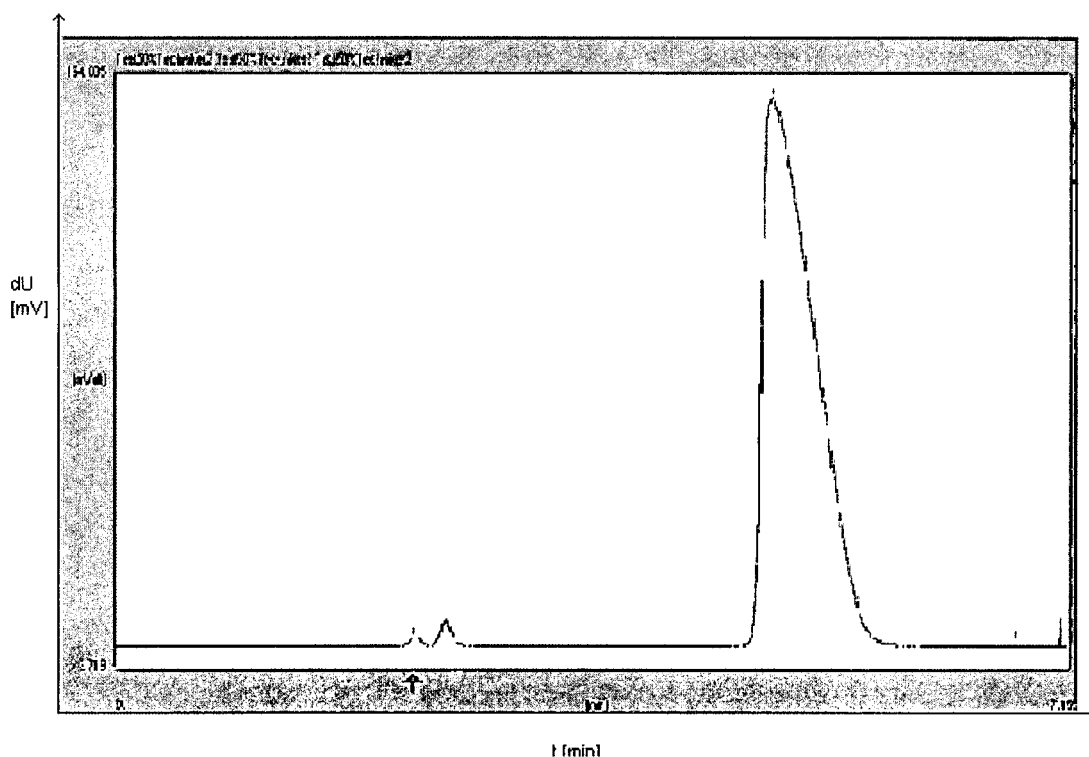


Figure 5-11: Overlay of the three chromatograms (26, 27, 28), data are given in Table 5-15

35% Xenon

	Area [mVs]	Retention time [min]
29-15.12.03	$2.896 \cdot 10^7$	5.02
30-15.12.03	$2.899 \cdot 10^7$	5.02
31-15.12.03	$2.901 \cdot 10^7$	5.02

Table 5-16: Results for the gas mixture 2

10.5% Xenon

	Area [mVs]	Retention time [min]
32-15.12.03	$8.9968 \cdot 10^6$	5.21
33-15.12.03	$8.9080 \cdot 10^6$	5.21
34-15.12.03	$8.9330 \cdot 10^6$	5.21

Table 5-17: Results for the gas mixture 3

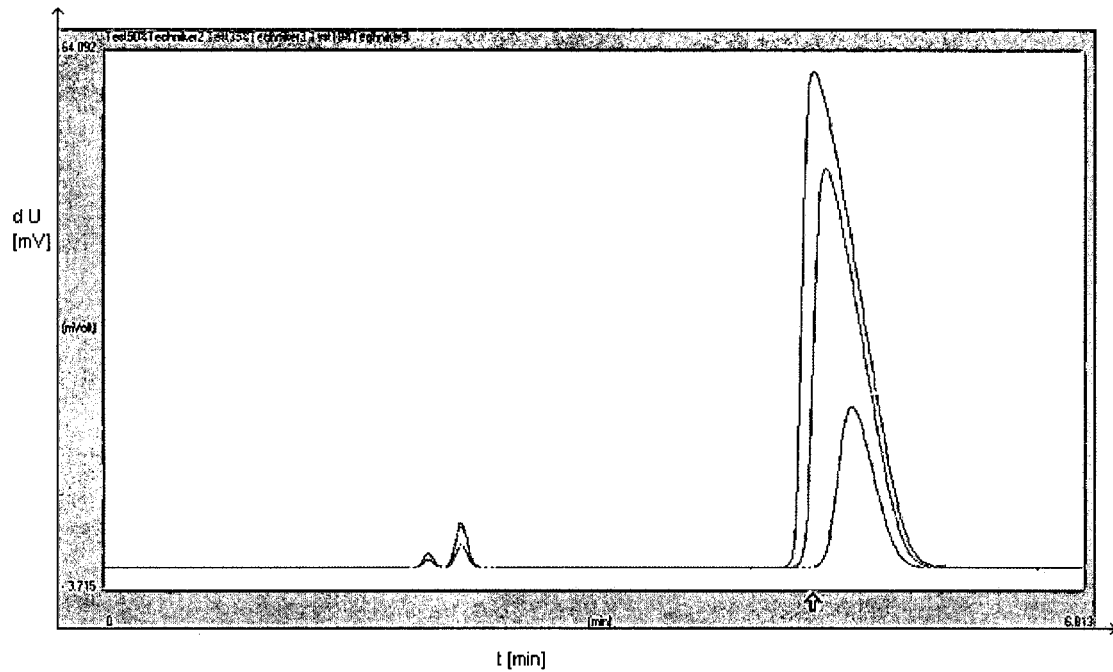


Figure 5-12: Overlay of chromatograms of the gas mixtures 1-3 (27, 30 and 33).

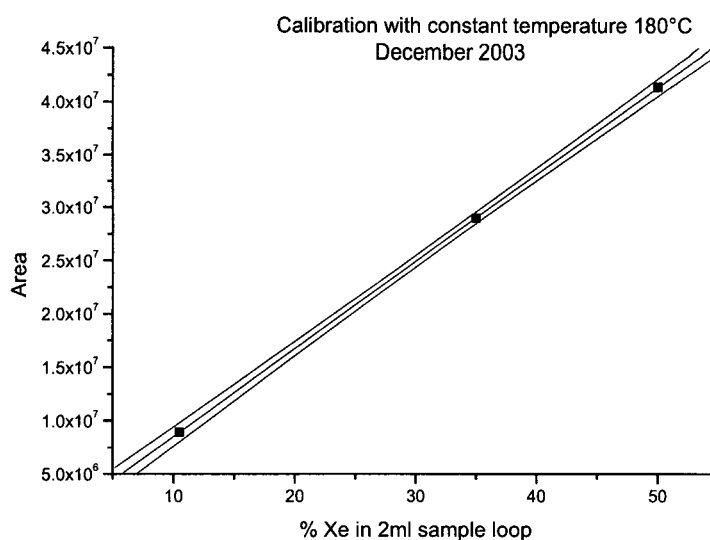


Figure 5-13: Calibration with a constant temperature program

% Xenon	Area [mVs]
10.5	$8.946 \cdot 10^6 \pm 0.046 \cdot 10^6$
35	$2.899 \cdot 10^7 \pm 0.002 \cdot 10^7$
50.05	$5.110 \cdot 10^7 \pm 0.005 \cdot 10^7$

Table 5-18: Data used for the calibration diagram in Figure 5-13

5.1.3.4 Calibration with a constant temperature of 190°C

The constant temperature was set at 190°C since this temperature is above the range within which Silicagel can be used and at this temperature it can be possible to avoid heating out of the Silicagel after few usages for purification. Furthermore the initial time and the hold time were reduced since the retention time of xenon is about five minutes, which does not require a longer analysis time and enables more measurements (calibration and gas transfer) per day.

Before this the calibration was performed, a few months lasting system check because the reconstruction of the gas transfer system had to be carried out.

For the validation of the system the calibration was controlled regularly over different periods with the following parameters:

<i>Oven parameters</i>		<i>TCD parameters</i>	
Initial temperature [°C]	190	Block temperature [°C]	150
Initial time [min]	6	Transfer temperature [°C]	150
Number of ramps	1	Filament temperature [°C]	250
Rate #1[deg/ min]	35	Filament voltage [V]	10
Final temperature [°C]	190	Reference flow [ml/min]	30
Hold time (min)	4		

Table 5-19: System parameters for the calibration with a constant temperature of 190°C

16.02.2005	50.05%	35%	19.9%	10.5%
	Area [mVs]	Area [mVs]	Area [mVs]	Area [mVs]
Mean value	$8.502 \cdot 10^7$	$5.422 \cdot 10^7$	$3.053 \cdot 10^7$	$1.724 \cdot 10^7$
Standard deviation	$0.007 \cdot 10^7$			

Table 5-20: Results of the calibration on February 16th, 2005

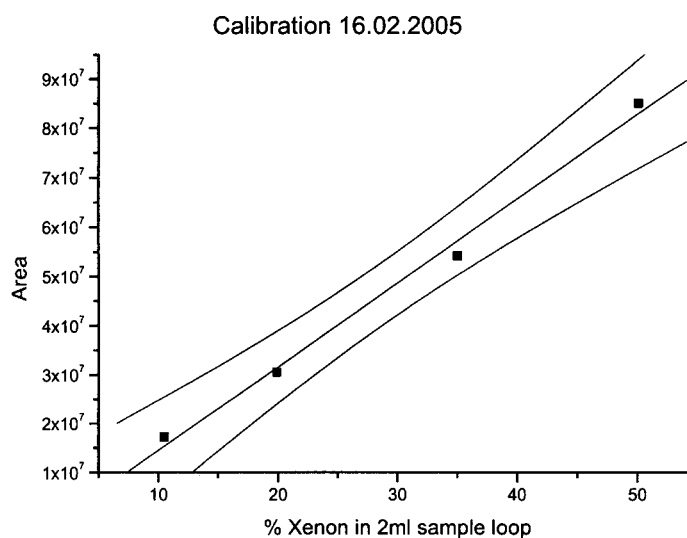


Figure 5-14: Calibration with all mixtures, data used are given in Table 5-20: Results of the calibration on February 16th, 2005

Equation of the calibration curve: $y = -2.54 \cdot 10^6 + 1.71 \cdot 10^6 x$ (Equation 2)

The detection limit is 0.01 μl .

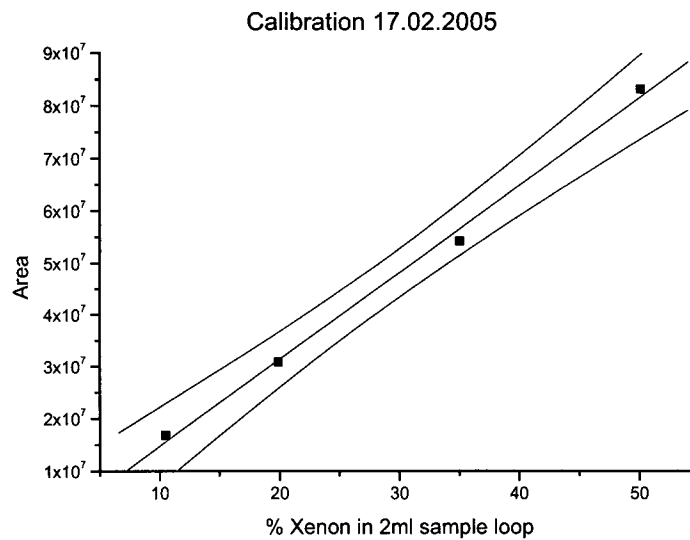


Figure 5-15: Calibration with all gas mixtures, data are given in Table 5-21

% Xenon	Area [mVs]
10.5	1.682·10 ⁷
19.9	3.087·10 ⁷ ± 0.001·10 ⁷
35	5.421·10 ⁷ ± 0.004·10 ⁷
50.05	8.318·10 ⁷ ± 0.008·10 ⁷

Table 5-21: Calibration data for Figure 5-15

Equation of the calibration curve: $y = -1.92 \cdot 10^6 + 1.67 \cdot 10^6 x$ (Equation 3)

The detection limit is 0.099 μl .

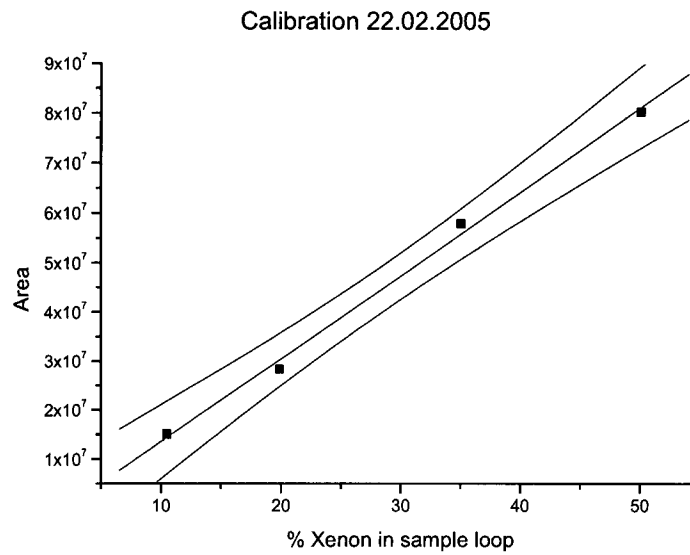


Figure 5-16: Calibration with all gas mixtures on February 22nd, 2005

% Xenon	Area [mVs]
10.5	$1.509 \cdot 10^7 \pm 0.006 \cdot 10^7$
19.9	$2.830 \cdot 10^7 \pm 0.001 \cdot 10^7$
35	$5.790 \cdot 10^7 \pm 0.330 \cdot 10^7$
50.05	$8.037 \cdot 10^7 \pm 0.002 \cdot 10^7$

Table 5-22: Calibration data for Figure 5-16

Equation of the calibration curve: $y = -3.35 \cdot 10^6 + 1.69 \cdot 10^6 x$ (Equation 4)

The detection limit is 0.006 μ l.

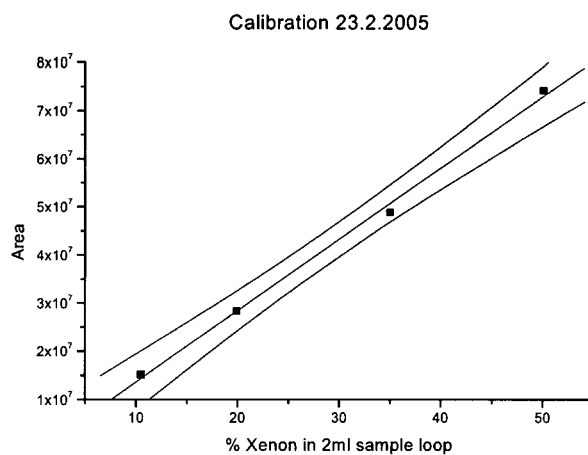


Figure 5-17: Calibration on February 23rd, 2005

% Xenon	Area [mVs]
10.5	$1.5150 \cdot 10^7 \pm 0.0003 \cdot 10^7$
19.9	$2.8300 \cdot 10^7$
35	$4.8820 \cdot 10^7 \pm 0.0002 \cdot 10^7$
50.05	$7.4230 \cdot 10^7 \pm 0.0235 \cdot 10^7$

Table 5-23: Data for the diagram in Figure 5-17

Equation of the calibration curve: $y = -1.17 \cdot 10^6 + 1.48 \cdot 10^6 x$ (Equation 5)

The detection limit is 0.012 μ l.

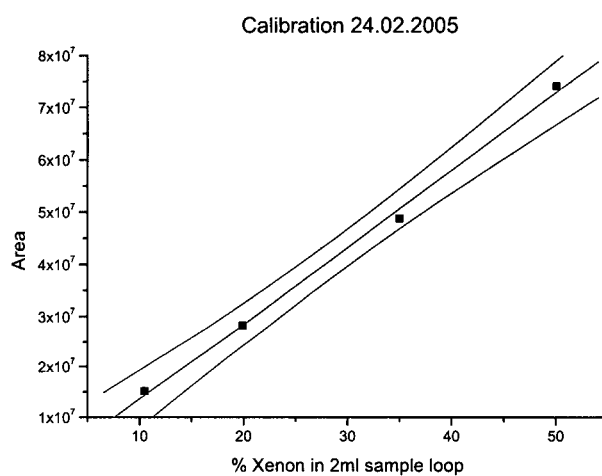


Figure 5-18: Calibration with all gas mixtures on February 24th, 2005

% Xenon	Area [mVs]
10.5	$1.513 \cdot 10^7 \pm 0.002 \cdot 10^7$
19.9	$2.824 \cdot 10^7 \pm 0.003 \cdot 10^7$
35	$4.876 \cdot 10^7 \pm 0.005 \cdot 10^7$
50.05	$7.406 \cdot 10^7 \pm 0.012 \cdot 10^7$

Table 5-24: Data for diagram in Figure 5-18

Equation of the calibration curve: $y = -1.15 \cdot 10^6 + 1.48 \cdot 10^6 x$ (Equation 6)

The detection limit is 0.012 μl .

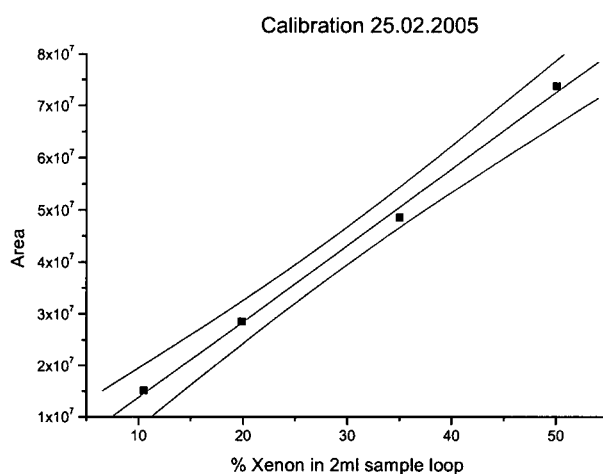


Figure 5-19: Calibration with all gas mixtures on February 25th, 2005

% Xenon	Area [mVs]
10.5	$1.513 \cdot 10^7 \pm 0.012 \cdot 10^7$
19.9	$2.852 \cdot 10^7 \pm 0.002 \cdot 10^7$
35	$4.855 \cdot 10^7 \pm 0.022 \cdot 10^7$
50.05	$7.377 \cdot 10^7 \pm 0.034 \cdot 10^7$

Table 5-25: Data used for diagram in Figure 5-19

Equation of the calibration curve: $y = -0.9 \cdot 10^6 + 1.47 \cdot 10^6 x$ (Equation 7)

The detection limit is 0.013 μl .

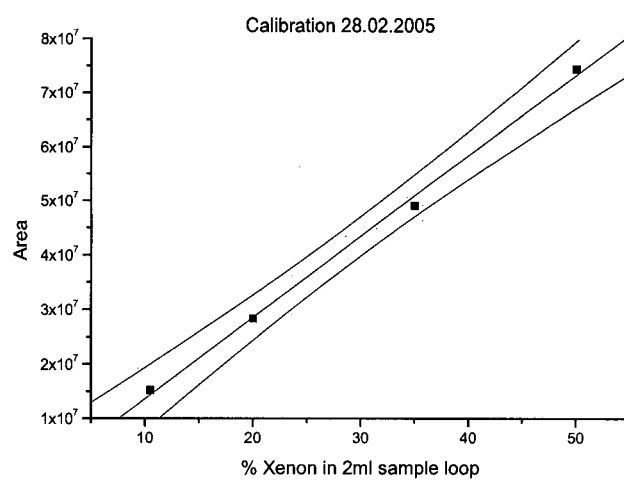


Figure 5-20: Calibration with all gas mixtures on February 28th, 2005

% Xenon	Area [mVs]
10.5	$1.518 \cdot 10^7 \pm 0.001 \cdot 10^7$
19.9	$2.835 \cdot 10^7 \pm 0.001 \cdot 10^7$
35	$4.908 \cdot 10^7 \pm 0.011 \cdot 10^7$
50.05	$7.452 \cdot 10^7 \pm 0.029 \cdot 10^7$

Table 5-26: Mean values used for Figure 5-20

Equation of the calibration curve: $y = -1.23 \cdot 10^6 + 1.49 \cdot 10^6 x$ (Equation 8)

The detection limit is 0.011 μl .

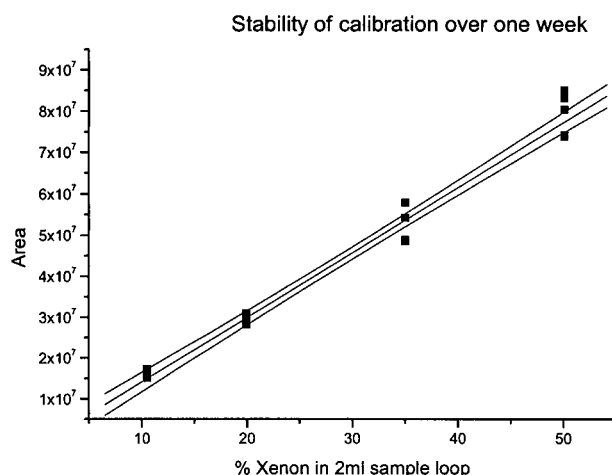


Figure 5-21: Stability of the calibration for one week

Data used for Figure 5-21 are given in Annex A.

Equation of the calibration curve: $y = -1.71 \cdot 10^6 + 1.58 \cdot 10^6 x$ (Equation 9)

The detection limit is 0.006 μl .

5.1.3.5 Influence of the carrier gas pressure

Three experiments with gas mixture 3 in a series showed the influence of the carrier gas pressure:

	Pressure [kPa]	Area [mVs]	$\Delta\text{kPa}/\Delta\text{Area}$
Measurement 1	190	18055620	$1.05 \cdot 10^{-5}$
Measurement 2	210	13322070	$1.57 \cdot 10^{-5}$
Measurement 3	200	15586440	$1.28 \cdot 10^{-5}$

Table 5-27: Results of measurements of studying the influence of the carrier gas pressure

These measurements have shown that it is necessary to control the carrier gas pressure before starting any analysis. The standard deviation of the peak area [mVs] is in the range of 10^4 within measurements testing the stability, but in this case by changing the carrier gas pressure plus/minus 10kPa, the range is changed to a value of 10^6 .

Earlier measurements have shown the effects of a change of the carrier gas pressure during a longer lasting measurement on the baseline:

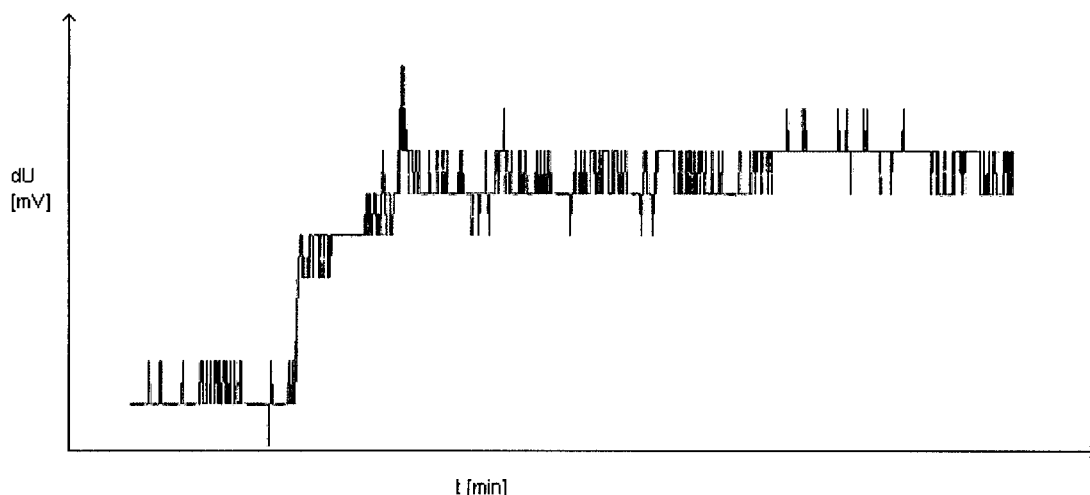


Figure 5-22: Increasing of carrier gas pressure from 4 to 5 bars

5.1.4 Validation

The stability and the calibration during March 2005 was tested for validation. These measurements included the determination of the detection limit, which is three times more than the background. The detection limit is given in μl , since this is the interesting unit, because all the samples amount are given in ml.

01.03.2005	50.05%	35%	19.9%	10.5%
Mean value (n=3)	$7.464 \cdot 10^7$	$4.912 \cdot 10^7$	$2.841 \cdot 10^7$	$1.521 \cdot 10^7$
Standard deviation	$0,003 \cdot 10^7$	$0.004 \cdot 10^7$	$0.002 \cdot 10^7$	$0.001 \cdot 10^7$

Table 5-28: Results of the calibration on March 1st, 2005

Equation of the calibration curve: $y = -1.22 \cdot 10^6 + 1.49 \cdot 10^6 x$ (Equation 10)

Detection limit: 0.011 μl .

02.03.2005	50.05%	35%	19.9%	10.5%
Mean value (n=3)	$7.418 \cdot 10^7$	$4.886 \cdot 10^7$	$2.824 \cdot 10^7$	$1.5170 \cdot 10^7$
Standard deviation	$0.007 \cdot 10^7$	$0.002 \cdot 10^7$	$0.001 \cdot 10^7$	$0.0003 \cdot 10^7$

Table 5-29: Results of the calibration on March 2nd, 2005

Equation of the calibration curve: $y = -1.16 \cdot 10^6 + 1.48 \cdot 10^6 x$ (Equation 11)

Detection limit: 0.012 μ l

03.03.2005	50.05%	35%	19.9%	10.5%
Mean value (n=3)	$7.430 \cdot 10^7$	$4.897 \cdot 10^7$	$2.833 \cdot 10^7$	$1.517 \cdot 10^7$
Standard deviation	$0.004 \cdot 10^7$	$0.007 \cdot 10^7$	$0.002 \cdot 10^7$	$0.002 \cdot 10^7$

Table 5-30: Results of calibration on 3rd March 2005

Equation of the calibration curve: $y = -1.16 \cdot 10^6 + 1.48 \cdot 10^6 x$ (Equation 12)

Detection limit: 0.012 μ l

07.03.2005	50.05%	35%	19.9%	10.5%
Mean value (n=3)	$7.416 \cdot 10^7$	$4.823 \cdot 10^7$	$2.800 \cdot 10^7$	$1.5030 \cdot 10^7$
Standard deviation	$0.233 \cdot 10^7$	$0.026 \cdot 10^7$	$0.003 \cdot 10^7$	$0.0002 \cdot 10^7$

Table 5-31: Results of the calibration on March 7th, 2005

Equation of the calibration curve: $y = -1.43 \cdot 10^6 + 1.48 \cdot 10^6 x$ (Equation 13)

Detection limit: 0.011 μ l

14.03.2005	50.05%	35%	19.9%	10.5%
Mean value (n=3)	$7.431 \cdot 10^7$	$4.898 \cdot 10^7$	$2.830 \cdot 10^7$	$1.518 \cdot 10^7$
Standard deviation	$0.012 \cdot 10^7$	$0.004 \cdot 10^7$	$0.002 \cdot 10^7$	$0.001 \cdot 10^7$

Table 5-32: Results of the calibration on March 14th, 2005

Equation of the calibration curve: $y = -1.17 \cdot 10^6 + 1.49 \cdot 10^6 x$ (Equation 14)

Detection limit: 0.011 μ l

30.03.2005	50.05%	35%	19.9%	10.5%
Mean value (n=3)	$7.612 \cdot 10^7$	$5.009 \cdot 10^7$	$2.899 \cdot 10^7$	$1.553 \cdot 10^7$
Standard deviation	$0.012 \cdot 10^7$	$0.002 \cdot 10^7$	$0.002 \cdot 10^7$	$0.007 \cdot 10^7$

Table 5-33: Results of the calibration on March 30th, 2005

Equation of the calibration curve: $y = -1.22 \cdot 10^6 + 1.52 \cdot 10^6 x$ (Equation 15)

Detection limit: 0.012 μ l

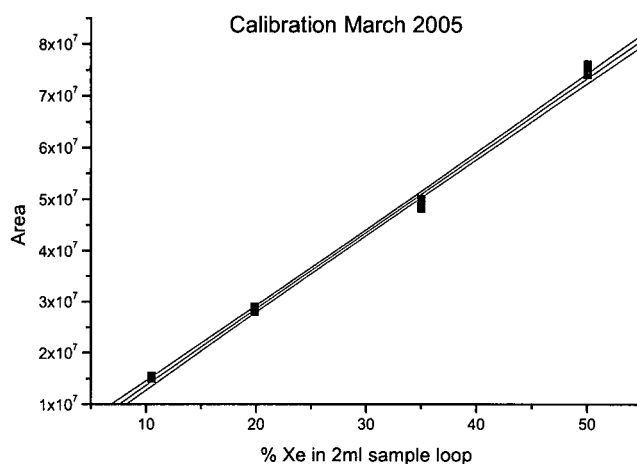


Figure 5-23: Calibration curve March 2005

Equation of the calibration curve: $y = -1.23 \cdot 10^6 + 1.49 \cdot 10^6 x$ (Equation 16)

Calculated detection limit: 0.010 μ l

These regular measurements have shown the stability of the system under different atmospheric conditions like temperature (variations from 21°C to 25°C) and pressure (varied from 991.6 mbar to 995.1 mbar).

During this period the system was never shut down, only the filaments from the TCD and the reference flow for the TCD were turned off.

The detection limit ranges from 567 ppm to 580 ppm; regarding all measurements for the observation period it is 513 ppm. The mean value for the detection limit is $(0.0110 \pm 0.0001) \mu\text{l}$.

5.1.5 Comparison of the calibration data for the validation

The calibration data were intercompared in order to evaluate the reliability. Based on the calibration equation for March 2005 and on the concentration of the gas mixture the calculation for the measurements of February was the following:

$$y = -1.23 \cdot 10^6 + 1.49 \cdot 10^6 x \quad \text{Equation 17: Calibration equation of March}$$

Calculation with data from measurements of February gave following results:

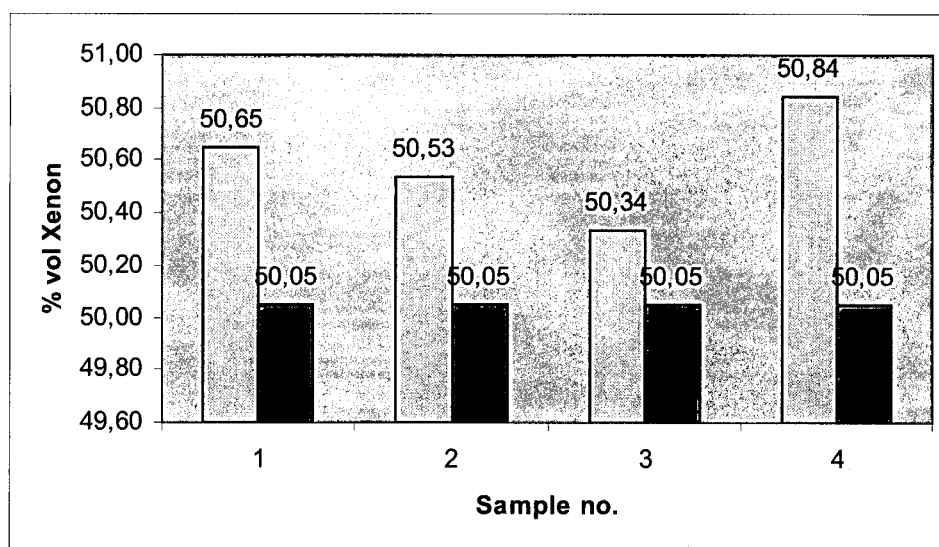


Figure 5-24: Plot of the comparison the calibration of March with the February data for gas mixture 1

Then based on the calibration equation for February 2005 with the results of the measurements from March 2005 the concentration of gas

mixture 1 was calculated:

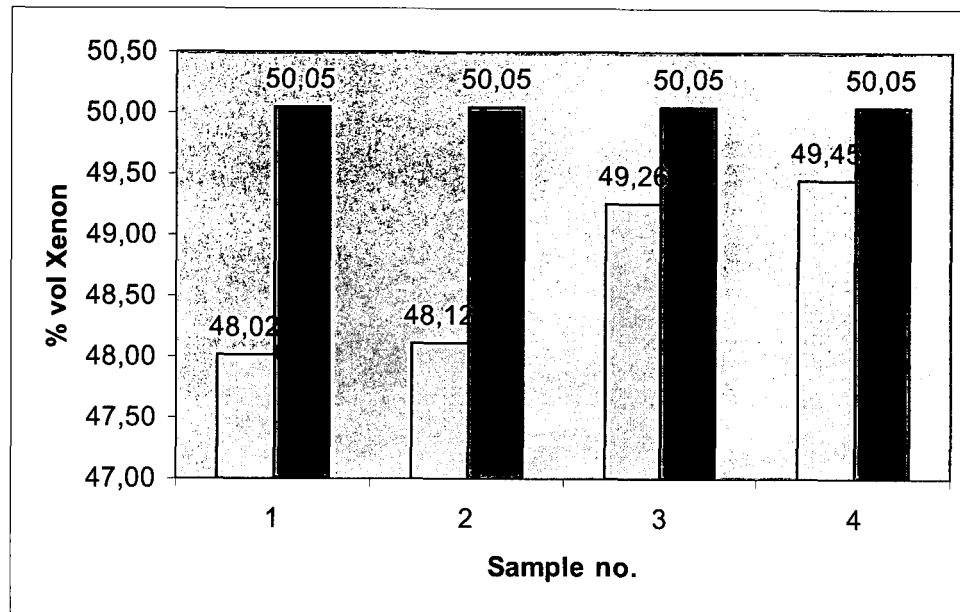


Figure 5-25: Graphic illustration of the comparison of February calibration with the March data for gas mixture 1

These data show a maximum discrepancy of 4.05%, which means that this system has a reliability better than 5%. This means that the volume of archive samples from noble gas stations can be determined with a reliability $\leq 5\%$.

5.1.6 Conclusion

A calibration period of two months has shown that the system is stable and that the values measured are reproducible. Nevertheless, if an IMS sample is analyzed always a calibration measurement has to be performed in advance to make sure that the configuration was not changed (e.g. carrier gas pressure) and for permanent changing of environmental conditions (temperature and pressure).

These experiments have shown that the peak areas [mVs] are constant, if the oven temperature is not shut down and the carrier gas flow is not turned off, only the filament power and the reference flow may be turned off. If the whole system is shut down, a new calibration with different gas standards must be performed and a new calibration line has to be defined.

5.2 Gas transfer

5.2.1 Design

The first step of building up a transfer system (requirements see chapter 5.1.2) was the construction of a system for trapping xenon from the calibration gas mixture after analysis in the gaschromatograph and then the remeasurement.

The aim of this procedure was to demonstrate a possible principle for a transfer system design and for calculation of losses.

Therefore a defined amount of xenon was analyzed and - after detection by TCD - collected in a gas bag which was remeasured for calculation of the loss, and in order to develop a system in which the archive samples are transferred into a gas bag and then analyzed by gaschromatography.

Description of the geometry of the gas bag used for sampling xenon after measurement by the gaschromatograph:

Material: plastic (Tedlar® Gas Sampling Bag) with two fittings:

UK4 Fitting (On/Off Septum Kynar Dual Valve)

JK4NNB4 Fitting (JACO ¼" Kynar Union Fitting w/blind cap)

Volume: 0.6 l

5.2.1.1 Description of the experiment

For the calibration of the gaschromatograph the certified gas mixture containing 35% vol. of xenon and the 2 ml sample loop were used. The xenon fraction was collected in the plastic gas bag for remeasurement.

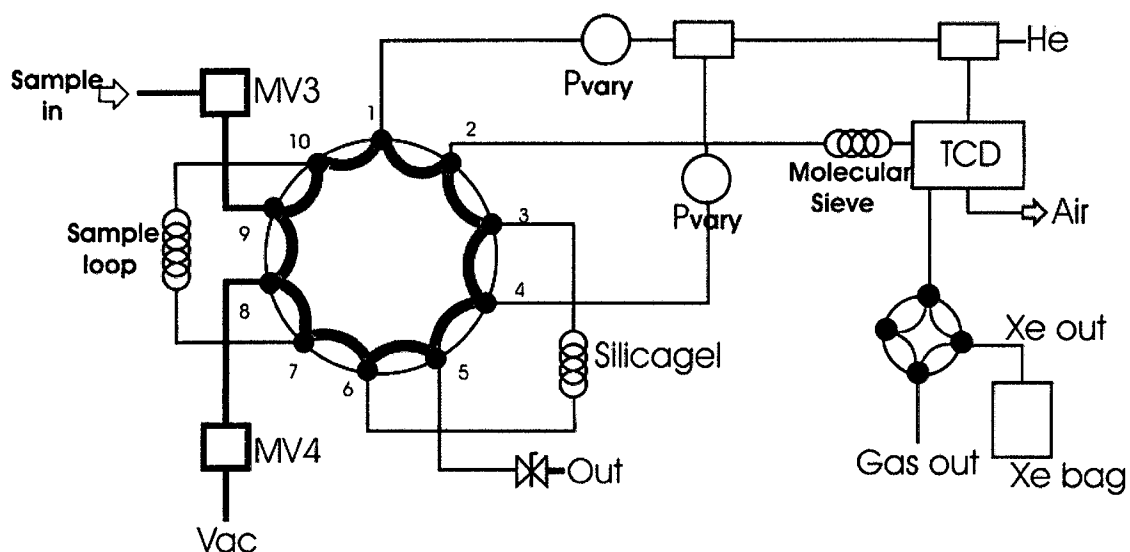


Figure 5-26: Diagram of the connections for the first gas transfer

The inlet "Sample IN" was connected with the gas mixture containing 35% vol. of xenon.

The first step was to inject the sample (calibration gas) under environmental conditions (ambient pressure and room temperature) for three times for the calibration of the chromatograph. Then a sample was injected and after the gaschromatographic analysis xenon was collected in the bag as shown in Figure 5-26 by switching the four port valve to the "Xe out" output (red line in figure). The switching of the four port valve was set two minutes before the retention time of xenon and switching back two minutes after the retention time of xenon. This experiment was performed once, and in this way a total of 0.7 ml of xenon was collected.

Accordingly the geometry was connected with the sample input connection "Sample IN" to the gaschromatograph. The sample loop of the gaschromatograph was evacuated to 4 mbar with a vacuum pump. Then the valve to the vacuum pump was closed and the valve which closed the connection between the sample input into the gaschromatograph and the sample loop was opened so that the gas mixture could flush into the loop. Then all connections were closed again and the sample was analyzed. This

procedure was performed for ten times in a series.

This experiment was carried out with the following oven program:

<i>Oven parameters</i>		<i>TCD parameters</i>	
Initial temperature [°C]	180	Block temperature [°C]	150
Initial time [min]	7	Transfer temperature [°C]	150
Number of ramps	1	Filament temperature [°C]	250
Rate #1[deg/min]	35	Filament voltage [V]	10
Final temperature [°C]	180	Reference flow [ml/min]	30
Hold time (min)	1		

Table 5-34: Parameters for gas transfer

Following table gives an overview of the results of the calibration:

No.	Area [mVs]	Xenon [ml]
1	28902770	0.69
2	30024020	0.71
3	28969300	0.69

Table 5-35: Calibration of the gaschromatograph for 35% vol. xenon

The next table shows the result of trapping of xenon in a gas bag:

Area [mVs]	Xenon [ml]
29447190	0.70

Table 5-36: Amount of xenon collected in the gas bag

Then this sample was taken from the gas bag and measured by ten steps in a series (see table 5-36):

No.	Area [mVs]	Xenon [ml]
01	577335	0.01372404
02	557683	0.01325689
03	577288	0.01372293
04	586173	0.01393413
05	572452	0.01360797
06	549930	0.01307259
07	524307	0.01246349

08	503696	0.01197354
09	494058	0.01174443
10	476800	0.01133419

Table 5-37: Results of the first transfer experiment

The total xenon content of the sample was calculated from the xenon concentration in the sample bag and the flow rate of the carrier gas during the xenon separation ($51,5 \pm 1$ ml)/min.

5.2.1.2 Result

With this experiment it could be demonstrated that $99.7\% \pm 3,1\%$ of the xenon separated could be collected with the carrier gas by directing the gas flow to a separate outlet during the xenon separation. From this result it can be assumed that this process can be performed quantitatively.

5.2.2 "TRANSFER 1"

A transfer line has been developed offering all possibilities, like direct transfer to the sample loop of the gaschromatograph in case the sample volume is small, or freezing out of xenon in a cool trap if the xenon volume is expected to be very large. It is also possible to flush the archive bottle without disconnecting it from the system.

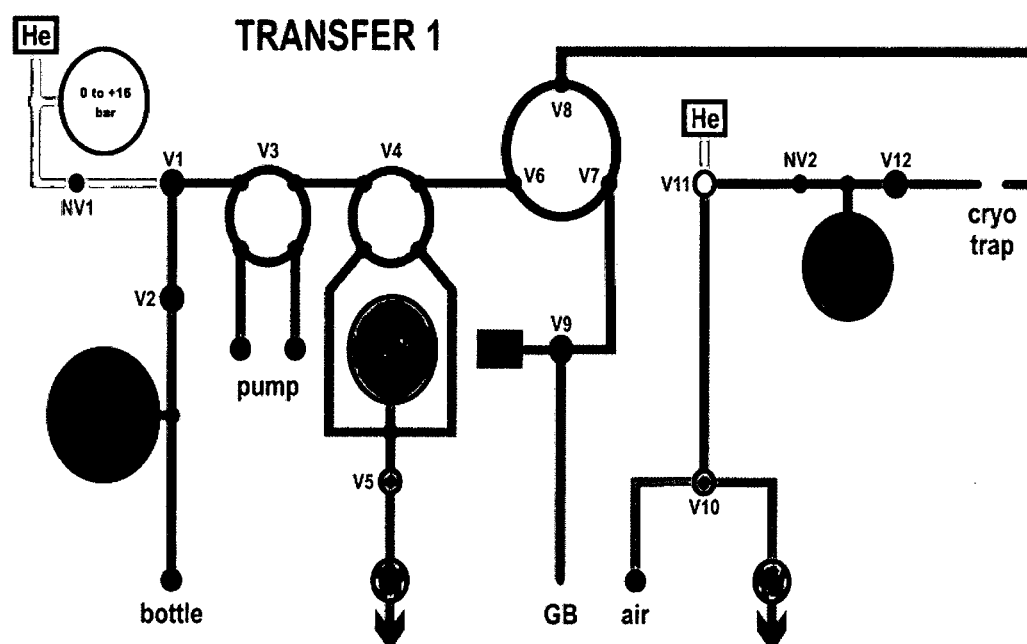


Figure 5-27: Diagram of the connection for the following gas transfers

The advantage of this system is the possibility of handling every type of archive bottle, of filling a bottle with low pressure to atmosphere pressure and the possibility to flush every bottle with Helium without disconnecting it. Due to the integrated cool trap it is possible to reduce the sample volume (freezing out of xenon).

The disadvantage of this system is the long transfer way from the

archive bottle to the sample loop of the gaschromatograph.

Processing

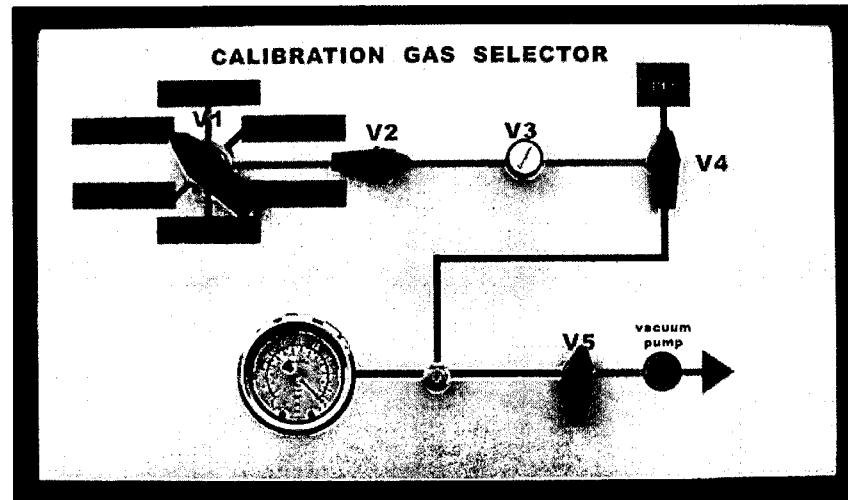


Figure 5-28: Control panel for the calibration of the gaschromatograph and for filling defined amounts of xenon into archive geometries

For testing of this gas transfer system a defined amount of xenon was filled in archive bottles.

General description of experiments with "TRANSFER 1":

The archive bottle was connected with the "bottle"-connection after it was filled with a known volume of xenon. With the "TRANSFER 1"-system it was filled up with helium to atmosphere pressure, flushed over the long transfer way to the sample loop, which was submerged in liquid nitrogen to serve as a cool trap.

5.2.2.1 Proficiency test with "TRANSFER 1"

The aim of this exercise was to gather experience with sample transport times, sample handling (different sample containers, how laboratories get along with them), measurement, and reporting of the results.

The archive container had a volume of 500 ml and the pressure of the bottle was 77 mbar. First measurements of 0.2 ml and 1 ml respectively were performed for the calibration of the gaschromatograph, measurements of 5 ml, 7.2 ml and 7.8 ml respectively were performed in order to test the transfer system and the gaschromatograph for larger sample volumes.

All connections and the transfer line were evacuated and the sample loop of the gaschromatograph was used as a cool trap by submerging it into liquid nitrogen. The transfer of the archive sample to the sample loop was made by means of a vacuum pump. The sample was transferred up to 50 mbar to the loop, and then the bottle was filled with helium up to 1.3 bar, which was then transferred to the loop with the vacuum pump. This process was performed for four times consecutively and then the sample loop was warmed to room temperature with a hot-air gun and then the sample was injected at the following oven and TCD parameters:

<i>Oven parameters</i>		<i>TCD parameters</i>	
Initial temperature [°C]	190	Block temperature [°C]	150
Initial time [min]	10	Transfer temperature [°C]	150
Number of ramps	1	Filament temperature [°C]	250
Rate #1[deg/min]	35	Filament voltage [V]	10
Final temperature [°C]	190	Reference flow [ml/min]	30
Hold time (min)	10		

Table 5-38: Parameters of the gaschromatograph for the gas transfer xenon proficiency test

	0.2 ml	1 ml	5 ml	7.2 ml	7.8 ml	Sample
Area [mVs] 1	$1.501 \cdot 10^7$	$7.276 \cdot 10^7$	$2.573 \cdot 10^8$	$3.494 \cdot 10^8$	$3.363 \cdot 10^8$	$2.119 \cdot 10^8$
Area [mVs] 2		$7.598 \cdot 10^7$				
Area [mVs] 3		$7.312 \cdot 10^7$				
σ		$1.762 \cdot 10^6$				
1 ml	$7.503 \cdot 10^7$	$7.395 \cdot 10^7$	$5.145 \cdot 10^7$	$4.854 \cdot 10^7$	$4.312 \cdot 10^7$	
sample	2.824 ml	2.865 ml	4.118 ml	4.365 ml	4.914 ml	

Table 5-39: Measurements and results of the xenon Exercise November 2004

Under consideration of the measurements before the amount of stable xenon was determined to be (4.45 ± 0.3) ml.

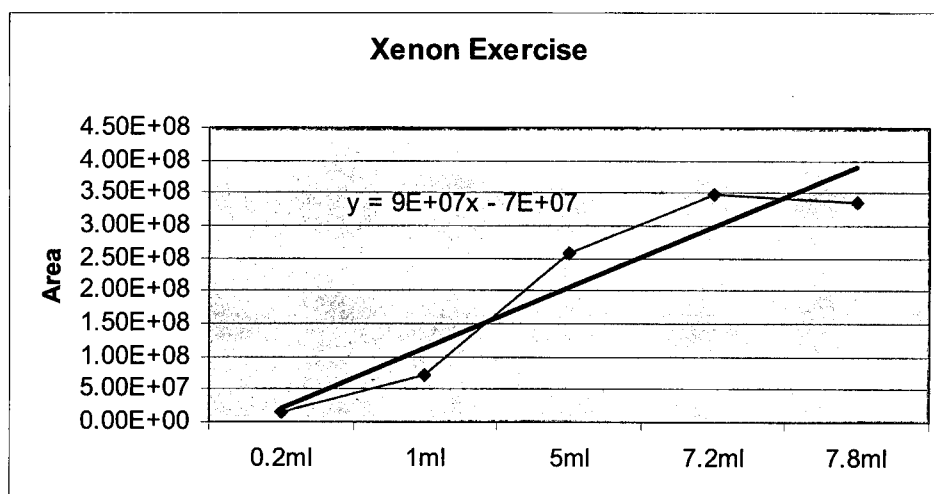


Figure 5-29: Graphic design of the calibration

This experiment has shown that the result was precise since the station had reported the following result: 4.1766 ml.

This result showed as well that the TCD is no longer linear for higher sample volumes (guaranteed linearity in the range of 10^6), therefore it is necessary to split the samples or to calibrate the gaschromatograph for higher sample volumes with determination of the reliability of these data.

5.2.2.2 Results of testing the influence of different pressures in the sample loop during injection

This experiment was performed in order to test both the influence on the analysis of different pressures in the sample loop during injection and the reliability of analysis results, since archive bottles are stored under different storage conditions (see chapter 5.1).

The first step was to vary the pressure of the gas in the sample loop during sample injection; by this procedure the amount of xenon could be raised and effects for different sample injection pressures could be evaluated.

Different sample injection pressures were first performed with a calibration mixture containing 50% vol. of xenon:

Atmosphere pressure (1013 mbar): 1ml is equivalent to the following area [mVs]: 73252780 with a retention time of the peak of $t = 4.66\text{min}$

Measurements with 3.5 bar overpressure (this equivalent to an amount of xenon of 3.48 ml in the sample loop):

First measurement: Area [mVs] = 238520000, retention time = 4.29 min

This area [mVs] is equivalent to an amount of 3.22 ml of xenon

Second measurement: Area [mVs] = 238420700, retention time = 4.29 min

This area [mVs] is equivalent to an amount of 3.22 ml of xenon

The two last results show a good stability of the gaschromatograph for higher sample volumes, but it also shows that the TCD is no longer linear for higher sample volumes since the measurement differs from calculation by 7.47%.

Other experiments were performed with a calibration gas mixture containing 10% vol. of xenon.

Measurement under environmental conditions (atmosphere pressure) resulted in an area [mVs] of 14937100 (corresponding to an amount of 0.2 ml of xenon) with a peak retention time of $t = 5.05$ min.

Two measurements were performed with an overpressure of 3.5 bar and the third (last) measurement was performed with an overpressure of 5 bar:

Pressure [bar]	Calculated volume [ml]	Measured volume [ml]	Area [mVs]	Retention time [min]
3.5	0.7	0.68	50251780	4.9567
3.5	0.7	0.68	50358150	4.9567
5	0.99	0.96	70204400	4.9617

Table 5-40: Results of sample injection with varying pressures with a gas mixture containing 10% vol. of xenon

These experiments have demonstrated that the TCD is no longer linear for large sample volumes (see experiments with 50% vol. xenon). For the same experiment with 10% vol. xenon the pressure in the sample loop could be risen even up to 5 bar and the result differs about 3% from calculation.

Since the system is calibrated on peak area [mVs] different pressures do not have an impact on the results of the analysis (as shown in chapter 5.1.3.5 the baseline changes) as long as the baseline is constant during the analysis of one peak.

5.2.3 Testing of the gas transfer system by using the sample loop of the gaschromatograph as cool trap with liquid nitrogen

The bottle ($V = 0.14951 \pm 0.00050$ l) was flushed two times with a gas mixture containing 50% vol. xenon (filling up to 1 bar and then evacuating two times consecutively), afterwards it was filled up to 0.015 bar with the gas mixture 1 on the calibration gas selector (see Figure 5-28). Additionally, after connecting it with the "TRANSFER 1" system it was filled up to 0.5 bar with helium.

The system was evacuated up to 0.002 mbar, the sample loop was put in liquid nitrogen and then the valve of the archive bottle was opened and the sample was slowly transferred over the cooled loop by means of a vacuum pump.

Time-Pressure-Table:

Time	Pressure [bar]	Comment
0	0.5	
10s	0.481	
20s	0.480	
1 min	0.475	
2.5 min	0.465	
3 min	0.461	
4min 15s	0.452	
6 min	0.441	
7 min	0.435	
10 min	0.417	Till this point max flow 30ml/min, needle valve closed, then opened slightly
15 min	0.386	
20 min	0.356	
25 min	0.328	
30 min	0.213	Needle valve opened slightly more
35 min	0.143	
40 min	0.111	Needle valve opened still more
45 min	0.071	
60 min	0.031	Needle valve opened completely

65 min	0.024	
75 min	0.016	
80 min	0.012	
90 min	0.008	

Table 5-41: Decreasing of the pressure by carefully raising the flow of the sample and the time needed.

Then the valves of the sample loop were closed and the loop was warmed slowly to room temperature before the injection into the gaschromatograph for analysis.

The measurement for the calibration and the result of this experiment is given in Table 5-42:

Gas mixture	Area [mVs]	Retention time [s]	Xenon amount [ml]
50% calibration	76251860	4.82	1
50% calibration	76596820	4.82	1
35% calibration	50348400	4.9667	0.7
20% calibration	29241930	5.11	0.4
10% calibration	15613240	5.2267	0.2
Bottle - 1ml	63103600	4.8367	0.86 in sum relating to measurements of 50% gas
Rest in connections/sample loop	2473138	5.4117	

Table 5-42: Results of the measurements for the analysis of the transfer experiment

The length of the connections from the bottle to the sample loop was about 150 cm, the inner diameter of them was 1/16" which is equivalent to 0.16 cm, which means that the dead volume is in the range of 2 ml. This large dead volume causes a transfer loss of 14%.

For the next transfer experiment the gaschromatograph was calibrated with the gas mixture containing 10% vol. of xenon corresponding to an amount of xenon of 0.2 ml.

This measurement resulted in a peak area [mVs] of $1.55 \cdot 10^7$, therefore the area [mVs] of 1 ml can be calculated to be $7.76 \cdot 10^7$, and this value is in

the range of linearity as can be seen from the results of the calibration measurements with the 50% vol. gas mixture.

The archive bottle (volume of 0.14951 l) was flushed two times with the gas mixture containing 50% vol. of xenon and then filled with 0.014 bar of this gas. The bottle was connected with "TRANSFER 1". Before opening the valve the system was flushed with helium and evacuated till 0.002 bar, then the valve was opened and the measurement of the pressure resulted in $p = 0.013$ bar.

Valve V4 of the gaschromatograph (connection with the vacuum pump) was closed, so that there was no connection with the vacuum pump. The archive bottle was filled with helium up to 1.001 bar, then the valve (connection to the gaschromatograph) was opened, and the gas flushed over the sample loop cooled with liquid nitrogen. After seven minutes valve V4 was opened .

After $t = 33$ min the pressure was $p = 0.565$ bar; the bottle was filled with helium up to $p = 1.021$ bar, then the gas was again frozen out in the sample loop up to $p = 0.664$ bar, and then again the bottle was filled with helium up to $p = 2.000$ bar and then frozen out until $p = 0.327$ bar, where the needle valve was opened a little bit.

The analysis resulted in the measurement of an area [mVs] of $7.765 \cdot 10^7$ which corresponds to an amount of 1.001 ml of xenon.

This experiment was repeated with the gas mixture containing 10% vol. of xenon. The archive bottle was flushed with this gas mixture and then filled up to $p = 0.068$ bar with this gas. The sample loop was evacuated and frozen out during filling the bottle with the sample. Then helium was added to the calibration gas system till the pressure reached a value of $p = 1.168$ bar. For this approach the bottle was closed, the connections were

evacuated, flushed with helium for three times and then the bottle was filled.

The measurement of the pressure after connection of the bottle with "TRANSFER 1" resulted in $p = 1.050$ bar. For freezing out the sample valve V4 was opened, so that the connection with the vacuum pump was given. The sample was flushed over the cooled loop until the pressure amounted to $p = 1.002$ bar, then the bottle was filled with helium till $p = 2.000$ bar; before the bottle was filled with helium to $p = 1.102$ bar again, the pressure had been $p = 0.644$ bar, and finally the pressure was $p = 0.602$ bar. The analysis resulted in a peak area [mVs] of $5.556 \cdot 10^7$ which corresponds to an amount of 0.73 ml of xenon. In this case the calculated loss amounts to 26.71%.

Since the result of this experiment was not satisfactory it was slightly modified and repeated.

The bottle was flushed and filled with a gas mixture containing 10% vol. xenon up to $p = 0.069$ bar, was then connected with "TRANSFER 1", which before had been flushed with helium and evacuated; then the pressure in the bottle was measured with the result of a pressure of $p = 0.066$ bar (the system was evacuated before up to $p = 0.002$ bar), then helium was added up to $p = 2.550$ bar. The vacuum pump was turned off, and valve V3 of the gaschromatograph (connection between the transfer system and the sample loop) was opened and valve V4 (connection between sample loop and vacuum pump) was closed. Opening of valve V4 resulted in a pressure of $p = 1.500$ bar. After the pressure had reached a value of $p = 1.140$ bar, the bottle was again filled with helium up to $p = 2.880$ bar and this mixture was frozen out up to $p = 1.028$ bar. During this step the needle valve was slightly open. Then the vacuum pump was turned on and the gas was flushed over the frozen out sample loop till the pressure reached a value of $p = 0.125$ bar. Then the sample loop was warmed to room temperature and analyzed. The measurement resulted in a peak area [mVs] of $5.392 \cdot 10^7$ which corresponds

to 0.71 ml – in this case the transfer loss was calculated to be 28.87%.

The following transfer experiment again was performed with the 50% vol. xenon gas mixture in order to reproduce the satisfactory results already reached. The bottle was flushed with this gas mixture and then filled up to $p = 0.017$ bar. Connection to "TRANSFER 1" showed a pressure of $p = 0.016$ bar and the bottle was filled with helium up to 1.001 bar. By means of the vacuum pump the sample was frozen out to $p = 0.490$ bar, then filled with helium to $p = 1.010$ bar, frozen out up to $p = 0.369$ bar, again filled to $p = 2.043$ bar with helium, and finally frozen out to $p = 0.326$ bar. The analysis of this sample resulted in an area [mVs] of $6.759 \cdot 10^7$ corresponding to an amount of 0.89 ml xenon, which means a transfer loss of 10.77%.

Since the transfer loss could be reduced significantly this experiment was repeated with a gas mixture containing 10% vol. of xenon. During flushing the bottle with helium the sample loop was frozen out. First step was the closing of valve V3 of the gaschromatograph (connection between transfer line and sample loop) and then the closing of valve V4 (connection between sample loop and vacuum pump). Afterwards the switching mechanism was changed from the "calibration" position to the "sample" position.

The archive bottle ($V = 0.14951$ l) was flushed two times with 1.5 bar xenon 10% vol., then the system was again evacuated and finally filled with the gas mixture up to a pressure of $p = 0.075$ bar.

The connections of "TRANSFER 1" were evacuated up to 0.002 bar, the bottle was connected with this system and the measurement of the pressure showed a pressure of $p = 0.073$ bar. The bottle was filled with helium to $p = 2.002$ bar, the connection to the transfer line was opened and valve V3 was opened, so the gas flushed over the frozen out sample loop. The pressure decreased to $p = 1.862$ bar after opening the valve V3, then

valve V4 was opened and after $t = 30$ min the pressure was $p = 1.800$ bar. Since the pressure was decreasing very slowly, the vacuum pump was turned on and after $t = 20$ min the pressure reached the value $p = 0.967$ bar. Opening of the needle valve slightly resulted in a pressure of $p = 0.372$ bar after $t = 60$ min. Still waiting for the emptying of the bottle, the pressure was $p = 0.180$ bar after $t = 30$ min, then $p = 0.111$ bar again after further $t = 30$ min. At this point the needle valve was opened slightly and after $t = 30$ min the pressure was $p = 0.047$ bar.

At this point the bottle was filled with helium up to $p = 1.007$ bar and by means of the vacuum pump the sample was transferred over the frozen sample loop until $p = 0.238$ bar.

Then the sample loop was warmed to room temperature and the analysis of the sample showed a peak area [mVs] of $6.240 \cdot 10^7$ which corresponds to an amount of 0.82 ml of xenon. The transfer loss was calculated to be 18.16%, which is better than the results of the experiments with the gas mixture containing 10% vol. of xenon which were performed before, but still the loss was too high.

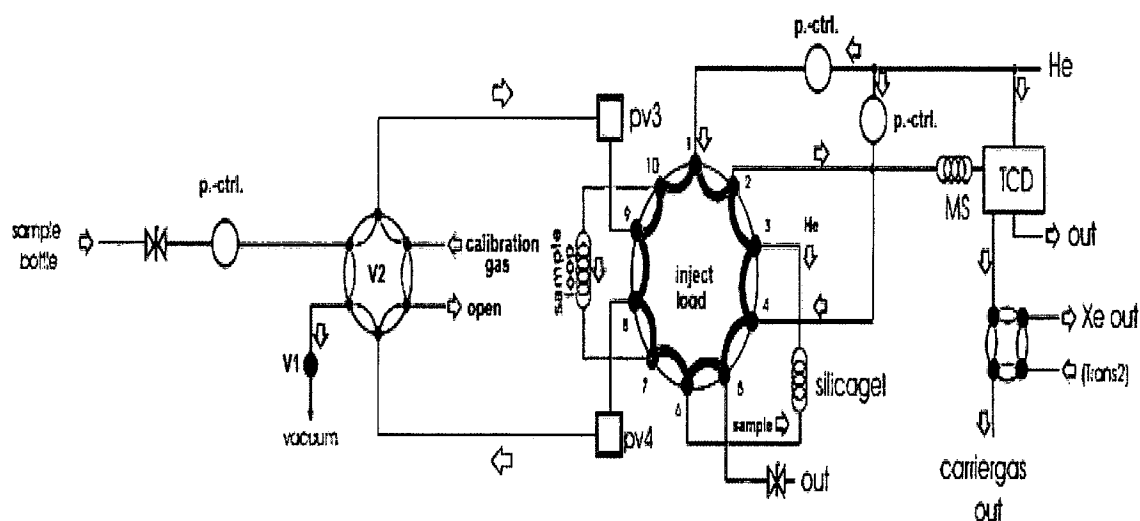


Figure 5-30: Diagram of the connections for following gas transfer experiments

In order to shorten the transfer way, the system "TRANSFER 1" was excluded and a shorter transfer line with a manometer for controlling the pressure in the sample bottle and a needle valve was installed (see Figure 5-30).

The bottle was flushed two times with 10% vol. of xenon and then filled up to 0.072 bar. Then helium was added up to 1.522 bar using the following procedure:

The bottle was closed, the connections were evacuated, flushed for three times with helium, and then the bottle was opened and filled up to 1.522 bar with helium.

Then the transfer system was evacuated to 2.8 mbar (connected with the closed archive bottle). The vacuum pump was turned off, the bottle was opened, and the pressure was $p = 1470.8$ mbar. Opening of valve V3 lead to a pressure of $p = 1391.8$ mbar, after $t = 15$ min the pressure was 1389.0 mbar, opening of valve V4 resulted in a pressure of $p = 1348.2$ mbar, after $t = 10$ min it was reduced to 1346.1 mbar.

The valves were closed, the sample loop was warmed, and the sample was analyzed. The result showed an amount of xenon of 0.16ml, therefore the next step was carried out. By means of the vacuum pump the bottle was slowly pumped out over the frozen sample loop down to 8.5 mbar, which resulted in 0.58 ml of xenon. Altogether the total quantity of xenon transferred was 0.74 ml and the transfer loss was 25.83%

5.2.4 Pumping the sample back and forth through the frozen sample loop

First the calibration of the gaschromatograph was evaluated with gas mixture 1. This measurement showed an area [mVs] of 76499760 which corresponds to 1 ml of xenon and was in the range of earlier calibrations.

For the transfer experiment the bottle was flushed two times with 10% vol. of xenon (2 bar) and then filled up with it to 0.077 bar (corresponding to 0.7 ml of xenon). The system was evacuated to 6.8 mbar.

Opening of the bottle showed a pressure of $p = 70.7$ mbar, when valve V3 was opened the pressure was $p = 66.9$ mbar, and when valve V4 was opened it was $p = 59.1$ mbar.

Pumping:	out	$p = 40$ mbar
	In	$p = 61.2$ mbar
	Out	$p = 38.9$ mbar
	In	$p = 61.9$ mbar
	Out	$p = 39.5$ mbar
	In	$p = 63.0$ mbar
	Out	$p = 37.4$ mbar
	In	$p = 63.1$ mbar
	Out	$p = 37.0$ mbar
	In	$p = 63.3$ mbar

The result of this analysis showed an amount of xenon of 0.58 ml (area [mVs] = 44556500), which means a transfer loss of 17%.

For the next experiment the small archive bottle was flushed two times with 10% vol. of xenon and then filled up to $p = 0.072$ bar. It was connected with the transfer system, the pressure first was $p = 70.8$ mbar (valves V3 and V4 closed) and then (V3 and V4 open) $p = 66.5$ mbar.

Process of pumping:

Pumping	Pressure [mbar]
In	46.8
Out	65.2
In	48.2
Out	65.4
In	57.9
Out	65.4

Table 5-43: Pressures during pumping

Measurement with the gaschromatograph showed that the amount of xenon transferred was 0.67 ml (area [mVs] = 51388110).

5.2.4.1 Calibration with new calibration gas mixtures

The first step was the calibration of the gaschromatograph with new gas mixtures containing xenon in vol % as given in Table 5-44:

Gas mixture	Area [mVs]	Retention time [min]	Xenon amount [ml]
50%	76748630	4.86	1
50%	77165390	4.88	1
10%	15518270	5.21	0.2
1%	1544191	5.36	0.02
0.1%	158053	5.42	0.002

Table 5-44: Results for the calibration of the gaschromatograph

After the calibration a new transfer experiment was performed.

The experiment was repeated with xenon 0.1% vol., the bottle was flushed and then filled with $p = 1442.0$ mbar (corresponding to 0.7 ml xenon).

With the same procedure the following pressures could be measured during the process of pumping:

No.	Pumping	Pressure [mbar]
1	Out	722
	In	1343
2	Out	722
	In	1342
3	Out	722
	In	1341
4	Out	723
	In	1340
5	Out	723
	In	1340
6	Out	724
	In	1339
7	Out	724
	In	1338
8	Out	724
	In	1337
9	Out	724
	In	1336
10	Out	723
	In	1335

Table 5-45: Pressures during pumping

The measurement showed a result of 0.58 ml, which means a transfer loss of 17.14%.

This experiment as well was repeated, but the pumping process was performed for twenty times, which resulted in a transfer of 0.56 ml xenon. However the quantity ought to have been 0.68 ml, which means that the loss was 17.64%.

After a following injection into the gaschromatograph additional 8.3 μ l could be found, so that the total amount was 0.57 ml of xenon and the transfer loss was 16.18%.

Under the assumption that there might still be a rest in the bottle, the procedure was repeated by cooling the sample loop in liquid nitrogen and pumping the sample again for five times. The result of this step was, that additionally 0.3 ml could be found. This procedure was repeated, and at this point further 0.01 ml were found. This means, by adding up all the single results the whole amount of xenon transferred is 0.61 ml and therefore the total transfer loss is 10.29%.

The experiment was repeated again with the large bottle ($V = 492.68$ ml), which was flushed three times and then filled up to $p = 1532$ mbar with Xe 0.1% vol. which corresponds to 0.75 ml. The pumping process was performed slowly for five times meaning that every step (out and in) lasted 10 minutes. Pressures can be seen in following table:

No.	Pumping	Pressure [mbar]
1	Out	769
	In	1427
2	Out	769
	In	1424
3	Out	769
	In	1420
4	Out	768
	In	1418
5	Out	766
	In	1417

Table 5-46: Pressures during pumping

Following results could be achieved this time: Area [mVs] = 50087129 = 0.66 ml (loss of 12%).

A new calibration was performed after the experiment, and with the new calibration 1 ml corresponds to an area [mVs] of 74868700. The amount measured was recalculated and the result was a quantity of 0.67 ml, which means a transfer loss of 10.67%.

5.2.5 *Transfer by adsorption on activated charcoal*

For this new transfer line a new sample loop was built equipped with activated charcoal for trapping xenon. The aim was the adsorption of the whole xenon present in the sample since losses with other transfer experiments are too high.

This new sample loop had a volume of (4.47 ± 0.05) ml and was made of stainless steel.

The gaschromatograph was calibrated three times with the gas mixture containing 10% vol. of xenon.

Processing for this transfer is a combination of adsorption and of pumping the sample back and forth for complete adsorption.

The small archive bottle was filled with 1% vol. xenon up to 504 mbar, which corresponds to 0.75 ml xenon in the bottle.

First the sample loop containing the activated charcoal was flushed with helium, and the system was evacuated and then the sample was connected with the transfer line. Then the valve of the bottle was opened and the sample was pumped back and forth for ten times with the sample loop submerged in liquid nitrogen.

The sample loop was warmed with a hot air gun up to $T = 190^{\circ}\text{C}$ and the measurement resulted in an area [mVs] of 52529530 which corresponds to 0.73 ml (calibration with an amount of 0.45 ml xenon resulted in an area [mVs] of 32178510). This result shows that 98% of the sample was detected.

This measurement was repeated and again the loss was in the same range (transfer of 97%).

6 Preparation of radioactive xenon isotopes

6.1 Introduction

For the preparation of relevant xenon isotopes samples containing 1 µg of 90% enriched U-235 were irradiated at the TRIGA (Training, Research, Isotope Production, General Atomic) Mark II research reactor at the Atomic Institute of the Austrian Universities in Vienna.

The reactor is a swimming pool reactor, which means that the reactor core is inside a pool filled with deionised, distilled water. This water serves both as coolant and as moderator [Friedlander *et. al.*, 1964].

The reactor core consists of 80 fuel elements and the fuel contains 20% uranium 235. There are different types of irradiation arrangements, the important ones for this work were the central irradiation tube in the centre of the core (neutron flux: $10^{13} \text{ cm}^{-2} \text{ s}^{-1}$) and the five reflector irradiation tubes (neutron flux: $1.7 \cdot 10^{12} \text{ cm}^{-2} \text{ s}^{-1}$).

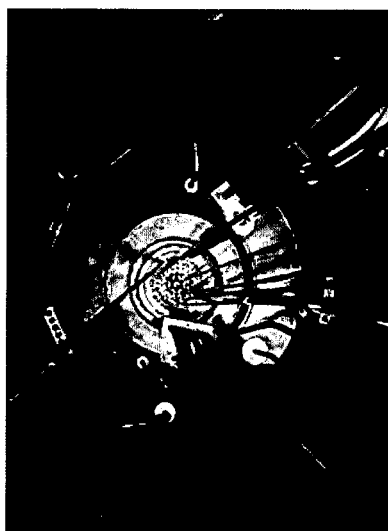


Figure 6-1: Reactor core TRIGA-Mark II Research reactor

The first irradiation was performed for testing whether these isotopes could be prepared and for an estimation of the activity of the irradiated sample. The result of this experiment was that all relevant isotopes could be produced and therefore calculations were performed first by solving the differential equations, which include building up and decay during irradiation and after irradiation taking into account growing in of daughters by decay of their mother. Then detailed calculations were performed using the program ORIGEN 2.2 designed for reactor burn-up calculations.

6.2 Calculations

Derivation and solution of differential equations

These calculations for xenon are based up on the relevant isobaric decay scheme. In the following the decay schemes are listed, where the number under the element gives the half life and the number in the boxes gives the branching ratio.

6.2.1.1 Xe-131m

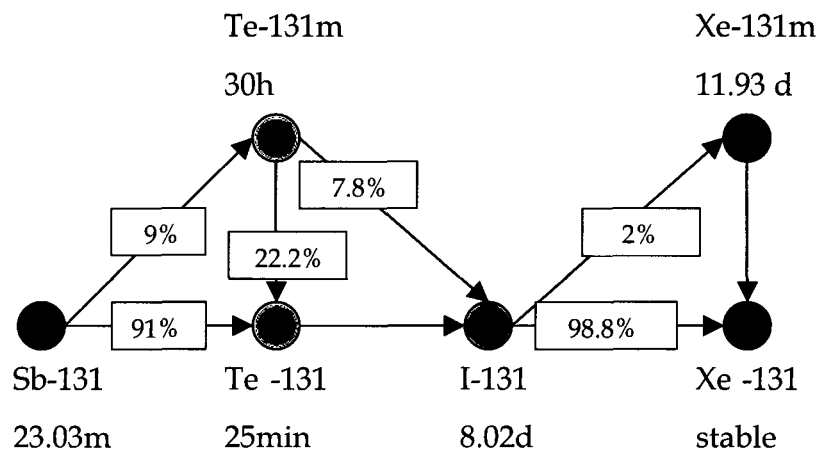


Figure 6-2: Decay scheme for the relevant isobaric chain 131

Nuclide	Independent fission yield	Cumulative fission yield
In-131	$1.11 \cdot 10^{-2}$	$2.49 \cdot 10^{-2}$
Sn-131	$8.81 \cdot 10^{-1}$	$9.06 \cdot 10^{-1}$
Sb-131	1.65	2.56
Te-131m	$2.33 \cdot 10^{-1}$	$4.12 \cdot 10^{-1}$
Te-131	$9.7 \cdot 10^{-2}$	2.55
I-131	$3.92 \cdot 10^{-3}$	2.89
Xe-131m	$3.48 \cdot 10^{-7}$	$4.05 \cdot 10^{-2}$

Table 6-1: Independent and cumulative fission yield per 100 fissions of isobaric chain 131 for U-235, thermal fission [data taken from: England and Rider, 1993]

Nuclide	Half life $T_{1/2}$ [s]	Decay constant λ [s^{-1}]
In-131	0.280 ± 0.003	2.48
Sn-131	39 ± 2	0.02
Sb-131	1380 ± 120	$5.02 \cdot 10^{-4}$
Te-131m	$1.08 \cdot 10^8 \pm 7.20 \cdot 10^3$	$4.62 \cdot 10^{-4}$
Te-131	1500 ± 6	$6.42 \cdot 10^{-6}$
I-131	$6.95 \cdot 10^5 \pm 8.64 \cdot 10^2$	$9.98 \cdot 10^{-7}$
Xe-131m	$1.03 \cdot 10^6 \pm 8.64 \cdot 10^2$	$6.47 \cdot 10^{-7}$

Table 6-2: Half life and decay constant for mass 131 [data taken from ENDF/B-IV]

With the known parameters like decay constant, neutron flux, neutron cross section for xenon and Iodine, cumulative and independent fission yields and half times differential equations for the calculation of the build up and decay of the xenon isotopes can be solved.

First the number of neutrons during irradiation was calculated by equation 17:

$$\Phi = \phi \cdot t$$

Equation 17: Number of neutrons during a defined irradiation interval

where

Φ ... Number of neutrons (fluence) during irradiation

ϕ ... Neutron flux [$\text{cm}^{-2} \text{s}^{-1}$]

t ... Irradiation time [s]

Calculation from direct decay of the mother nuclide is done with equation 18:

$$N_1(t) = N_0 \cdot \frac{\lambda_0}{\lambda_1 - \lambda_0} \cdot (e^{-\lambda_0 t} - e^{-\lambda_1 t})$$

Equation 18: Number of daughter nuclides by direct decay of the mother nuclide

where

$N_1(t)$... Number of daughter nuclides after time t by decay of the mother

N_0 ... Number of mother nuclides for $t = 0$

λ_0 ... Decay constant of the mother

λ_1 ... Decay constant of the daughter

The following differential equation includes the in-growth from Xe-135m by Iodine and decay of it:

$$\frac{dN_{\text{Xe131m}}}{dt} = \lambda_{\text{Jm}} N_{\text{J}} - N_{\text{Xe131m}} \cdot \sigma_{\text{a,Xe131m}} \cdot \Phi - \lambda_{\text{Xe131m}} N_{\text{Xe131m}} + \mu_{\text{Xe131m}} \Sigma_f \Phi$$

Equation 19: Approach for the calculation of Xe-131m

where

N_{Xe131m} ... Number of Xe-131m atoms

λ_{Jm} ... Decay constant of decaying from I-131 \rightarrow Xe-131m [s^{-1}]

N_{J} ... Number of I-131 atoms

λ_{Xe131m} ... Decay constant of Xe-135m [s^{-1}]

$\sigma_{a,Xe-131m}$... Cross section for absorption of Xe-131m [10^{-24} cm^2]

Φ ... Neutron flux [$\text{cm}^{-2} \text{ s}^{-1}$]

μ_{Xe131m} ... direct relative fission yield for Xe-131m ($\mu_{Xe131m} = 4.05 \cdot 10^{-4}$)

Σ_f ... macroscopic cross section for fission, calculated by Equation 23

Initial condition:

for $t = 0$

$$N_J(0) = N_{Xe131m}(0) = 0$$

Equation 20: Initial condition for solving the differential equation

with

$$N_J(t) = \frac{\mu_J \Phi \Sigma_f}{\lambda_J} \cdot (1 - e^{-\lambda_J t})$$

Equation 21: Equation for the number of Iodine atoms at time t

where

$N_J(t)$... Number of Iodine atoms at time t

μ_J ... direct relative fission yield for I-135 ($\mu_J = 2.89 \cdot 10^{-2}$)

Φ ... Neutron flux [$\text{cm}^{-2} \text{ s}^{-1}$]

Σ_f ... macroscopic cross section for fission, calculated by Equation 23

λ_J ... Decay constant for I-131 [s^{-1}]

Solution for Xe-131m:

$$N_{Xe131m}(t) = \lambda_{Jm} \frac{\mu_J \Phi \Sigma_f}{\alpha \cdot \lambda_J} (1 - e^{-\alpha t}) - \lambda_{Jm} \frac{\mu_J \Phi \Sigma_f}{\lambda_J (\alpha - \lambda_J)} (e^{-\lambda_J t} + e^{-\alpha t}) + \frac{1}{\alpha} \mu_{Xe131m} \Sigma_f \Phi (1 - e^{-\alpha t})$$

Equation 22: Solution for Xe-131m

where

N_{Xe131m} ... Number of Xe-131m atoms

λ_{jm} ... Decay constant of decaying from I-131 \rightarrow Xe-131m [s^{-1}]

μ_{j} ... direct relative fission yield for I-131 ($\mu_{\text{j}} = 2.89 \cdot 10^{-2}$)

Φ ... Neutron flux [$\text{cm}^{-2} \text{s}^{-1}$]

Σ_{f} ... macroscopic cross section for fission, calculated by Equation 23

$$\Sigma_{\text{f}} = \frac{m \cdot A \cdot \rho \cdot \sigma_{\text{f}}}{A} [10^{-24} \text{ cm}^2]$$

Equation 23: Calculation of the macroscopic cross section for U-235

where

m ... mass in [g], 90% enriched U-235

A ... Avogadro constant ($A = 6.0221415 \cdot 10^{23} \text{ mol}^{-1}$)

ρ ... Density of natural uranium ($\rho = 18.7 \text{ g/cm}^3$)

σ_{f} ... Cross section for neutron induced fission (for U-235: $577 \cdot 10^{-24}$; [Smidt, 1971])

α ... $\alpha = \sigma_{\text{a, Xe131m}} \cdot \Phi + \lambda_{\text{Xe131m}}$

λ_{j} ... Decay constant of I-131 [s^{-1}]

λ_{Xe131m} ... Decay constant of Xe-131m [s^{-1}]

$\sigma_{\text{a, Xe-131m}}$... cross section for absorption of Xe-131m [10^{-24} cm^2]

μ_{Xe131m} ... direct relative fission yield for Xe-131m ($\mu_{\text{Xe131m}} = 4.05 \cdot 10^{-4}$)

6.2.1.2 Xe-133m and Xe-133

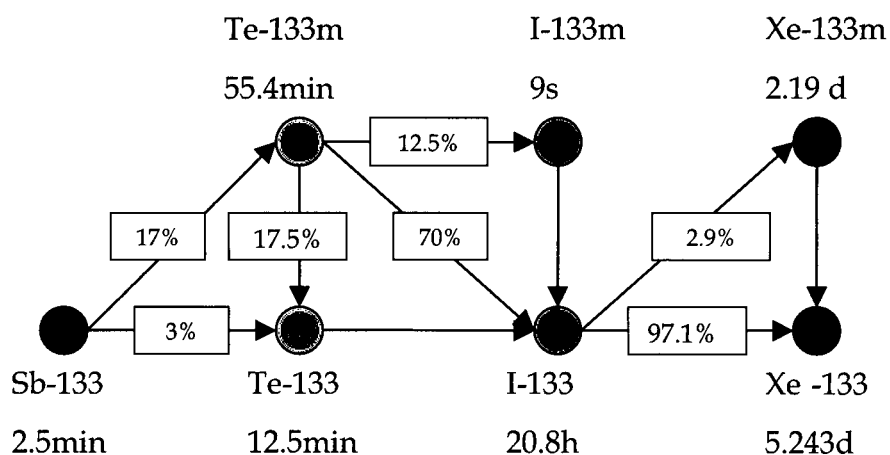


Figure 6-3: Decay scheme for the relevant isobaric chain 133

Nuclide	Independent fission yield	Cumulative fission yield
Sb-133	2.26	2.40
Te-133m	2.99	3.99
Te-133	1.15	3.06
I-133	$1.65 \cdot 10^{-1}$	6.70
Xe-133m	$1.89 \cdot 10^{-3}$	$1.89 \cdot 10^{-1}$
Xe-133	$6.66 \cdot 10^{-4}$	6.7

Table 6-3: Independent and cumulative fission yield per 100 fissions of isobaric chain 133 for U-235, thermal fission [data taken from: England and Rider, 1993]

Nuclide	Half life $T_{1/2}$ [s]	Decay constant λ [s^{-1}]
Sb-133	150 ± 6	0.005
Te-133m	3324 ± 24	$2.09 \cdot 10^{-4}$
Te-133	750 ± 18	$9.24 \cdot 10^{-4}$
I-133	$7.49 \cdot 10^4 \pm 3.60 \cdot 10^2$	$9.26 \cdot 10^{-6}$
Xe-133m	$1.89 \cdot 10^5 \pm 8.64 \cdot 10^2$	$3.66 \cdot 10^{-6}$
Xe-133	$4.53 \cdot 10^5 \pm 8.64 \cdot 10^1$	$1.53 \cdot 10^{-6}$

Table 6-4: Half life and decay constant for mass 133 [data taken from ENDF/B-IV]

The following differential equation includes the in-growth from Xe-133 by Iodine and Xe-133m and its decay:

$$\frac{dN_{Xe133}}{dt} = \lambda_{J_x} N_J + \lambda_{Xe133m} N_{Xe133m} - N_{Xe133} \cdot \sigma_{a,Xe133} \cdot \Phi - \lambda_{Xe133} N_{Xe133} + \mu_{Xe133} \Sigma_f \Phi$$

Equation 24: Approach for the calculation of Xe-133

where

N_{Xe133} ... Number of Xe-133 atoms

λ_{J_x} ... Decay constant of decaying from I-133 \rightarrow Xe-133m \rightarrow Xe-133 [s^{-1}]

N_J ... Number of I-133 atoms

λ_{Xe133m} ... Decay constant of Xe-133m [s^{-1}]

N_{Xe133m} ... Number of Xe-133m atoms

N_{Xe133} ... Number of Xe-133 atoms

$\sigma_{a,Xe-133}$... cross section for absorption of Xe-133 [10^{-24} cm^2]

Φ ... Neutron flux [$\text{cm}^{-2} \text{ s}^{-1}$]

λ_{Xe133} ... Decay constant of Xe-133 [s^{-1}]

μ_{Xe133} ... direct relative fission yield for Xe-133 ($\mu_{Xe133} = 6.70 \cdot 10^{-2}$)

Σ_f ... macroscopic cross section for fission, calculated by Equation 23

The following differential equation includes the in-growth from Xe-133m by Iodine and its decay:

$$\frac{dN_{Xe133m}}{dt} = \lambda_{J_m} N_J - N_{Xe133m} \cdot \sigma_{a,Xe133m} \cdot \Phi - \lambda_{Xe133m} N_{Xe133m} + \mu_{Xe133m} \Sigma_f \Phi$$

Equation 25: Approach for the calculation of Xe-133m

where

N_{Xe133m} ... Number of Xe-133m atoms

λ_{Jm} ... Decay constant of decaying from I-133 \rightarrow Xe-133m [s^{-1}]

N_{J} ... Number of I-133 atoms

λ_{Xe133m} ... Decay constant of Xe-133m [s^{-1}]

$\sigma_{\text{a,Xe-133m}}$... cross section for absorption of Xe-133m [10^{-24} cm^2]

Φ ... Neutron flux [$\text{cm}^{-2} \text{ s}^{-1}$]

μ_{Xe133m} ... direct relative fission yield for Xe-133m ($\mu_{\text{Xe133m}} = 1.89 \cdot 10^{-3}$)

Σ_{f} ... macroscopic cross section for fission, calculated by Equation 23

Initial condition:

For $t = 0$

$$N_{\text{J}}(0) = N_{\text{Xe133m}}(0) = N_{\text{Xe133}}(0) = 0$$

Equation 26: Initial condition for solving the differential equation

with

$$N_{\text{J}}(t) = \frac{\mu_{\text{J}} \Phi \Sigma_{\text{f}}}{\lambda_{\text{J}}} \cdot (1 - e^{-\lambda_{\text{J}} t})$$

Equation 27: Equation for the number of Iodine atoms at time t

where

$N_{\text{J}}(t)$... Number of Iodine atoms at time t

μ_{J} ... direct relative fission yield for I-133 ($\mu_{\text{J}} = 6.70 \cdot 10^{-2}$)

Φ ... Neutron flux [$\text{cm}^{-2} \text{ s}^{-1}$]

Σ_{f} ... macroscopic cross section for fission, calculated by Equation 23

λ_{J} ... Decay constant for I-133 [s^{-1}]

Solution for Xe-133m:

$$N_{\text{Xe133m}}(t) = \lambda_{\text{Jm}} \frac{\mu_{\text{J}} \Phi \Sigma_{\text{f}}}{\alpha \cdot \lambda_{\text{J}}} (1 - e^{-\alpha t}) - \lambda_{\text{Jm}} \frac{\mu_{\text{J}} \Phi \Sigma_{\text{f}}}{\lambda_{\text{J}} (\alpha - \lambda_{\text{J}})} (e^{-\lambda_{\text{J}} t} + e^{-\alpha t}) + \frac{1}{\alpha} \mu_{\text{Xe133m}} \Sigma_{\text{f}} \Phi (1 - e^{-\alpha t})$$

Equation 28: Solution for Xe-133m

where

N_{Xe133m} ... Number of Xe-133m atoms

λ_{Jm} ... Decay constant of decaying from I-133 \rightarrow Xe-133m [s^{-1}]

μ_{J} ... direct relative fission yield for I-133 ($\mu_{\text{J}} = 6.70 \cdot 10^{-2}$)

Φ ... Neutron flux [$\text{cm}^{-2} \text{s}^{-1}$]

Σ_{f} ... macroscopic cross section for fission, calculated by Equation 23

α ... $\alpha = \sigma_{\text{a, Xe133m}} \cdot \Phi + \lambda_{\text{Xe133m}}$

λ_{J} ... Decay constant of I-133 [s^{-1}]

λ_{Xe133m} ... Decay constant of Xe-133m [s^{-1}]

$\sigma_{\text{a, Xe-133m}}$... cross section for absorption of Xe-133m [10^{-24}cm^2]

μ_{Xe133m} ... direct relative fission yield for Xe-133m ($\mu_{\text{Xe133m}} = 1.89 \cdot 10^{-3}$)

Solution for Xe-133:

$$\begin{aligned} N_{\text{Xe133}}(t) = & \lambda_{\text{Jx}} \frac{\mu_{\text{J}} \Phi \Sigma_{\text{f}}}{\lambda_{\text{J}} \cdot \beta} (1 - e^{-\beta t}) - \frac{\lambda_{\text{Jx}}}{\beta - \lambda_{\text{J}}} \frac{\mu_{\text{J}} \Phi \Sigma_{\text{f}}}{\lambda_{\text{J}}} (e^{-\lambda_{\text{J}} t} - e^{-\beta t}) + \\ & + \lambda_{\text{Xe135}} \cdot \left[\begin{aligned} & \left(\frac{\lambda_{\text{Jm}} \mu_{\text{J}} \Phi \Sigma_{\text{f}}}{\alpha \cdot \beta \cdot \lambda_{\text{J}}} \cdot (1 - e^{-\beta t}) - \frac{\lambda_{\text{Jm}} \mu_{\text{J}} \Phi \Sigma_{\text{f}}}{(\beta - \alpha) \alpha \cdot \lambda_{\text{J}}} \cdot (e^{-\alpha t} - 1) \right) - \\ & \frac{\lambda_{\text{Jm}} \mu_{\text{J}} \Phi \Sigma_{\text{f}}}{(\beta - \lambda_{\text{J}}) \cdot \lambda_{\text{J}} (\alpha - \lambda_{\text{J}})} \cdot (e^{-\lambda_{\text{J}} t} - e^{-\beta t}) - \frac{\lambda_{\text{Jm}} \mu_{\text{J}} \Phi \Sigma_{\text{f}}}{(\beta - \alpha) \cdot \lambda_{\text{J}} (\alpha - \lambda_{\text{J}})} \cdot (e^{-\alpha t} - e^{-\beta t}) - \\ & - \frac{\mu_{\text{Xe133m}} \Phi \Sigma_{\text{f}}}{\alpha \cdot \beta} \cdot (1 - e^{-\beta t}) - \frac{\mu_{\text{Xe133m}} \Phi \Sigma_{\text{f}}}{\alpha (\beta - \alpha)} \cdot (e^{-\alpha t} - e^{-\beta t}) \end{aligned} \right] + \\ & + \frac{1}{\beta} \cdot \mu_{\text{Xe133}} \Phi \Sigma_{\text{f}} \cdot (1 - e^{-\beta t}) \end{aligned}$$

Equation 29: Solution for Xe-133

where

$N_{\text{Xe133}}(t)$... Number of Xe-133 atoms at time t

λ_{Jx} ... Decay constant of decaying from I-133 \rightarrow Xe-133m \rightarrow Xe-133 [s^{-1}]

λ_{Jm} ... Decay constant of decaying from I-133 \rightarrow Xe-133m [s^{-1}]

μ_{J} ... direct relative fission yield for I-133 ($\mu_{\text{J}} = 6.70 \cdot 10^{-2}$)

Φ ... Neutron flux [$\text{cm}^{-2} \text{s}^{-1}$]

λ_{J} ... Decay constant of I-133 [s^{-1}]

Σ_{f} ... macroscopic cross section for fission, calculated by Equation 23

α ... $\alpha = \sigma_{\text{a, Xe133m}} \cdot \Phi + \lambda_{\text{Xe133m}}$

β ... $\beta = \sigma_{\text{a, Xe133}} \cdot \Phi + \lambda_{\text{Xe133}}$

$\lambda_{\text{Xe133(m)}}$... Decay constant of Xe-133m [s^{-1}]

$\sigma_{\text{a, Xe-133(m)}}$... cross section for absorption of Xe-133m [10^{-24}cm^2]

$\mu_{\text{Xe133(m)}}$... direct relative fission yield for Xe-133(m) ($\mu_{\text{Xe133m}} = 1.89 \cdot 10^{-3}$,
 $\mu_{\text{Xe133}} = 6.70 \cdot 10^{-2}$)

6.2.1.3 Xe-135

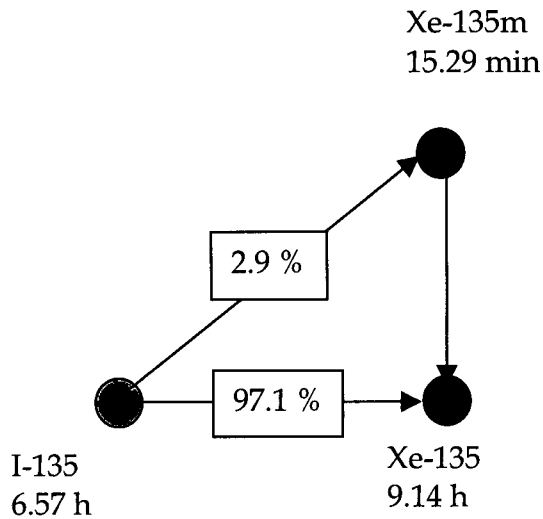


Figure 6-4: Decay scheme for the relevant isobaric chain 135

Nuclide	Independent fission yield	Cumulative fission yield
I-135	2.93	6.28
Xe-135m	$1.78 \cdot 10^{-1}$	1.1
Xe-135	$7.85 \cdot 10^{-2}$	6.54

Table 6-5: Independent and cumulative fission yield per 100 fissions of isobaric chain 135 for U-235, thermal fission [data taken from: England and Rider, 1993]

Nuclide	Half life $T_{1/2}$ [s]	Decay constant λ [s^{-1}]
I-135	$2.37 \cdot 10^4 \pm 7.20 \cdot 10^1$	$2.93 \cdot 10^{-5}$
Xe-135m	$9.17 \cdot 10^2 \pm 3.00 \cdot 10^0$	$7.56 \cdot 10^{-4}$
Xe-135	$3.29 \cdot 10^4 \pm 7.20 \cdot 10^1$	$2.11 \cdot 10^{-5}$

Table 6-6: Half life and decay constant for the mass 135 [data taken from ENDF/B-IV]

The following differential equation includes the in-growth from Xe-135 by Iodine and Xe-135m and its decay:

$$\frac{dN_{Xe135}}{dt} = \lambda_{J_x} N_J + \lambda_{Xe135m} N_{Xe135m} - N_{Xe135} \cdot \sigma_{a,Xe135} \cdot \Phi - \lambda_{Xe135} N_{Xe135} + \mu_{Xe135} \Sigma_f \Phi$$

Equation 30: Approach for the calculation of Xe-135

where

N_{Xe135} ... Number of Xe-135 atoms

λ_{Jx} ... Decay constant of decaying from I-135 \rightarrow Xe-135m \rightarrow Xe-135 [s^{-1}]

N_J ... Number of I-135 atoms

λ_{Xe135m} ... Decay constant of Xe-135m [s^{-1}]

N_{Xe135m} ... Number of Xe-135m atoms

N_{Xe135} ... Number of Xe-135 atoms

$\sigma_{a,Xe-135}$... cross section for absorption of Xe-135 [10^{-24} cm^2]

Φ ... Neutron flux [$\text{cm}^{-2} \text{ s}^{-1}$]

λ_{Xe135} ... Decay constant of Xe-135 [s^{-1}]

μ_{Xe135} ... direct relative fission yield for Xe-135 ($\mu_{Xe135} = 0.003$, [Smidt, 1971])

Σ_f ... macroscopic cross section for fission, calculated by Equation 23

The following differential equation includes the in-growth from Xe-135m by Iodine and its decay:

$$\frac{dN_{Xe135m}}{dt} = \lambda_{Jm} N_J - N_{Xe135m} \cdot \sigma_{a,Xe135m} \cdot \Phi - \lambda_{Xe135m} N_{Xe135m} + \mu_{Xe135m} \Sigma_f \Phi$$

Equation 31: Approach for calculation of Xe-135m

where

N_{Xe135m} ... Number of Xe-135m atoms

λ_{Jm} ... Decay constant of decaying from I-135 \rightarrow Xe-135m [s^{-1}]

N_J ... Number of I-135 atoms

λ_{Xe135m} ... Decay constant of Xe-135m [s^{-1}]

$\sigma_{a,Xe-135m}$... cross section for absorption of Xe-135m [10^{-24} cm^2]

Φ ... Neutron flux [$\text{cm}^{-2} \text{ s}^{-1}$]

μ_{Xe135m} ... direct relative fission yield for Xe-135m ($\mu_{Xe135} = 0.003$, [Smidt, 1971])

Σ_f ... macroscopic cross section for fission, calculated by Equation 23

Initial condition:

For $t = 0$

$$N_J(0) = N_{Xe135m}(0) = N_{Xe135}(0) = 0$$

Equation 32: Initial condition for solving the differential equation

with

$$N_J(t) = \frac{\mu_J \Phi \Sigma_f}{\lambda_J} \cdot (1 - e^{-\lambda_J t})$$

Equation 33: Equation for number of Iodine atoms at time t

where

$N_J(t)$... Number of Iodine atoms at time t

μ_J ... direct relative fission yield for I-135 ($\mu_J = 0.056$, *Smidt, 1971*)

Φ ... Neutron flux [$\text{cm}^{-2} \text{s}^{-1}$]

Σ_f ... macroscopic cross section for fission, calculated by Equation 23

λ_J ... Decay constant for I-135 [s^{-1}]

Solution for Xe-135m:

$$N_{Xe135m}(t) = \lambda_{Jm} \frac{\mu_J \Phi \Sigma_f}{\alpha \cdot \lambda_J} (1 - e^{-\alpha t}) - \lambda_{Jm} \frac{\mu_J \Phi \Sigma_f}{\lambda_J (\alpha - \lambda_J)} (e^{-\lambda_J t} + e^{-\alpha t}) + \frac{1}{\alpha} \mu_{Xe135m} \Sigma_f \Phi (1 - e^{-\alpha t})$$

Equation 34: Solution for Xe-135m

where

N_{Xe135m} ... Number of Xe-135m atoms

λ_{Jm} ... Decay constant of decaying from I-135 \rightarrow Xe-135m [s^{-1}]

μ_J ... direct relative fission yield for I-135 ($\mu_J = 0.056$, *Smidt, 1971*)

Φ ... Neutron flux [$\text{cm}^{-2} \text{s}^{-1}$]

Σ_f ... macroscopic cross section for fission, calculated by Equation 23

$\alpha \dots \alpha = \sigma_{a, Xe135m} \cdot \Phi + \lambda_{Xe135m}$

λ_J ... Decay constant of I-135 [s^{-1}]

λ_{Xe135m} ... Decay constant of Xe-135m [s^{-1}]

$\sigma_{a, Xe-135m}$... cross section for absorption of Xe-135m [10^{-24} cm^2]

μ_{Xe135m} ... direct relative fission yield for I-135 ($\mu_J = 0.003$, *Smidt, 1971*)

Solution for Xe-135:

$$N_{Xe135}(t) = \lambda_{Jx} \frac{\mu_J \Phi \Sigma_f}{\lambda_J \cdot \beta} (1 - e^{-\beta t}) - \frac{\lambda_{Jx}}{\beta - \lambda_J} \frac{\mu_J \Phi \Sigma_f}{\lambda_J} (e^{-\lambda_J t} - e^{-\beta t}) +$$

$$+ \lambda_{Xe135m} \cdot \left[\begin{aligned} & \left(\frac{\lambda_{Jm} \mu_J \Phi \Sigma_f}{\alpha \cdot \beta \cdot \lambda_J} \cdot (1 - e^{-\beta t}) - \frac{\lambda_{Jm} \mu_J \Phi \Sigma_f}{(\beta - \alpha) \alpha \cdot \lambda_J} \cdot (e^{-\alpha t} - 1) - \right. \\ & \left. - \frac{\lambda_{Jm} \mu_J \Phi \Sigma_f}{(\beta - \lambda_J) \cdot \lambda_J (\alpha - \lambda_J)} \cdot (e^{-\lambda_J t} - e^{-\beta t}) - \frac{\lambda_{Jm} \mu_J \Phi \Sigma_f}{(\beta - \alpha) \cdot \lambda_J (\alpha - \lambda_J)} \cdot (e^{-\alpha t} - e^{-\beta t}) - \right. \\ & \left. - \frac{\mu_{Xe135m} \Phi \Sigma_f}{\alpha \cdot \beta} \cdot (1 - e^{-\beta t}) - \frac{\mu_{Xe135m} \Phi \Sigma_f}{\alpha (\beta - \alpha)} \cdot (e^{-\alpha t} - e^{-\beta t}) \right] + \\ & + \frac{1}{\beta} \cdot \mu_{Xe135} \Phi \Sigma_f \cdot (1 - e^{-\beta t}) \end{aligned} \right]$$

Equation 35: Solution for Xe-135

where

$N_{Xe135}(t)$... Number of Xe-135 atoms at time t

λ_{Jx} ... Decay constant of decaying from I-135 \rightarrow Xe-135m \rightarrow Xe-135 [s^{-1}]

λ_{Jm} ... Decay constant of decaying from I-135 \rightarrow Xe-135m [s^{-1}]

μ_J ... direct relative fission yield for I-135 ($\mu_J = 0.056$, *Smidt, 1971*)

Φ ... Neutron flux [$\text{cm}^{-2} \text{ s}^{-1}$]

λ_J ... Decay constant of I-135 [s^{-1}]

Σ_f ... macroscopic cross section for fission, calculated by Equation 23

$\alpha \dots \alpha = \sigma_{a, Xe135m} \cdot \Phi + \lambda_{Xe135m}$

$\beta \dots \beta = \sigma_{a, Xe135} \cdot \Phi + \lambda_{Xe135}$

$\lambda_{Xe135(m)}$... Decay constant of Xe-135(m)

$\sigma_{a, Xe-135(m)}$... cross section for absorption of Xe-135m [10^{-24} cm^2]

$\mu_{Xe135(m)}$... direct relative fission yield for X-135m ($\mu_{Xe135(m)} = 0.003$, [*Smidt, 1971*])

6.2.2 Description of ORIGEN-2.2

ORIGEN-2.2 is a computer code for build-up, decay and processing of radioactive material calculations.

Compared to earlier models (ORIGEN-2, ORIGEN-2.1) this version considers updates from power plant models, cross sections, fission product yields, decay data, decay photon data and the source code [Croff; 1983].

This program uses a matrix exponential method to solve a large system of coupled, linear first order ordinary differential equations with constant coefficients [<http://www.nea.fr/abs/html/ccc-0371.html>, October 2005].

An example for an input file is given in Annex B.

6.3 Experimental

First step was the planning of the irradiation itself, the amount of uranium 235 needed, and for how long the irradiation should last. The amount was chosen to be 1 μg for the first experiment and it turned out that this was enough for producing all relevant isotopes of xenon. An irradiation time of three hours was chosen for the first experiment [Reeder *et al.*, 2001]. Then for the following experiments with calculations (see chapter 6.2), planned for measuring different isotope ratios different times were chosen.

At the beginning a sample of 11.83 mg of 90% enriched uranium 235 was taken. Since 1 μg U-235 was needed, the following procedure was performed in order to obtain a uranium solution easy to handle:

8.07 mg of 90% U-235 were dissolved in 7 ml 65% of Nitric acid, which was heated and evaporated. The residue was transferred with 4 x 2.5 ml 1 M Nitric acid to a teflon flask giving a concentration of 0.7905 mg U / g_{solution}. Since the aim was a solution containing 0.1 mg U / g_{solution}, 1.183 g were

taken from the original solution, transferred into a second teflon flask and diluted with 8.857 g 1 M Nitric acid. The resulting solution had a concentration of 0.11208 mg U / g_{solution}, calculated with the density of 1 M Nitric acid; $\rho_{1\text{MCHNO}_3} = (1.032 \text{ g/cm}^3)$ at $T = 20^\circ\text{C}$. The concentration of U-235 for this solution was calculated to be 0.09775 mg U-235/ml.

The preparation of the samples for the irradiation was performed by transferring 10 μl of this solution into a quartz glass vial. After evaporation of the solution on a heating plate and glowing the vial for a short time with a Bunsen burner, it was sealed.

6.4 Gamma spectroscopy of samples

The ATL03 ultra low level laboratory is located in a bunker with 30 cm concrete walls. This material is the major shielding for environmental radiation.

In this bunker a steel chamber with walls of 5cm thickness was constructed as a second shielding. There are two detector systems (HPGe) located.

The detector specifications are given in Annex C.

6.4.1 Calibration

The irradiated samples were measured in the quartz glass vial in a plastic container surrounded by plastic foil in a distance of 10cm from the detector. For the calibration of this geometry a calibration point source (KG236, AEA Technology QSA GmbH Germany) with different nuclides (see Table 6-7) was fixed and measured in the same distance.

Nuclide	Half life [d]	Activity [kBq]	Uncertainty [%]
Am-241	157850	3.47	1.5
Cd-109	462.1	17.5	1.5
Co-57	271.79	0.675	1.5
Ce-139	137.66	0.702	1.5
Hg-203	46.595	1.09	1.5
Sn-113	115.09	2.42	1.5
Sr-85	64.849	2.28	1.5
Cs-137	10999.97	3.17	1.5
Y-88	106.65	5.01	1.5
Co-60	1925.5	3.74	1.5

Table 6-7: KG-236-Nuclide list with activities for 01.01.2002

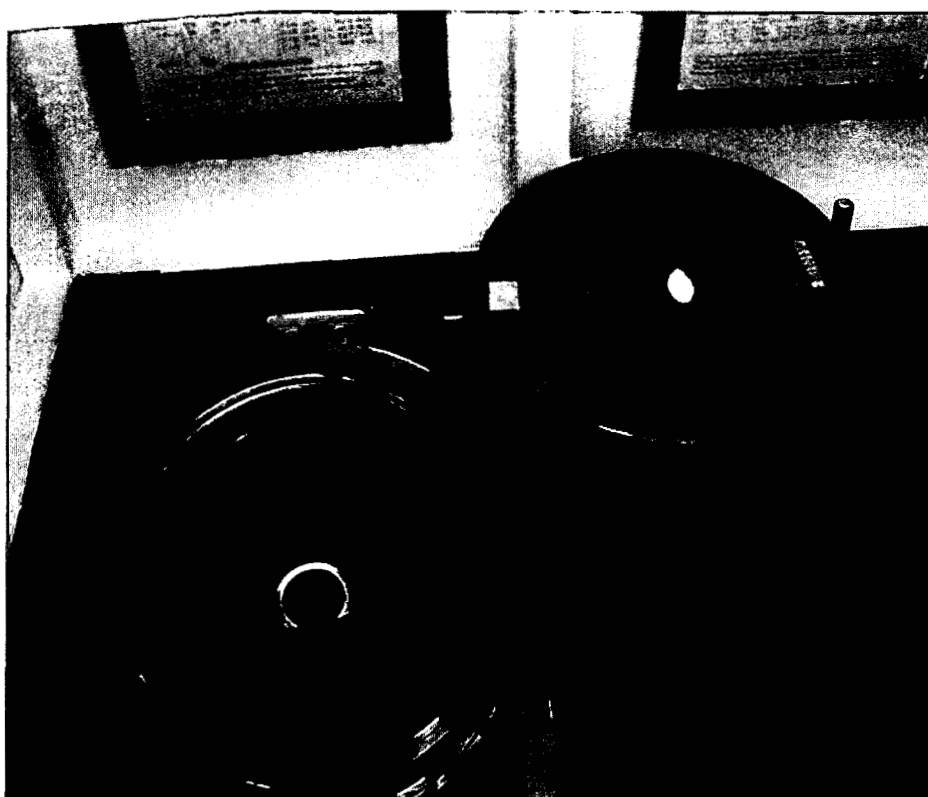


Figure 6-5: Detector ATL03_003

6.5 Results

6.5.1 Before separation

Following results show a good accordance between experiment and theory, therefore it is possible to calibrate the detector system with irradiated uranium samples and in this way to simulate nuclear weapons testing.

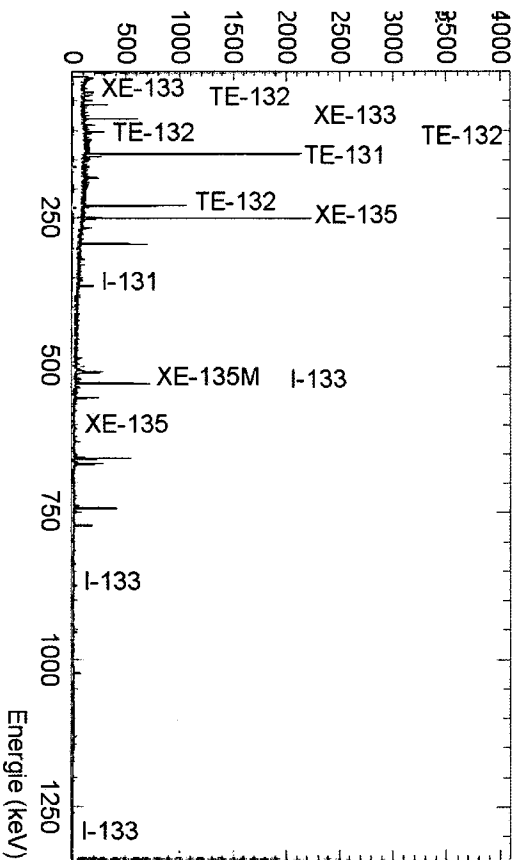


Figure 6-6: Spectrum of a sample irradiated for one hour

For the results only isotope ratios were taken into account, since the activities of the fission products depend on the neutron flux, which is approximately in the order of $1.7 \cdot 10^{12} \text{cm}^{-2} \text{s}^{-1}$.

Results are listed in Table 6-98:

	Sample-irradiation time	Experimental Measurement after irradiation			ORIGEN 2.2		
		50 h	170 h		50 h	170 h	
Isotope ratio	Xe133m/Xe133	$8.79 \cdot 10^{-2}$	$2.36 \cdot 10^{-2}$		$5.63 \cdot 10^{-2}$	$2.49 \cdot 10^{-2}$	
	Xe135/Xe133	1.55			1.13		
	MR10-3.5 h	25 h			25 h		
Isotope ratio	Xe133m/Xe133	$7.79 \cdot 10^{-2}$			$6.39 \cdot 10^{-2}$		
	Xe135/Xe133	5.34			6.31		
	MR11-1.75h	25 h			25 h		
Isotope ratio	Xe133m/Xe133	$5.54 \cdot 10^{-2}$			$6.44 \cdot 10^{-2}$		
	Xe135/Xe133	9.1			6.83		
	MR14-1h	4 h	22 h	77 h	4 h	22 h	77 h
Isotope ratio	Xe133m/Xe133			0.05	0.08	0.06	0.05
	Xe135/Xe133	38	5.6	0.5	39	8.2	0.2

Table 6-8: Measured and calculated isotope ratios

6.5.2 After separation

After a defined time interval the sample was separated from Iodine with activated charcoal, so further ingrowth of xenon by Iodine was stopped. This is necessary for the sample preparation for different tests like simulation of nuclear power operation or nuclear weapons testing.

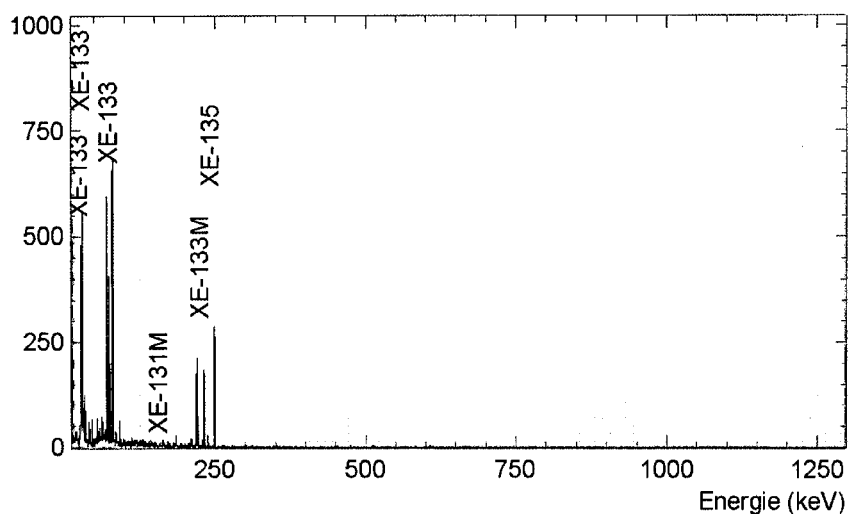


Figure 6-7: Spectrum after separation

		Experimental Measurement after separation			ORIGEN 2.2		
		1.25 h	9 h	19 h	1.25 h	9 h	19 h
Isotope ratio	MR14-Separation after 10 h Xe133m/Xe133	$3.99 \cdot 10^{-2}$	$2.73 \cdot 10^{-2}$	$2.67 \cdot 10^{-2}$	$4.07 \cdot 10^{-2}$	$3.84 \cdot 10^{-2}$	$3.55 \cdot 10^{-2}$
	Xe135/Xe133	$3.31 \cdot 10^{-2}$	$1.86 \cdot 10^{-2}$	$7.06 \cdot 10^{-3}$	$2.79 \cdot 10^{-2}$	$1.61 \cdot 10^{-2}$	$7.96 \cdot 10^{-3}$

Table 6-9: Measured and calculated isotope ratios for MR 14

The separation factor for sample MR14 was 1500, which was determined by the activity of Iodine 131 before separation and after separation. After separation no Iodine could be found, therefore the calculated MDA was taken for the determination of the separation factor.

6.5.3 Conclusion

It could be shown that a simulation of nuclear weapons testing is possible by irradiation of 1 μg 90% enriched uranium and that the result is in the range as calculated before with ORIGEN 2.2.

Since the identification of the source is determined by isotope activity ratios and not by activities themselves, this is a reliable method for the testing of measurement equipments for On-Site-Inspection or for quality assurance in a small European network.

7 Summary and conclusion

The aim of this work was the development and quantification of a well suited processing of noble gas sample transfer from an archive bottle to a radiometric measurement system. During this work a new task has been arisen from the need of the four radioactive xenon isotopes: Irradiation of 90% enriched uranium 235 for preparation of the xenon radionuclides of interest and finally simulation of nuclear weapons testing.

The phrasing “well suited” refers to the requirements given by the (P)TS. These requirements include a gas transfer with a minimum loss. In this case this is an important point since the amount of the xenon sample is in the range of 1 ml to 10 ml mixed with other components. Additionally the determination of the stable xenon amount is required and the separation of other elements which could disturb the radiometric measurement like radon or krypton.

For the determination of the amount of xenon collected the method of gas chromatography was chosen, since the sample composition varies from sample to sample and these compounds have to be separated before radiometric measurement for verification that there is no radioactive component which may disturb the radiometric measurement like radon or krypton. Furthermore not only the separation was possible but as well the collection in device for gamma-spectroscopy.

After installation of the gas chromatograph it was tested for stability and for reproducibility for a long time period and then a transfer system from the archive bottle via the gas chromatograph to the radiometric measurement device was developed.

After numerous experiments beginning with sample freezing out in the sample loop, pumping the sample in a circle it turned out that the efficient way is adsorption on a sample loop filled with activated charcoal and submerged in liquid nitrogen.

The first experiments have shown transfer losses in the range of 30 % to 2 % which means losses of a 1 ml sample of 0.3 ml to 0.02 ml.

Within this work an intercomparison test organised by the (P)TS is described and analyzed, for further measurement no archive samples were available.

The other part of this work was the preparation of relevant xenon isotopes by irradiation of 90% enriched U-235 at the TRIGA Mark II research reactor at the Atomic Institute of the Austrian Universities in Vienna, since the substance is very expensive and the procurement is quite complicated.

This task has developed in this way, that finally nuclear weapons testing carried out can be simulated by changing the irradiation conditions and by combining different irradiated samples.

This will be used for testing the equipments developed for on-site inspections for their fulfillment of the requirements given by the (P)TS.

The planing of irradiation was performed by solution of linear differential equations. Since this was a very complicated process the program Origen 2.2 was used for further calculations. Comparison between theory and experiments have shown, that a simulation of nuclear explosions is possible in this way. For such a simulation it is necessary to have a high Xe-135 activity concentration. Due to its short half life, the activity concentration of the other isotopes will be too low for representing nuclear weapons testing. In this case a shortly (about half an hour) irradiated sample and a long (in the range of 3.5 hours to 7 hours) irradiated sample, which has

decayed for a longer time period (ingrowth xenon from Iodine), have to be combined for simulation the xenon isotope composition originating from nuclear weapons testing.

Finally it has to be emphasized, especially for testing the OSI-equipment, that the complete system is only efficient, if the transport time of the archive bottle is kept short and if the bottles are tight.

Annex A – Data regarding Chapter

5.1.3.4

16.02.2005	50.05%	35%	19.9%	10.5%
	$8.495 \cdot 10^7$	$5.422 \cdot 10^7$	$3.053 \cdot 10^7$	$1.724 \cdot 10^7$
	$8.509 \cdot 10^7$			
	$8.502 \cdot 10^7$			
Mean value	$8.502 \cdot 10^7$	$5.422 \cdot 10^7$	$3.053 \cdot 10^7$	$1.724 \cdot 10^7$
Standard deviation	$6.705 \cdot 10^4$			

Table- A1: Results of calibration on February 16th 2005

17.02.2005	50.05%	35%	19.9%	10.5%
Measurement 1	$8.309 \cdot 10^7$	$5.425 \cdot 10^7$	$3.088 \cdot 10^7$	$1.682 \cdot 10^7$
Measurement 2	$8.325 \cdot 10^7$	$5.415 \cdot 10^7$	$3.085 \cdot 10^7$	
Measurement 3	$8.320 \cdot 10^7$	$5.420 \cdot 10^7$	$3.088 \cdot 10^7$	
Measurement 4		$5.423 \cdot 10^7$	$3.087 \cdot 10^7$	
Mean value	$8.318 \cdot 10^7$	$5.421 \cdot 10^7$	$3.087 \cdot 10^7$	$1.682 \cdot 10^7$
Standard deviation	$8.272 \cdot 10^4$	$4.082 \cdot 10^4$	$1.277 \cdot 10^4$	

Table - A2: Results of calibration on February 17th 2005

22.02.2005	50.05%	35%	19.9%	10.5%
Measurement 1	$8.036 \cdot 10^7$	$5.407 \cdot 10^7$	$2.829 \cdot 10^7$	$1.513 \cdot 10^7$
Measurement 2	$8.039 \cdot 10^7$	$5.967 \cdot 10^7$	$2.830 \cdot 10^7$	$1.503 \cdot 10^7$
Measurement 3	$7.808 \cdot 10^7$	$5.989 \cdot 10^7$		$1.512 \cdot 10^7$
Mean value	$8.037 \cdot 10^7$	$5.788 \cdot 10^7$	$2.830 \cdot 10^7$	$1.509 \cdot 10^7$
Standard deviation	$1.324 \cdot 10^6$	$3.296 \cdot 10^6$	$1.135 \cdot 10^4$	$5.671 \cdot 10^4$

Table -A3: Results of calibration on February 22nd 2005

23.02.2005	50.05%	35%	19.9%	10.5%
Measurement 1	$7.440 \cdot 10^7$	$4.882 \cdot 10^7$	$2.830 \cdot 10^7$	$1.514 \cdot 10^7$
Measurement 2	$7.407 \cdot 10^7$	$4.882 \cdot 10^7$		$1.515 \cdot 10^7$
Mean values	$7.423 \cdot 10^7$	$4.882 \cdot 10^7$	$2.830 \cdot 10^7$	$1.515 \cdot 10^7$
Standard deviation	$2.352 \cdot 10^5$	$2.128 \cdot 10^3$		$3.041 \cdot 10^3$

Table -A4: Results of calibration on February 23rd 2005

24.02.2005	50.05%	35%	19.9%	10.5%
Measurement 1	$7.391 \cdot 10^7$	$4.881 \cdot 10^7$	$2.821 \cdot 10^7$	$1.514 \cdot 10^7$
Measurement 2	$7.413 \cdot 10^7$	$4.871 \cdot 10^7$	$2.823 \cdot 10^7$	$1.512 \cdot 10^7$
Measurement 3	$7.415 \cdot 10^7$	$4.875 \cdot 10^7$	$2.827 \cdot 10^7$	
Mean value	$7.406 \cdot 10^7$	$4.876 \cdot 10^7$	$2.824 \cdot 10^7$	$1.513 \cdot 10^7$
Standard deviation	$1.370 \cdot 10^5$	$4.908 \cdot 10^4$	$2.832 \cdot 10^4$	$1.662 \cdot 10^4$

Table-A5: Results of calibration on February 24th 2005

25.02.2005	50.05%	35%	19.9%	10.5%
Measurement 1	$7.400 \cdot 10^7$	$4.844 \cdot 10^7$	$2.852 \cdot 10^7$	$1.526 \cdot 10^7$
Measurement 2	$7.339 \cdot 10^7$	$4.841 \cdot 10^7$	$2.850 \cdot 10^7$	$1.508 \cdot 10^7$
Measurement 3	$7.393 \cdot 10^7$	$4.880 \cdot 10^7$	$2.854 \cdot 10^7$	$1.503 \cdot 10^7$
Mean value	$7.377 \cdot 10^7$	$4.855 \cdot 10^7$	$2.852 \cdot 10^7$	$1.512 \cdot 10^7$
Standard deviation	$3.358 \cdot 10^5$	$2.165 \cdot 10^5$	$1.609 \cdot 10^4$	$1.161 \cdot 10^5$

Table -A6: Results of calibration on February 25th 2005

28.02.2005	50.05%	35%	19.9%	10.5%
Measurement 1	$7.432 \cdot 10^7$	$4.920 \cdot 10^7$	$2.834 \cdot 10^7$	$1.517 \cdot 10^7$
Measurement 2	$7.439 \cdot 10^7$	$4.907 \cdot 10^7$	$2.835 \cdot 10^7$	$1.519 \cdot 10^7$
Measurement 3	$7.486 \cdot 10^7$	$4.898 \cdot 10^7$	$2.836 \cdot 10^7$	$1.517 \cdot 10^7$
Mean values	$7.452 \cdot 10^7$	$4.908 \cdot 10^7$	$2.835 \cdot 10^7$	$1.518 \cdot 10^7$
Standard deviation	$2.933 \cdot 10^5$	$1.105 \cdot 10^5$	$6.162 \cdot 10^3$	$1.150 \cdot 10^4$

Table -A7: Results of calibration on February 28th 2005

Data used for stability testing:

% Xenon	Area [mVs]
10.5	$1.51 \cdot 10^7$
10.5	$1.51 \cdot 10^7$
10.5	$1.52 \cdot 10^7$
10.5	$1.51 \cdot 10^7$
10.5	$1.68 \cdot 10^7$
10.5	$1.72 \cdot 10^7$
19.9	$2.85 \cdot 10^7$
19.9	$2.82 \cdot 10^7$
19.9	$2.83 \cdot 10^7$
19.9	$3.09 \cdot 10^7$
19.9	$3.05 \cdot 10^7$
35	$4.86 \cdot 10^7$
35	$4.88 \cdot 10^7$

35	$4.88 \cdot 10^7$
35	$5.79 \cdot 10^7$
35	$5.42 \cdot 10^7$
35	$5.42 \cdot 10^7$
50.05	$7.38 \cdot 10^7$
50.05	$7.41 \cdot 10^7$
50.05	$7.42 \cdot 10^7$
50.05	$8.04 \cdot 10^7$
50.05	$8.32 \cdot 10^7$
50.05	$8.50 \cdot 10^7$

Table-A8: Data used for testing the stability of the calibration for one week

01.03.2005	50.05%	35%	19.9%	10.5%
Measurement 1	$7.467 \cdot 10^7$	$4.911 \cdot 10^7$	$2.839 \cdot 10^7$	$1.523 \cdot 10^7$
Measurement 2	$7.462 \cdot 10^7$	$4.910 \cdot 10^7$	$2.842 \cdot 10^7$	$1.521 \cdot 10^7$
Measurement 3	$7.461 \cdot 10^7$	$4.917 \cdot 10^7$	$2.841 \cdot 10^7$	$1.520 \cdot 10^7$
Mean value	$7.464 \cdot 10^7$	$4.912 \cdot 10^7$	$2.841 \cdot 10^7$	$1.521 \cdot 10^7$
Standard deviation	$3.377 \cdot 10^4$	$3.843 \cdot 10^4$	$1.767 \cdot 10^4$	$1.335 \cdot 10^4$

Table A9: Results of calibration on March 1st 2005

02.03.2005	50.05%	35%	19.9%	10.5%
Measurement 1	$7.424 \cdot 10^7$	$4.888 \cdot 10^7$	$2.823 \cdot 10^7$	$1.513 \cdot 10^7$
Measurement 2	$7.411 \cdot 10^7$	$4.883 \cdot 10^7$	$2.824 \cdot 10^7$	$1.519 \cdot 10^7$
Measurement 3	$7.420 \cdot 10^7$	$4.886 \cdot 10^7$	$2.824 \cdot 10^7$	$1.518 \cdot 10^7$
Mean value	$7.418 \cdot 10^7$	$4.886 \cdot 10^7$	$2.824 \cdot 10^7$	$1.517 \cdot 10^7$
Standard deviation	$6.762 \cdot 10^4$	$2.479 \cdot 10^4$	$5.947 \cdot 10^3$	$3.039 \cdot 10^4$

Table -A10: Results of calibration on March 1st 2005

03.03.2005	50.05%	35%	19.9%	10.5%
Measurement 1	$7.426 \cdot 10^7$	$4.890 \cdot 10^7$	$2.832 \cdot 10^7$	$1.514 \cdot 10^7$
Measurement 2	$7.434 \cdot 10^7$	$4.898 \cdot 10^7$	$2.835 \cdot 10^7$	$1.518 \cdot 10^7$
Measurement 3	$7.430 \cdot 10^7$	$4.903 \cdot 10^7$	$2.832 \cdot 10^7$	$1.519 \cdot 10^7$
Mean value	$7.430 \cdot 10^7$	$4.897 \cdot 10^7$	$2.833 \cdot 10^7$	$1.517 \cdot 10^7$
Standard deviation	$4.090 \cdot 10^4$	$6.711 \cdot 10^4$	$2.051 \cdot 10^4$	$2.536 \cdot 10^4$

Table A11: Results of calibration on March 3rd 2005

07.03.2005	50.05%	35%	19.9%	10.5%
Measurement 1	$7.685 \cdot 10^7$	$4.793 \cdot 10^7$	$2.797 \cdot 10^7$	$1.503 \cdot 10^7$
Measurement 2	$7.279 \cdot 10^7$	$4.839 \cdot 10^7$	$2.799 \cdot 10^7$	$1.503 \cdot 10^7$
Measurement 3	$7.286 \cdot 10^7$	$4.837 \cdot 10^7$	$2.804 \cdot 10^7$	$1.503 \cdot 10^7$
Mean value	$7.416 \cdot 10^7$	$4.823 \cdot 10^7$	$2.800 \cdot 10^7$	$1.503 \cdot 10^7$
Standard deviation	$2.326 \cdot 10^6$	$2.597 \cdot 10^5$	$3.466 \cdot 10^4$	$2.045 \cdot 10^3$

Table A12: Results of calibration on March 7th 2005

14.03.2005	50.05%	35%	19.9%	10.5%
Measurement 1	$7.445 \cdot 10^7$	$4.896 \cdot 10^7$	$2.830 \cdot 10^7$	$1.520 \cdot 10^7$
Measurement 2	$7.425 \cdot 10^7$	$4.902 \cdot 10^7$	$2.832 \cdot 10^7$	$1.518 \cdot 10^7$
Measurement 3	$7.424 \cdot 10^7$	$4.895 \cdot 10^7$	$2.828 \cdot 10^7$	$1.517 \cdot 10^7$
Mean value	$7.431 \cdot 10^7$	$4.898 \cdot 10^7$	$2.830 \cdot 10^7$	$1.518 \cdot 10^7$
Standard deviation	$1.197 \cdot 10^5$	$4.048 \cdot 10^4$	$1.722 \cdot 10^4$	$1.414 \cdot 10^4$

Table A13: Results of calibration on March 14th 2005

30.03.2005	50.05%	35%	19.9%	10.5%
Measurement 1	$7.598 \cdot 10^7$	$5.007 \cdot 10^7$	$2.897 \cdot 10^7$	$1.556 \cdot 10^7$
Measurement 2	$7.617 \cdot 10^7$	$5.011 \cdot 10^7$	$2.902 \cdot 10^7$	$1.557 \cdot 10^7$
Measurement 3	$7.621 \cdot 10^7$	$5.009 \cdot 10^7$	$2.898 \cdot 10^7$	$1.545 \cdot 10^7$
Mean value	$7.612 \cdot 10^7$	$5.009 \cdot 10^7$	$2.899 \cdot 10^7$	$1.553 \cdot 10^7$
Standard deviation	$1.235 \cdot 10^5$	$2.426 \cdot 10^4$	$2.326 \cdot 10^4$	$6.954 \cdot 10^4$

Table A14: Results of calibration on March 30th 2005

31.03.2005	50.05%	35%	19.9%	10.5%
Measurement 1	$7.625 \cdot 10^7$	$5.035 \cdot 10^7$	$2.924 \cdot 10^7$	$1.561 \cdot 10^7$
Measurement 2	$7.660 \cdot 10^7$			
Mean value	$7.642 \cdot 10^7$			
Standard deviation	$2.439 \cdot 10^5$			

Table A15: Results of calibration on March 31st 2005

Annex B - Origen 2.2 INPUT

```
-1  
-1  
-1  
RDA  
RDA ***** BURNUP OF 90% U235 *****  
RDA  
RDA  
RDA  
LIP 0 0 0  
RDA DECAY LIB THERMAL LIB  
LIB 0 1 2 3 201 202 203 9 50 0 1 0  
RDA PHOTON LIB  
PHO 101 102 103 10  
RDA READ FUEL COMPOSITION (1g)  
INP -1 1 -1 -1 1 1  
MOV -1 1 0 1.0  
HED 1 CHARGE  
RDA  
RDA ****FUEL HISTORY COMMANDS****  
RDA ****IRRADIATION****  
RDA  
BUP  
IRF 1 2.0E+12 1 2 3 2  
BUP  
HED 2 FUELS DIS  
RDA  
RDA ****DECAY****  
DEC 3 2 3 3 1  
DEC 4 3 4 3 0  
DEC 5 4 5 3 0  
RDA  
RDA ****OUTPUT COMMANDS****  
RDA  
TIT BURNUP OF 1g 90% 2.0E+12  
BAS 1g  
CUT 5 1.0E-05 7 1.0E-5 -1  
OPTL 24*8  
OPTA 24*8  
OPTF 8 8 8 8 8 8 5 8 8 8 8 8 8 8 8 8 8 8 8 8 8 8 8 8  
OUT 5 1 -1 0  
END  
2 922340 0.0095 922350 0.8991 922360 0.0068 922380 0.0846 0 0.0 FUEL 90%
```


Annex C-Detector specification

Detector ATL03_003

Detector name:	BE5035.
Serial No.:	b 03098,
Type:	HP-Ge, p-type, cryal endcap and electrolytic cooper mounting.
Cryostat:	Vertical streamline.
Cool-Down Time:	16 hours.
Efficiency:	55% relative efficiency.
Crystal shape:	80 mm diameter, 35 mm length.
End Cap to Crystal:	5 mm.
Absorbing Layers:	0.5 mm Carbon Epoxy.
Window:	Carbon window, teflon cap.
Remote Preamplifier:	Outside of shielding equipment.
Recommended High Voltage Operating Bias:	+ 4500 V.

Technical specifications

Resolution (FWHM) at 1.33 MeV, Co-60:	< 2.0 keV (warranted).
Resolution (FWHM) at 122 keV, Co-57:	< 0.7 keV (warranted).
FWTM / FWHM at 13332.5 keV	≤ 2.0.
DSpec Peaking Time:	13 μs.

The data available were certified by Canberra in August 2002.

Detector ATL03_004

Detector name: BE5035.

Serial No.: b 03102,

Type: HP-Ge, p-type, cryal endcap and electrolytic cooper mounting.

Cryostat: Vertical streamline.

Cool-Down Time: 16 hours.

Efficiency: 55% relative efficiency.

Crystal shape: 80 mm diameter, 35 mm length.

End Cap to Crystal: 5 mm.

Absorbing Layers: 0.5 mm Carbon Epoxy.

Window: Carbon window, teflon cap.

Remote Preamplifier: Outside of shielding equipment.

Recommended High Voltage Operating Bias: + 5000 V.

Technical specifications

Resolution (FWHM) at 1.33 MeV, Co-60: < 2.0 keV (warranted).

Resolution (FWHM) at 122 keV, Co-57: < 0.7 keV (warranted).

FWTM / FWHM at 13332.5 keV \leq 2.0.

DSPEC Peaking Time: 13 μ s.

The data available were certified by Canberra in October 2002.

Annex D-Calculation of MDA

$$MDA(Bq) = \frac{L_D}{T \cdot \varepsilon \cdot \gamma_i \cdot K_c}$$

where:

L_D Lower limit of detection at the 95 % confidence level.

$$L_D = 2.71 + 4.65\sqrt{\mu_B}$$

$\sqrt{\mu_B}$ Standard deviation of the background at the energy of interest.

$$\mu_B = \sum^{ROI} counts_i$$

ROI: Defined as ± 1.25 FWHM ($\pm 3 \sigma$) on either side of the hypothetical peak centroid.

T Acquisition life time (s).

ε Attenuation corrected efficiency (counts per gamma) at the energy of interest.

γ_i Branching ratio of gamma energy (gamma per decay) of the isotope 'i'.

K_c Decay correction during acquisition time.

$$K_c = \frac{1 - e^{-\lambda_i t_c}}{\lambda_i \cdot t_c}$$

λ_i Decay constant for the isotope 'i' (s^{-1}).

t_c Clock real time between start and end of acquisition (s).

Notice:

This calculation of the MDA is provided by the (P)TS especially for the nuclide Ba-140, since the laboratory system requirements for certification is being capable of measuring this nuclide in seven days with a MDA of ≤ 24 mBq. [PTS, 2005]

Futhermore the calculation of the limit of detection is based upon the paper from L. Currie. [Lloyd A. Currie; 1968]

Literature:

- Auer M.*, 2002: "Laboratory analysis of xenon samples during the Noble Gas Equipment Test"; Presentation on the Radionuclide Workshop August 2002, Blumau, Austria
- Botsch*, 2000: Wolfgang Botsch: "Untersuchung zur Strahlenexposition von Einwohnern kontaminierter Ortschaften der nördlichen Ukraine"; Dissertation Hannover 2001
- Bowyer et al.*; 1996: T.W. Bowyer, K.H. Abel, W.K. Hensley, C.W. Hubbard, A.D. McKinnon, M.E. Panisko, R.W. Perkins, P.L. Reeder, R.C. Thompson, R.A. Warner: "Automatic Radioxenon Analyzer for CTBT Monitoring"; PNNL-11424, UC-713; December 1996
- Bowyer et al.*; 1998: T.W. Bowyer, R.W. Perkins, K.H. Abel, W.K. Hensley, C.W. Hubbard, A.D. McKinnon, M.E. Panisko, P.L. Reeder, R.C. Thompson, R.A. Warner: "Xenon Radionuclides, Atmospheric: Monitoring"; Encyclopedia of Environmental Analysis and Remediation, Editor: Robert A. Meyers; John Wiley & Sons, Inc., 1998. ISBN: 0-471-11708-0
- Bowyer et al.*; 2002: T.W. Bowyer, C. Schlosser, K.H. Abel, M. Auer, J.C. Hayes, T.R. Heimbigner, J.I. McIntyre, M.E. Panisko, P.L. Reeder, H. Sartorius, J. Schulze, W. Weiss: "Detection and analysis of xenon isotopes for the comprehensive nuclear-test-ban treaty international monitoring system", Journal of Environmental Radioactivity 59 (2002), 139-151
- Böcker J.*, 1997: Chromatographie: Instrumentelle Analytik mit Chromatographie und Kapillarelektrophorese, Würzburg, Vogel (Laborpraxis)

- Croff*, 1983: Allen G. Croff: „Origen 2: A versatile computer code for calculating the nuclide compositions and characteristics of nuclear materials“, Nuclear Technology, Vol. 62, p. 335-352; 1983
- CTBT* 1996: Preparatory Commission for the Comprehensive Nuclear-Test-Ban Treaty Organization, Provisional Technical Secretariat, 1996. Comprehensive Nuclear-Test-Ban Treaty and Text on the Establishment of a Preparatory Commission for the Comprehensive Nuclear-Test-Ban Treaty Organization. A/50/1027, Austria, 139p.
- De Geer*; 2002: “Basic nuclear data for PTS xenon analysis“, PTS/IDC/RS/RD; 9 April 2002
- ENDF/B-IV*: URL: <http://t2.lanl.gov> (October 2005)
- England and Rider*, 1993: T.R. England and B.F. Rider, Los Alamos National Laboratory, LA-UR-94-3106; ENDF-349 (1993), URL: <http://ie.lbl.gov/fission.html> (October 2005)
- Finkelstein Y.*: “Fission product isotope ratios as event characterization tools- Part II: Radioxenon isotopic activity ratios“, Kerntechnik 66 (2001) 5-6, p.229-236
- Friedlander et al.*, 1964: Gerhart Friedlander, Joseph W. Kennedy, Julian Malcolm Miller: “Nuclear and Radiochemistry” Second Edition, 1964, John Wiley & Sons
- Lloyd A. Currie*: “Limits for Qualitative Detection and Quantitative Determination“, Analytical Chemistry, Vol. 40, No. 3 (1968); p. 586-593

- NPT*, 1968: Treaty on the Non-Proliferation of Nuclear Weapons, UNTS 729, p. 161; 1968
- Perkins and Casey*, 1996: Richard W. Perkins, Leslie A. Casey: "Radionuclides: Their role in monitoring a comprehensive test ban treaty"; DOE/RL-96-51
- PRIS*, 2005: Power Reactor Information System by the IAEA (International Atomic Energy Agency),
<http://www.iaea.org/programmes/a2/index.html>,
12.11.2005
- PTBT*, 1963: Partial Test Ban Treaty (Treaty banning Nuclear Weapon Tests in the Atmosphere, in Outer Space and Under Water), UNTS 480, p.43; 1963
- PTS*, 2003: CTBTO, "Detailed technical specifications and requirements for the development of on-site inspection equipment for xenon sampling, separation and measurement", CTBT/PTS/INF.578; March 2003
- PTS*, 2005: Certification of radionuclide laboratories, CTBT/PTS/INF96.REV 7
- Reeder et al.*, 2001 : P.L. Reeder, T.W. Bowyer, J.I. McIntyre, W.K. Pitts : "Determination of ^{131m}Xe and ^{133m}Xe in the presence of ^{133g}Xe via combined beta-spectroscopy and delayed coincidence", Journal of Radioanalytical and Nuclear Chemistry, Vol. 248, No. 3 (2001); 617-622

Schulze et al., 2000: Joachim Schulze, Matthias Auer, Robert Werzi: "Low level radioactivity measurement in support of the CTBTO", *Applied Radiation and Isotopes* 53 (2000); 23-30

Smidt, 1971: Dieter Smidt, "Reaktortechnik, Band 1 Grundlagen", G. Braun Karlsruhe, 1971

Technical report, 1998: Report by an international advisory committee (Working Group 3): The radiological situation at the atolls of Mururoa and Fangataufa; Inventory of radionuclides underground at the atolls Volume 3, June 1998

UNSCEAR, 1977: UNSCEAR (United Nations Scientific Committee on the Effects of Atomic Radiation) Report 1977, Annex D, III A. Effluents

UNSCEAR, 1982: UNSCEAR (United Nations Scientific Committee on the Effects of Atomic Radiation) Report 1982, Annex F "Exposures resulting from nuclear power production", III., Reactor operation, A. Effluents, Table 13 and Table 15

UNSCEAR, 1993: UNSCEAR (United Nations Scientific Committee on the Effects of Atomic Radiation) Report 1993, Annex B "Exposures from man made sources of radiation", IV., Nuclear Power Production, C. Reactor operation, Effluents, Table 27 and Table 28.

UNSCEAR, 2000: UNSCEAR (United Nations Scientific Committee on the Effects of Atomic Radiation) Report 2000, Volume I.

Wotawa et al, 2003.: Gerhard Wotawa, Lars-Erik De Geer, Philippe Denier, Martin Kalinowski, Harri Toivonen, Real D'Amours, Franco Desiato, Jean-Pierre Issartel, Matthias Langer, Petra Seibert, Andreas Frank, Craig Sloan, Hiromi Yamazawa: "Atmospheric transport modelling in support of CTBT

verification-overview and basic concepts"; Atmospheric Environment 37, 2529-2537 (2003).

<http://ie.lbl.gov>: WWW Table of Radioactive Isotopes, last access: 11.03.2006

<http://www.ctbto.org>: Official Homepage of CTBTO, last access: 08.11.2005.

<http://www.eia.doe.gov>: Boiling Water Reactor and Diagrams for a Pressurized-

Water Reactor and a Reactor Vessel

(http://www.eia.doe.gov/cneaf/nuclear/page/nuc_reactors/pwr.html and

http://www.eia.doe.gov/cneaf/nuclear/page/nuc_reactors/bwr.html), last access: 19.10.2005

http://www.ga.gov.au/oracle/nukexp_form.jsp: Homepage of Australia's national agency for geoscience research and geospatial information, last access: 08.11.2005.

<http://www.nukeworker.com>: last access: 26.02.2006

<http://www.pugwash.org>: Conferences on Science and World Affairs; last access: 25.03.2006.

<http://www.visitcumbria.com;2005>: Sellafield Visitor Center;

<http://www.visitcumbria.com/wc/svc.htm>, last access: 13.11.2005

<http://www.world-nuclear.org>: Information and Issue Briefs, "Nuclear fuel cycle" (updated in August 2005); last access: 18.10.2005

Lebenslauf

Name: RAITH Maria

Geb. Datum: 08. Dezember 1975

Ausbildung:

- 1982-1986 Volksschule, 1210 Wien, Prießnitzgasse 1
- 1986-1994 hum. Gymnasium, 1020 Wien, Zirkusgasse 48
- Reifeprüfung am 31.5.1994
- 1994 Beginn des Physik-Diplom Studiums an der Universität Wien
- 2002 Abschluss des Studiums (Titel der Diplomarbeit: „Verbesserungsschritte beim Prozessieren von Silizium-Solarzellen“ durchgeführt bei Hrn. Doz. Dr. Johann Summhammer am Atominstitut der Österreichischen Universitäten)
- 2003 Beginn des Doktoratsstudiums an der Technischen Universität Wien, Titel der Arbeit: „Determination of short-lived xenon isotopes for verification of the Comprehensive Nuclear Test Ban Treaty“ ausgeführt im Forschungszentrum Seibersdorf (Health Physics, Radionuklidlabor), betreut im Zentrum von Dr. Erich Hrncsek und an der TU-Wien von Prof. Dr. Manfred Tschurlovits
- Absolvierung Strahlenschutzkurse (Grundkurs, Umgang mit geschlossenen radioaktiven Stoffen und Umgang mit offenen radioaktiven Stoffen)
- Beginn des Universitätslehrgangs „Medizinische Physik“ im Wintersemester 2005/06

Publikation:

- GALVANIC CONTACTING ON GRAIN BOUNDARIES OF MULTICRYSTALLINE SILICON SOLAR CELLS (R. Ebner, M. Raith, V. Schlosser, J. Summhammer; "PV in Europe from PV Technology to Energy Solutions", Conference and Exhibition (7-11 October 2002 in Rome, Italy))

Konferenzen/Workshops:

- Radionuclide Laboratory Workshop & Noble Gas Workshop, August 2004, Strassoldo, Italien
- 8th Int. Conf. on Applications of Nuclear Techniques, Kreta, Griechenland

Präsentationen:

- "Determination of short lived xenon isotopes for verification of the Comprehensive Nuclear Test Ban Treaty"-BfS Freiburg, April 2003, Seminarvortrag
- "Determination of short lived xenon isotopes for verification of the Comprehensive Nuclear Test Ban Treaty"-ARCS, März 2004, Diplomanden/Dissertantenseminar
- "Messung von Xe-Isotopen zum Nachweis von Kernwaffentests", Atominstitut der Österr. Universitäten, Mai 2004, Seminarvortrag
- „Preparation of xenon Isotopes by Irradiation of Enriched uranium“, Strassoldo, August 2004, Edelgas-Workshop
- „Preparation of xenon Isotopes by Irradiation of Enriched uranium“, Kreta, September 2004, 8th Int. Conf. on Applications of Nuclear Techniques
- "Determination of short lived xenon isotopes for verification of the Comprehensive Nuclear Test Ban Treaty"-ARCS, März 2005, Diplomanden/Dissertantenseminar